



PUBLIC FINAL REPORT

UTD PROJECT NUMBERS 1.19.I, 1.19.D

GTI PROJECT NUMBERS 22580 and 22582

Comparative Assessment of Space and Water Heating Systems in the Virtual Test Home

Report Issued:

January 2021



Prepared For:

Utilization Technology Development, NFP

Des Plaines, IL

UTD Document No. UTD-21-001

GTI Project Managers:

Alejandro Baez Guada

aguada@gti.energy

Tim Kingston

tkingston@gti.energy

1700 S. Mount Prospect Rd.

Des Plaines, Illinois 60018

www.gti.energy

Legal Notice

This information was prepared by Gas Technology Institute (“GTI”) for Utilization Technology Development NFP (“UTD”).

Neither GTI, the members of GTI, the Sponsor(s), nor any person acting on behalf of any of them:

a. Makes any warranty or representation, express or implied with respect to the accuracy, completeness, or usefulness of the information contained in this report, or that the use of any information, apparatus, method, or process disclosed in this report may not infringe privately-owned rights. Inasmuch as this project is experimental in nature, the technical information, results, or conclusions cannot be predicted. Conclusions and analysis of results by GTI represent GTI's opinion based on inferences from measurements and empirical relationships, which inferences and assumptions are not infallible, and with respect to which competent specialists may differ.

b. Assumes any liability with respect to the use of, or for any and all damages resulting from the use of, any information, apparatus, method, or process disclosed in this report; any other use of, or reliance on, this report by any third party is at the third party's sole risk.

c. The results within this report relate only to the items tested.

Table of Contents

Legal Notice	i
Table of Contents.....	ii
Table of Figures	vi
List of Tables.....	ix
Executive Summary – Comparative Assessment of Space and Water Heating Systems in the Virtual Test Home	10
Introduction & Background.....	12
Background.....	12
End-use Electrification	13
Objective	14
General Methodologies.....	14
VTH Evaluation	14
Advanced Gas-fired Systems.....	14
Electric Air-source Heat Pump Technologies.....	15
Air-source Heat Pump	16
Cold-climate Air-source Heat Pumps	17
Heat Pump Water Heaters	20
Building Energy Modeling	21
Field Validation	22
ccASHP Space Heating Performance Characterizations	22
Background.....	22
Space Heating Capacity Characterization	23
Coefficient of Performance Characterization	24
Additional Operation Characterizations	25
ASHP and ccASHP Performance Comparison.....	26
Validation	30
Manufacturer Specifications	30
Field Demonstration	31
EHPWH Water Heating Performance Characterizations	32
Background.....	32
EHPWH Heat Pump Capacity and COP Characterization.....	33
EHPWH Operation Characterization.....	34
EHPWH Performance Comparison.....	34

Validation	37
Manufacturer Specifications	37
Field Demonstration	38
Performance Perspective.....	39
Individual Space and Water Heating Performance Comparison.....	40
Annual COP and Energy Consumption	41
Annual Operating Cost.....	43
Annual GHG Emissions	44
Discussion.....	45
System Market Impact Considerations	45
Annual COP	47
Annual Source-Energy COP	47
Annual Source-Energy	48
Annual GHG Emissions	49
Annual Operating Cost.....	49
Conclusion & Next Steps	50
Next Steps	50
Appendix A – VTH Evaluation Methods.....	51
Space Heating	51
Tankless Water Heating.....	51
Appendix B – iFLOW + Navien Combi Space and Water Heating Performance Curves.....	53
iFLOW + Navien.....	53
Navien Tankless	53
Appendix C – ASHP and ccASHP Evaluation Test Plan	54
Evaluation Matrix	54
Instrument Plan.....	54
Data Sampling	58
Air Source Electric Heat Pump and System Boundary conditions	58
ASHP Boundary	59
System Boundary.....	59
Calculation of Performance Parameters	59
Electrical Input.....	59
ASHP Electrical Input.....	59
System Electrical Input.....	59
Thermal Output	60

ASHP Heating Output.....	60
AHU Heating Output	60
Cooling Output Associated to Defrost Events	60
Enthalpy Calculation	61
Net Thermal Output.....	61
ASHP Efficiency	61
System Efficiency.....	61
Appendix D – EHPWH Evaluation Test Plan	63
Evaluation Matrix	63
Instrument Plan.....	63
Data Sampling	65
Calculation of Performance Parameters	65
Electrical Input.....	65
Thermal Output	65
EHPWH COP	66
EHPWH Heat Recovery	66
Appendix E – ASHP and ccASHP Additional Characterizations.....	67
Part-load Degradation.....	67
Compressor Speed	67
Defrost Cycles.....	68
Power Consumption and Cooling Delivered	68
Defrost Duration	68
Defrost Activation Cycles	68
Appendix F – Modeling Individual Space and Water Heating Performance Comparison.....	71
Appendix G – Modeling System Market Impact Considerations.....	73
ccASHP + EHPWH Space Heating and Cooling Loads.....	73
Air Conditioning Performance Characterization.....	73
Cooling Capacity	73
Coefficient of Performance.....	73
Goodman Two-stage 10HSPF ASHP Heating Performance Characterization.....	74
Heating Capacity	74
Coefficient of Performance.....	74
Defrost Operation.....	75
Additional Operating Features	75
THP Performance Characterization	75

mCHP Performance Characterization.....78

Table of Figures

Figure 1 – Annual EHPWH COP (left) and Baseline and Cold-climate ASHP Heating COP (right)	10
Figure 2 – Annual Non-baseload Source-energy Consumptions (left) and GHG emissions (right) of Five HVAC and Water Heating Systems	11
Figure 3 – VTH Approach	12
Figure 4 – Condensing Furnace Performance Characterization and Space Heating Distribution (left) and VTH vs Manufacturer (MFR) Annual Gas Efficiencies (right) in Multiple Climate Zones	13
Figure 5 – VTH vs Manufacturer (MFR) Annual Efficiencies for a Condensing Tankless (right), Electric Heat Pump (center) and Gas-fired Combination System (left) in Multiple Climate Zones	13
Figure 6 – Residential PV Installed Cost Break Down (Source: NREL)	14
Figure 7 – Advanced Gas-fired Space Heating Systems VTH Characterizations	15
Figure 8 – Gas-fired Water Heating Systems VTH Characterizations	15
Figure 9 – 10HSPF ASHP VTH Characterization	16
Figure 10 – 10HSPF EHP VTH Characterization in IECC Climate Zones 5, 6 and 7	17
Figure 11 – Hybrid VTH/Field Demonstration Evaluation Approach	18
Figure 12 – Simplified ccASHP P&ID	19
Figure 13 – Indoor (left) and Outdoor (right) ASHP Component Installations	20
Figure 14 – EHPWH Simplified P&ID	21
Figure 15 – Goodman ASHP Steady-state Heating Capacity Characterization	23
Figure 16 – Mitsubishi (left) and Fujitsu (right) ccASHP Steady-state Heating Capacity Characterizations	24
Figure 17 – Goodman ASHP Steady-state COP Characterization	24
Figure 18 – Mitsubishi (left) and Fujitsu (right) ccASHP Steady-state COP Characterizations	25
Figure 19 – Standby Power Consumption of the Electric Heat Pump Systems	25
Figure 20 – ANSI/AHRI 210/240 Heating Regions	26
Figure 21 – ASHP and ccASHP Sizing in Modeling Home Located in Region IV with Humid Air Conditions	27
Figure 22 – ASHP and ccASHPs Daily COP in the Humid/Region IV	28
Figure 23 – Goodman Baseline ASHP COP Waterfall Chart at 0°F (left), 20°F (center), and 50°F (right)	28
Figure 24 – Mitsubishi ccASHP COP Waterfall Chart at 0°F (left), 20°F (center), and 50°F (right)	29
Figure 25 – ASHP and ccASHPs Annual Heating COPs in all CSA EXP 07 Climate Zones (left) and Heating Load Distribution as a Function of OATdb (right)	29

Figure 26 – Goodman ASHP Steady-state Heating Capacity (left) and COP (right) As a Function of OAT: VTH and MFR Comparison	30
Figure 27 – Mitsubishi ccASHP Steady-State Heating Capacity (left) and COP (right) As a Function of OAT: VTH and MFR Comparison	30
Figure 28 – Fujitsu ccASHP Steady-State Heating Capacity (left) and COP (right) As a Function of OAT: VTH and MFR Comparison	31
Figure 29 – ASHP and ccASHPs HSPF Calculation VTH and MFR Comparison	31
Figure 30 – HSPF, HSPF2 and VTH Calculation (left) and Heating Distribution as a Function of OATdb (right)	31
Figure 31 – Third-party Field Demonstration and VTH Comparison (Source: CEE).....	32
Figure 32 – Rheem (left) and AO Smith (right) EHPWH Heat Pump Component Heating Capacity Characterizations	33
Figure 33 – Rheem (left) and AO Smith (right) EHPWH Heat Pump Component COP Characterizations	34
Figure 34 – EHPWH Daily COP for Indoor Installation in the Humid/Region IV	35
Figure 35 – Baseline Electric Water Heater Waterfall Charts for 32-gallon (left), 58-gallon (center), and 84-gallon (right) days	35
Figure 36 – Rheem EHPWH Water Heater Waterfall Charts for 32-gallon (left), 58-gallon (center), and 84-gallon (right) days	36
Figure 37 – EHPWHs Annual COPs in all CSA EXP 07 Climate Zones (left) and Water Heating Load Distributions as a Function of OATdb (right).....	36
Figure 38 – Rheem EHPWH Annual COP for Conventional and Ducted Installations	37
Figure 39 – EHPWH UEF Calculation Comparison	37
Figure 40 – UEF and VTH Calculation (left) and Entering Air Temperature (right) Comparison	38
Figure 41 – Third-party Field Demonstration and VTH Comparison for the AO Smith EHPWHH with Conventional Installation (Source: DOE).....	38
Figure 42 – Third-party Field Demonstration and VTH Comparison for the Rheem EHPWHH with Ducted Installation (Source: Energy 350).....	39
Figure 43 – EHPWH and ccASHP Energy Streams in the Cooling and Heating Seasons.....	39
Figure 44 – Rheem EHPWH Annual COPs for Conventional with- and without HVAC Impact and Ducted Installations.....	40
Figure 45 – Market Impact Considerations Cities in the IECC (left) and CSA EXP 07(right) Maps	41
Figure 46 – Space (left) and Water (right) Heating Equipment Annual COPs	42
Figure 47 – Space (left) and Water (right) Heating Equipment Annual Energy (Gas + Electricity) Consumption.....	43
Figure 48 – Space (left) and Water (right) Heating Equipment Annual Non-baseload Source-energy (Gas + Electricity) Consumptions.....	43
Figure 49 – Space (left) and Water (right) Heating Equipment Annual Total Source-energy (Gas + Electricity) Consumptions	43

Figure 50 – Space (left) and Water (right) Heating Equipment Annual Operating Costs.....	44
Figure 51 – Space (left) and Water (right) Heating Equipment Annual Non-baseload GHG Emissions.....	45
Figure 52 – Space (left) and Water (right) Heating Equipment Annual Total GHG Emissions ...	45
Figure 53 – Market Impact Consideration System Configurations. Baseline Electric (upper left), Advanced Electric (middle left), Advanced Gas (lower left), THP + AC (upper right) and IES-mCHP (lower right)	47
Figure 54 – Annual COPs for the Five HVAC & DHW Systems	47
Figure 55 – Annual Total (left) and Non-baseload (right) SCOPs for the Five HVAC & DHW Systems	48
Figure 56 – Annual Total (left) and Non-baseload (right) Source-energy Consumptions for the Five HVAC & DHW Systems	49
Figure 57 – Annual Total (left) and Non-baseload (right) GHG Emissions for the Five HVAC & DHW Systems.....	49
Figure 58 – Annual Operating Costs for the Five HVAC & DHW Systems	50
Figure 59 – Thermostat Simulation Strategies.....	51
Figure 60 – iFLOW + Navien Performance Characterization.....	53
Figure 61 – Navien Tankless Performance Characterization	53
Figure 62 – Mechanical Room P&ID.....	57
Figure 63 – Outdoor Testing Bay P&ID	57
Figure 64 – AHU Test Rig P&ID	58
Figure 65 – ASHP and System Boundary.....	59
Figure 66 – EHPWH Evaluation P&ID	65
Figure 67 – Goodman ASHP Part-load Degradation Characterization	67
Figure 68 – Mitsubishi (left) and Fujitsu (right) ccASHP Part-load Degradation Characterizations	67
Figure 69 – Goodman ASHP Compressor Speed Characterization	68
Figure 70 – Mitsubishi (left) and Fujitsu (right) ccASHP Maximum Compressor Speed Characterizations	68
Figure 71 – Goodman ASHP Defrost Cooling (left Y-axis) and Power Consumption (right Y-axis) Characterizations	69
Figure 72 – Mitsubishi (left) and Fujitsu (right) ccASHP Defrost Power Consumption Characterizations	69
Figure 73 – Goodman ASHP Defrost Duration Characterization	69
Figure 74 – Mitsubishi (left) and Fujitsu (right) ccASHP Defrost Duration Characterizations	70
Figure 75 – Mitsubishi (left) and Fujitsu (right) ccASHP Defrost Duration Characterizations	70
Figure 76 – Steady-state Cooling Capacity Curves for the Mitsubishi ccASHP (left) and Both Goodman 15SEER (center) and 18SEER (right) ASHPs	73

Figure 77 – Cooling Capacity OATdb Derating Factor for the Mitsubishi ccASHP (left) and Both Goodman 15SEER (center) and 18SEER (right) ASHPs	73
Figure 78 – Cooling COP Curves for the Mitsubishi ccASHP (left) and Both Goodman 15SEER (center) and 18SEER (right) ASHPs	74
Figure 79 – Goodman 10HSPF ASHP Steady-state Heating Capacity	74
Figure 80 – Goodman 10HSPF ASHP Steady-state COP	75
Figure 81 – Goodman 10HSPF ASHP Defrost Operation Duration (left) and Cooling Delivered (right).....	75

List of Tables

Table 1 – ccASHP Evaluation: Devices Under Test	17
Table 2 – EHPWH Evaluation: Devices Under Test	20
Table 3 – ASHP and ccASHP Basic Principles	22
Table 4 – Electric and Mechanical Component Matrix of Electric Heat Pumps	26
Table 5 – EHPWH Basic Principles	32
Table 6 – EHPWH Tank Heat Loss Factor and Heating Elements Lower Thermostat Limit	34
Table 7 – Space and Water Heating Equipment System Performance Comparison.....	41
Table 8 – Market Impact Consideration Equipment.....	46
Table 9 – ASHP and ccASHP Evaluation Mechanical Room Instrumentation	54
Table 10 – ASHP and ccASHP Evaluation Outdoor Testing Bay Instrumentation	54
Table 11 – ASHP and ccASHP Evaluation Indoor Instrumentation	55
Table 12 – EHPWH Evaluation Instrumentation List	63
Table 13 – EIA State Electricity Monthly Rates	71
Table 14 – EIA State Natural Gas Monthly Rates.....	71
Table 15 – eGRID Source-energy Factor and GHG Emissions for Natural Gas and Electricity Per City	72

Executive Summary – Comparative Assessment of Space and Water Heating Systems in the Virtual Test Home

Advancements in gas and electric heat pump technology make it possible to achieve source-energy annual space heating efficiencies greater than 100%. However, heat pumps inherently suffer efficiency losses due to ambient temperatures and, like other heating technologies, part-load cycling conditions. This report investigates the detailed performance of electric heat pumps (traditional and cold-climate) to better understand how hybrid gas-electric systems can be implemented to achieve the most efficient, cost-effective and comfortable space heating.

Maximizing efficiency and greenhouse gas (GHG) savings and minimizing operating cost can sometimes be conflicting goals. For example, heat pump operations may be very efficient at times, but very costly to operate depending on electric utility tariffs. Moreover, GHG emission intensities from fuel-fired equipment, including many sources of electricity, must be considered.

Industry projections indicate GHG emission intensities from the electric grid are expected to decrease as market penetration of renewable power generation increases. Projections also indicate the energy cost ratio of electricity to gas may increase due to increasing electricity demands and required infrastructure buildout to support certain beneficial end-use electrification.

GTI’s Virtual Test Home (VTH) methods have demonstrated insightful assessments on HVAC, water heating and power generation equipment. Unlike standard rating-point test methods such as Annual Fuel Utilization Efficiency (AFUE) and Heating Seasonal Performance Factor (HSPF) for space heating equipment, the VTH can be used to evaluate and characterize the performance of complex systems in a wide range of as-installed operating conditions to estimate annual GHG emissions and operating cost via building energy modeling. VTH assessments on cold-climate air-source heat pumps (ccASHPs) and electric-driven heat pump water heaters (EHPWHs) provided an understanding of their coefficient of performance (COP) across multiple climate zones under as-installed conditions (as shown in Figure 1) to better understand how hybrid gas-electric systems can be implemented to achieve the most efficient, cost-effective and comfortable space heating.

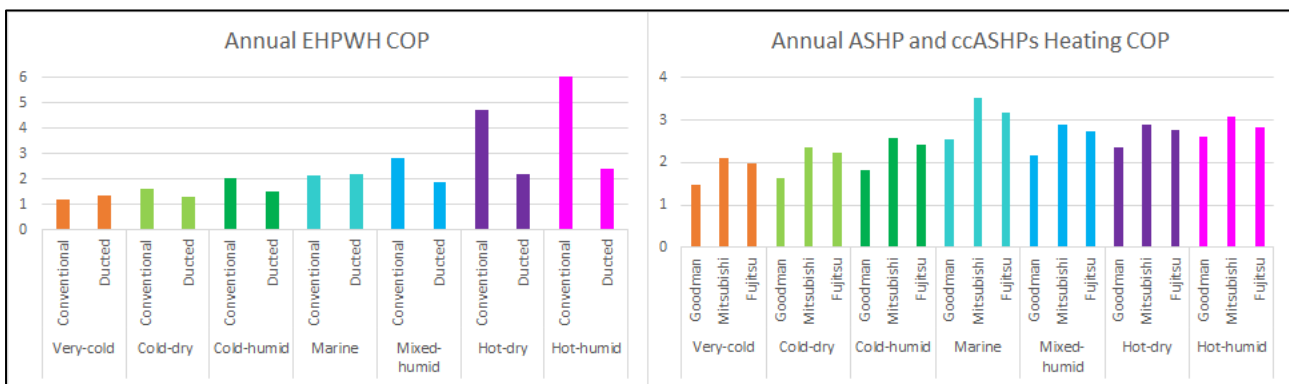


Figure 1 – Annual EHPWH COP (left) and Baseline and Cold-climate ASHP Heating COP (right)

The combination of these two advanced electric-driven HVAC and water heating systems were compared with other combinations of HVAC and water heating systems that have been evaluated in the VTH, as shown in Figure 2. Results from energy modeling indicates ccASHPs in combination with EHPWHs are very competitive with non-heat pump gas-fired systems such as the iFLOW + Navien advanced combination space and water heating (combi) system. However, data collected on emerging

advanced gas-fired combi systems developed and evaluated by GTI show lower source-energy GHG emissions with commercially available gas-fired than electric-driven technologies.

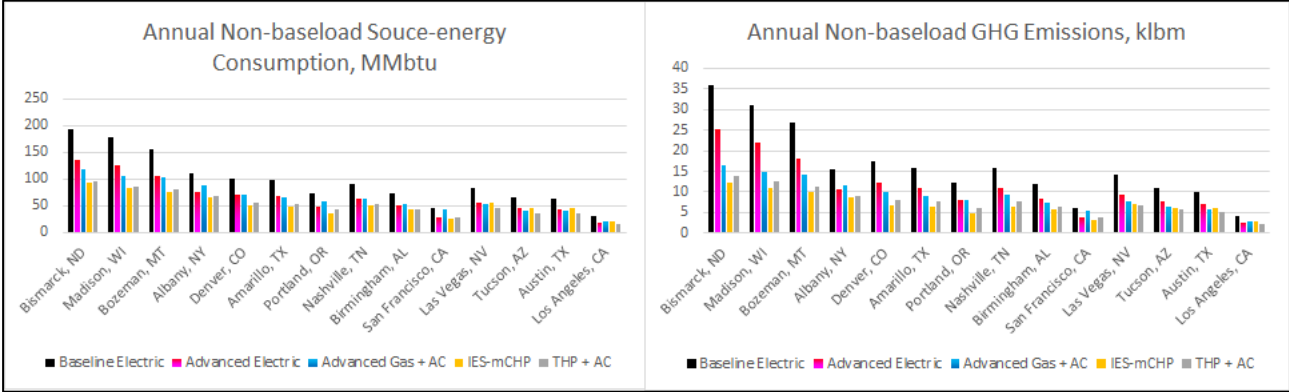


Figure 2 – Annual Non-baseload Source-energy Consumptions (left) and GHG emissions (right) of Five HVAC and Water Heating Systems

Introduction & Background

As the energy industry continues to drive toward net-zero energy (NZE) homes and reducing GHG emissions, new gas-fired, electric-driven, renewable and resilient integrated systems technologies have emerged. For these complex and integrated systems, single rating point descriptors from federal test methods (e.g. AFUE, UEF and HSPF) fail to capture their as-installed performance. As a result, it is difficult to make energy savings assessments on complex systems with space heating/cooling and water heating capabilities.

Background

The VTH experimental approach is a novel testing method developed by GTI. It emerged from the need to better understand equipment performance in various scenarios representative of real-world operation including part-loads and ambient conditions. Field demonstrations often provide inconsistent performance data across sites, resulting in a very costly and time-consuming approach for energy efficiency assessments that sometimes result in inconclusive data. On the other hand, energy accounting (simple gas/electric consumptions), and operating cost and comfort are valuable metrics obtained from field demonstration projects. As a laboratory-based compromise, this VTH approach seeks a comprehensive understanding of component and system performance, focusing on mechanical equipment retrofit measures applied to the field demonstrations. The intent of this holistic approach can be summarized as characterizing performance in a laboratory using a combination of steady-state and transient tests, extrapolating savings through modeling, and later validating performance characterizations and modeled savings in the field as illustrated in Figure 3. Such a holistic approach can provide performance datasets rich in detail that can be used by key stakeholders to assess energy impacts for single- and multi-family building applications.

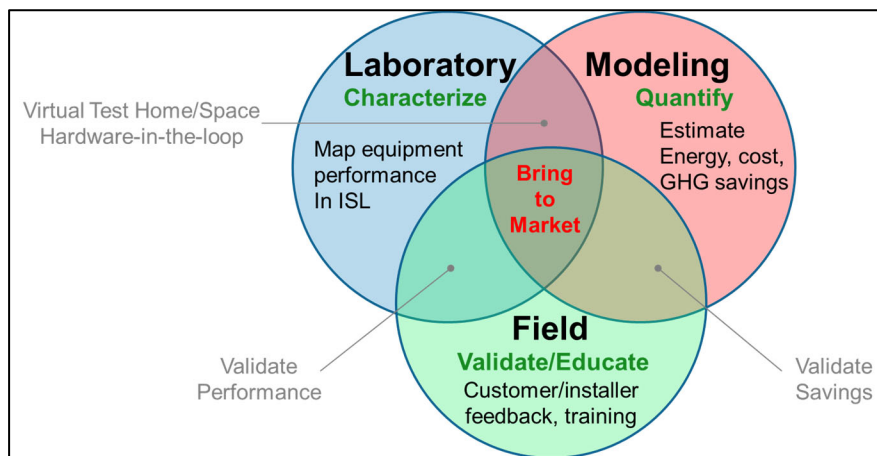


Figure 3 – VTH Approach

The VTH evaluations can serve as a valuable tool to investigate the discrepancies between equipment performance as rated by single-rating point test methods and as-installed performance. For example, Figure 4 shows the gaps between single-rating point test methods and VTH evaluations for annual gas efficiencies across various climates for a single-stage condensing gas furnace. Estimated annual gas efficiencies obtained from ANSI/ASHRAE 103 Method of Test (MOT), generating the AFUE metric for residential furnaces and boilers, is based on combustion efficiency. Similar analyses have been performed in water heating appliances, electrically driven air-source heat pumps (ASHP) and gas-fired combination systems as shown in Figure 5. Unlike Uniform Energy Factor (UEF), HSPF and CSA P.9 – *Test method for determining the performance of combined space and water heating systems (combis)*

MOTs, VTH analyses can provide insightful results to the energy efficiency community as they compare systems in similar operating conditions in different building types, climates, utility costs and GHG emission factor locations as a result of power generation mix.

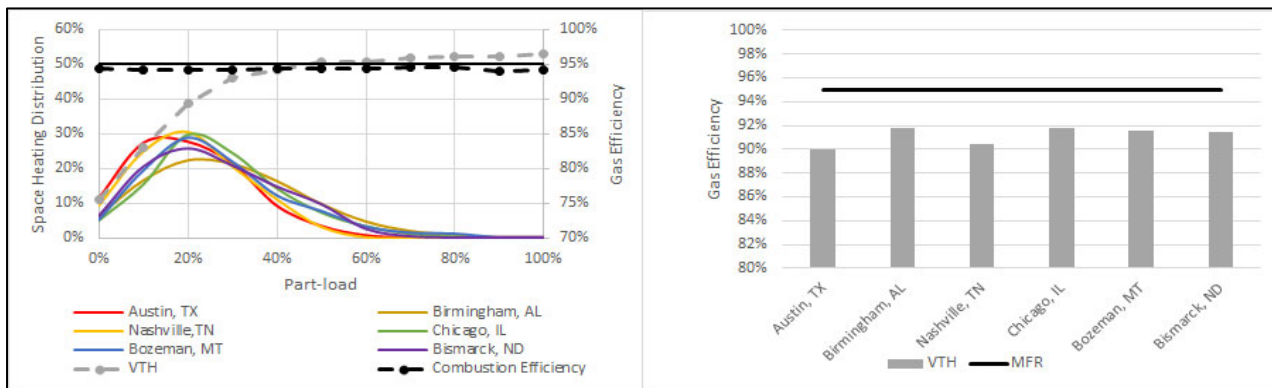


Figure 4 – Condensing Furnace Performance Characterization and Space Heating Distribution (left) and VTH vs Manufacturer (MFR) Annual Gas Efficiencies (right) in Multiple Climate Zones

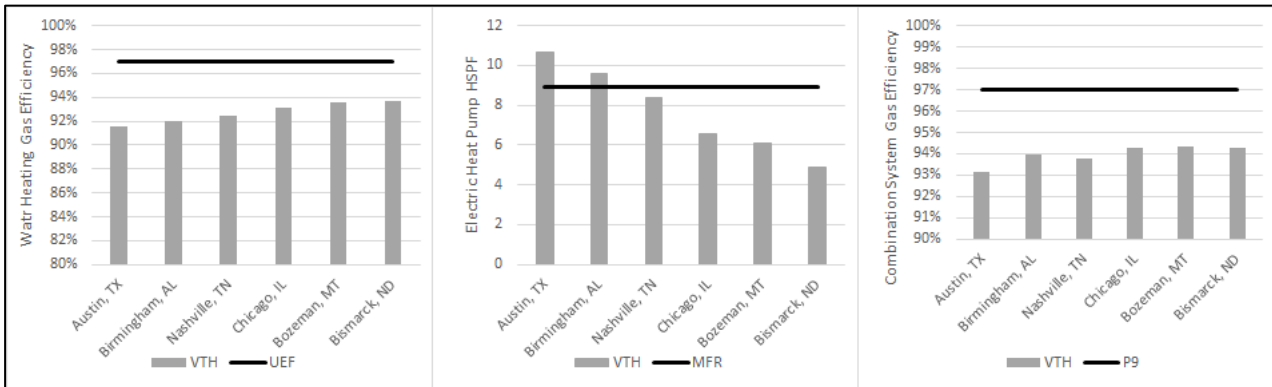


Figure 5 – VTH vs Manufacturer (MFR) Annual Efficiencies for a Condensing Tankless (right), Electric Heat Pump (center) and Gas-fired Combination System (left) in Multiple Climate Zones

End-use Electrification

GHG emissions from the electricity grid are expected to decline as renewable power generation increases. However, it is possible that the energy cost ratio of electricity to gas will continue to increase due to the massive infrastructure and electricity consumption required for the nascent end-use electrification movement. Additionally, residential photovoltaic (PV) market adoption continues to expand and transform residential power strategies. The National Renewable Energy Laboratory (NREL) has documented in the [U.S. Solar Photovoltaic System Cost](#) report the significant decline in both procurement and installation costs for PV. Costs of PV without battery storage declined from greater than \$7/kW to less than \$3/kW within 8 years, as shown in Figure 6. The growth of residential rooftop PV has allowed the U.S. electric industry to envision an aggressive electrification plan. This movement has changed consumers, homebuilders and manufacturers views of home energy and inclination to use advanced electrically driven technologies for heating, cooling and water heating applications. ccASHPs and EHPWHs are the most efficient appliances that are commercially available for the electrification of space and water heating end-use. A VTH assessment of these systems was necessary to compare annual operating cost and GHG emissions relative to advanced gas-fired systems.

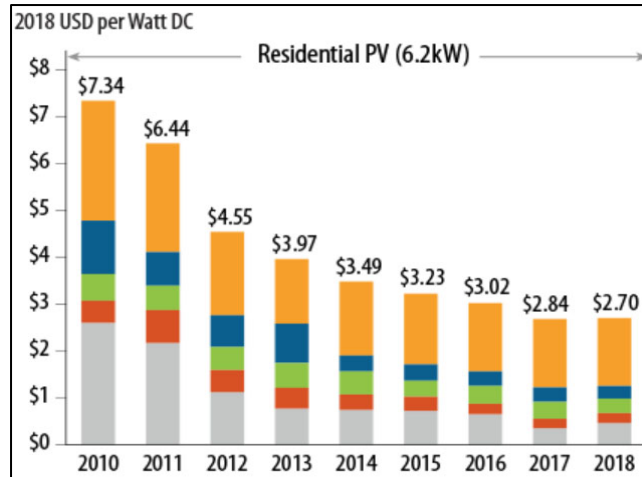


Figure 6 – Residential PV Installed Cost Break Down (Source: NREL)

Objective

GTI has characterized a 10 HSPF ASHP and compared it to gas-fired combi systems in UTD Report 1.16.E: *Low Capacity Heating Systems Portfolio – Phase 2*. The objective of this project was to compare gas/ liquefied petroleum gas (LPG) space and water heating against electric heat pump space and water heating technologies on a level basis by characterizing equipment part-load performances in GTI’s VTH and using those characterizations in modeling software. Tangible goals included:

- Characterizing at least two cold-climate and one baseline air-source electric heat pump systems for space heating in the VTH. Gas space heating including furnaces and combis have already been characterized in other UTD projects. LPG space heating is inferred from natural gas research given similarities in fuel performance.
- Characterizing at least two electric heat pump water heaters in the VTH. Gas space heating including furnaces and combis have already been characterized in other UTD projects. LPG space heating is inferred from natural gas research given similarities in fuel performance.
- Implementing the characterizations in EnergyPlus building energy modeling software to quantify relative annual space and water heating energy consumptions and GHG emissions in 14 states across five climate zones.

General Methodologies

VTH Evaluation

Advanced Gas-fired Systems

As shown in Figure 7, the VTH research sponsored by UTD (1.17.E) and NEEA provided performance characterizations for, among others a Rheem single-stage furnace, Dettson modulating furnace and iFLOW + Navien combi system. These gas forced-air space heating systems were all rated at about 60 MBH capacity, and they tested best-in-class in the VTH. Details for VTH test methods used to evaluate these systems are provided in Appendix A – VTH Evaluation Methods.

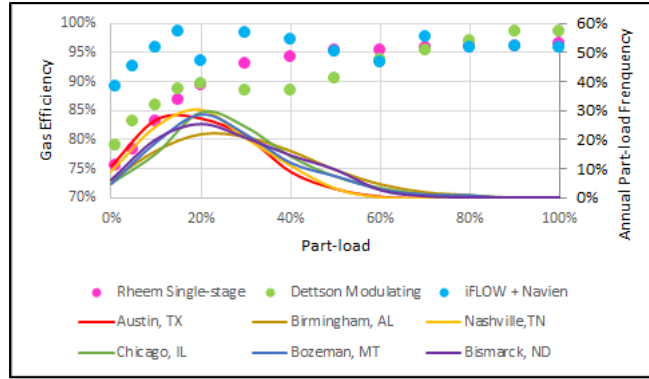


Figure 7 – Advanced Gas-fired Space Heating Systems VTH Characterizations

GTI has focused gas space heating VTH research on gaining an understanding of exactly why furnace and combi system performance suffers in part-load conditions, and more importantly, what can be done to improve low-load performance, including hybrid gas/electric solutions. GTI believes forced-air combis using condensing tankless water heaters offer a unique opportunity to improve gas space heating performance at very low loads by controlling water and air flows, and temperatures to modulate capacity. Figure 8 shows tankless and tank efficiencies presented in tandem with part-load frequencies at which the space heating systems would operate in several IECC climate zones in a 1,600-sqft IECC 2009 home. This figure illustrates why it is so important for these space heating systems to be able to operate efficiently at loads less than 50% of full capacity.

Similar to space heating systems VTH characterizations, gas-fired water heating technologies have been evaluated in VTH research sponsored by UTD (1.17.E), NEEA and CEC. Figure 8 shows gas efficiency curves for water heating technologies as a function of daily water heating loads. The daily domestic hot water (DHW) load frequency curves for a three-bedroom occupancy home in various IECC climate locations are shown in Figure 8. These frequency curves demonstrate why water heating technologies perform differently based on average daily DHW loads in different climate zones. Figure 8 also illustrates the need for these systems to operate at greater efficiencies for daily DHW loads between 5 MBTU to 20 MBTU, which correspond to about 9 to 36 gallons of hot water per day heated from 58°F to 125°F. Details for VTH test methods used to evaluate these systems are also provided in Appendix A – VTH Evaluation Methods

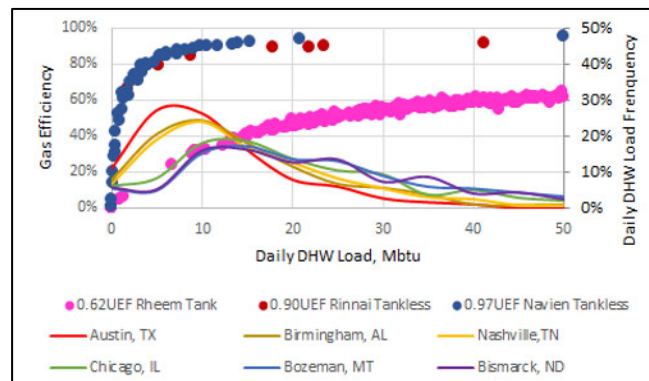


Figure 8 – Gas-fired Water Heating Systems VTH Characterizations

Electric Air-source Heat Pump Technologies

Unlike gas-fired systems, electric heat pump technology operation is defined by:

- Heating capacity as a function of entering air wet-bulb temperature and condenser fluid dry-bulb temperature
- Compressor electric input as a function of condenser fluid dry-bulb temperature
- Standby power consumption and thermal losses
- Defrost controls

Air-source Heat Pump

Figure 9 summarizes the VTH research sponsored by UTD (1.16.E) on an 18 SEER/10 HSPF two-stage ASHP. The system daily COP is shown as a function of daily outdoor air dry-bulb temperature (OATdb), which includes the impact of standby power consumption, defrost cycles, part-load degradation and auxiliary heating. Here again, details for VTH test methods used to evaluate these systems are provided in Appendix A – VTH Evaluation Methods

Figure 9 shows the performance of this system sized per ACCA Manuals J and S in the Region IV/Humid referenced in ANSI/AHRI 210/240: *Performance Rating of Unitary Air-conditioning & Air-source Heat Pump Equipment* for HSPF rating calculations. The VTH performance of this ASHP significantly deviates with manufacturer steady-state COP data due to the impact of auxiliary heating, defrost cycles, part-load degradation and standby-power consumption.

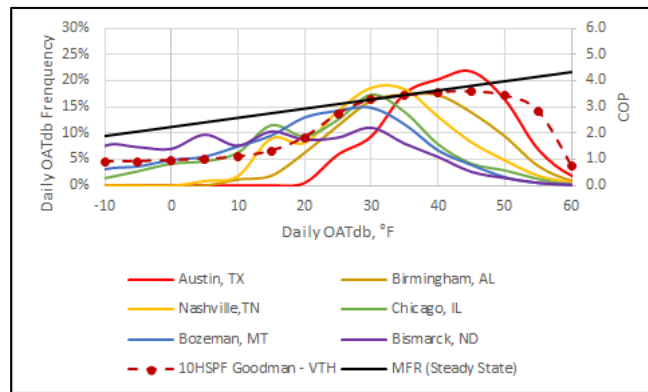


Figure 9 – 10 HSPF ASHP VTH Characterization

Additionally, the daily OATdb frequency curves for different IECC climate zones are shown in Figure 9. These frequency curves are useful to understand the impacts on HSPF calculations due to various ambient conditions such as those that might be seen in various IECC climate zones. For IECC climates 5, 6 and 7 (Chicago, IL, Bozeman, MT and Bismarck, ND), this ASHP operates with significant auxiliary heating elements for at least 40% of the heating season as shown in Figure 10. For these cold climates, ccASHPs are preferred over ASHPs since they can maintain heating capacity down to OATdb of 5°F.

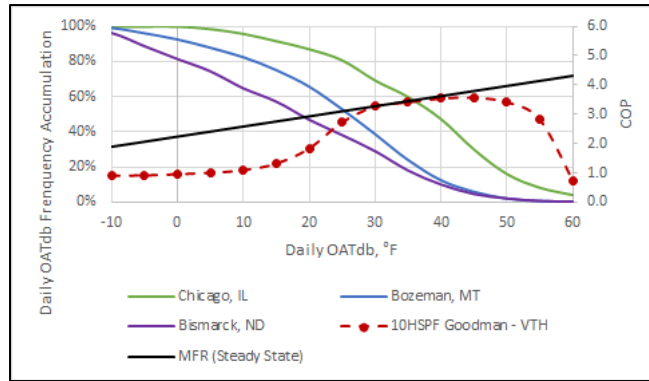


Figure 10 – 10 HSPF EHP VTH Characterization in IECC Climate Zones 5, 6 and 7

Cold-climate Air-source Heat Pumps

Two ccASHPs and one baseline ASHP as listed in Table 1 were evaluated using the hybrid VTH/field demonstration approach mentioned in the UTD Report for 1.18.D, 1.18.G, 2.18.G: *Integrating Micro-CHP & PV; Gas Heating & Cooling; Thermal Energy Storage; and in Advanced Gas/Renewable Homes*. These electric heat pump systems were operated in actual outdoor air temperature and humidity conditions and compressor speeds for 4 months. Each heat pump required communicating thermostats for operation. Therefore, they were installed with their corresponding thermostats, as shown in Figure 11, and were configured to respond to heat calls for the entire test period. The thermostats were driven by the heating loads in a GTI laboratory space. A roof top unit (RTU) was used for auxiliary heating. Figure 12 shows a simple P&ID illustration implemented for the hybrid VTH/field demonstration evaluation. Detailed instrumentation and data collection methods are provided in Appendix C – ASHP and ccASHP Evaluation Test Plan.

Table 1 – ccASHP Evaluation: Devices Under Test

Brand		Goodman	Mitsubishi	Fujitsu
Model Number	Indoor Unit	ARUF37C14	PUZ-A36AA7	ARU18RLF x 2
	Outdoor Unit	GSZ140361K	PUZ-HA36NHA5	AOU36RLXFZH
Cooling @ 95°F OATdb	Capacity MBH	Max	N/A	36.0
		Rated	35.2	33.0
		Min	N/A	18.0
	Rated Input Power, kW	3.04	2.6	2.9
SEER		15.0	17.8	18.0
Heating @ 47°F OATdb	Capacity MBH	Max	N/A	40.0
		Rated	32.8	38.0
		Min	N/A	18.0

Rated Input Power, kW	2.63	3.0	2.7
HSPF	9.0	11.0	9.3
NEEP Certified	No	Yes	Yes

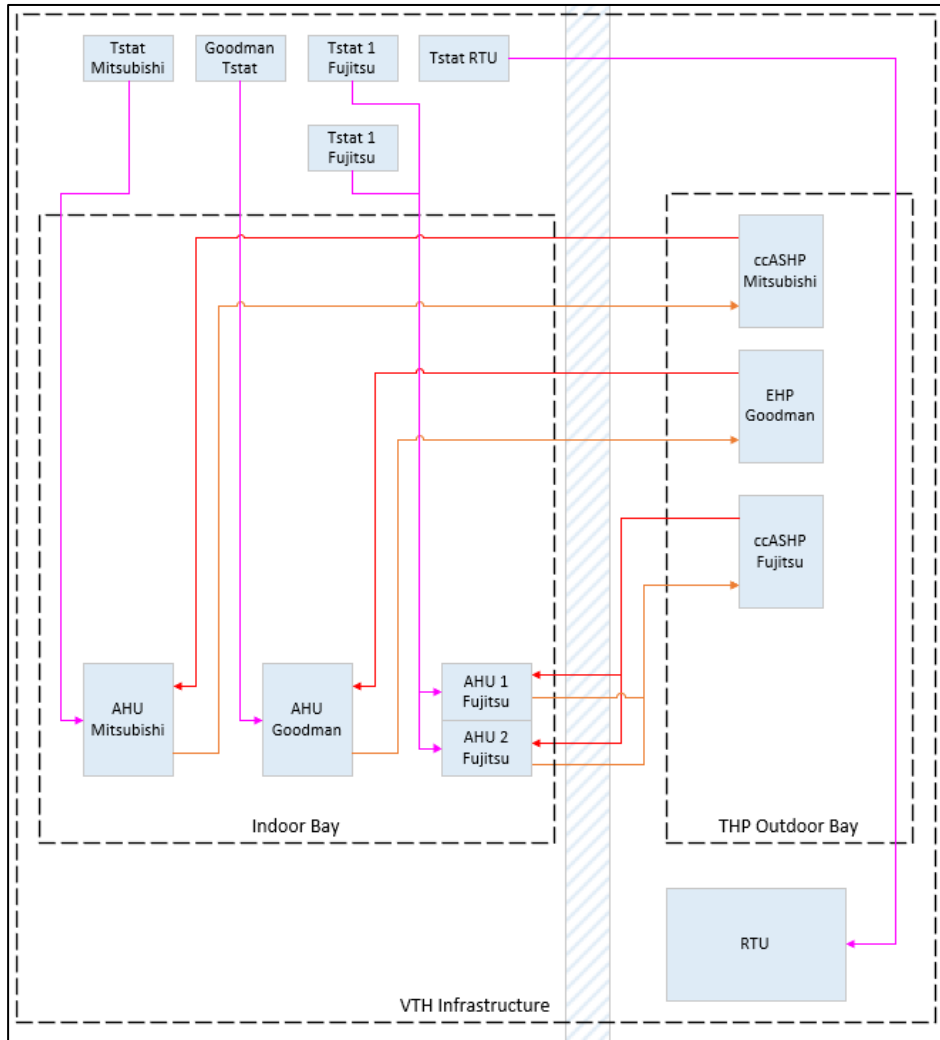


Figure 11 – Hybrid VTH/Field Demonstration Evaluation Approach

The simplified P&ID for hybrid VTH/Field Demonstration evaluation is shown in Figure 12. The energy delivered to the air was measured by a thermocouple array (TCA) and relative humidity transmitter (RHT) in both supply and return ductwork. A pitot traverse airflow station attached to the low-pressure transmitter shown as FT in Figure 12 was used to measure the air handler unit (AHU) airflow. A TCA and RHT were installed on the return grill of the outdoor unit to measure the outdoor air entering temperature and relative humidity. Two power meters shown as JT in Figure 12, were used to measure the system total and air handler power consumption.

The electric heat pump system’s period of operation was from February 2020 to April 2020, providing enough data points to build performance curves for these systems that included operation in -5°F to 70°F OATdb. Detailed information regarding the instrumentation and test plan can be found in Appendix C – ASHP and ccASHP Evaluation Test Plan.

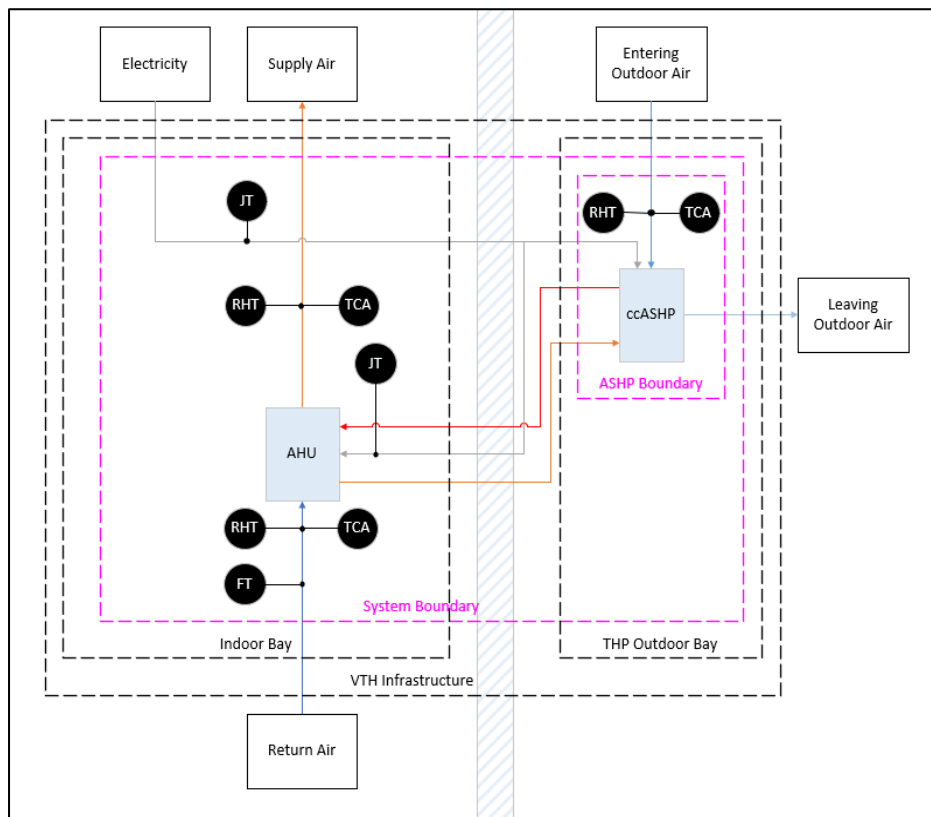


Figure 12 – Simplified ccASHP P&ID

Laboratory infrastructure was developed to evaluate three of these systems in the VTH/field approach. The installations of the indoor and outdoor units are shown on the left and right sides of Figure 13, respectively. General qualifications for the three AHUs evaluated as integral parts of the ccASHP systems shown on the left side of Figure 13 were:

- Capable for space heating and cooling assessment
- Airflow range up to 2000 cfm / 5 tons
- Modulating return air condition capabilities



Figure 13 – Indoor (left) and Outdoor (right) ASHP Component Installations

Heat Pump Water Heaters

Two heat pump water heaters (EHPWHs) listed in Table 2 were evaluated using the VTH approach. Similar to ASHP evaluations, EHPWH VTH evaluation consisted of characterizing:

- Heating capacity as a function of entering air wet-bulb temperature and average tank water dry-bulb temperature
- Compressor electric input as a function of condenser average tank water dry-bulb temperature
- Standby power consumption and thermal losses

The simplified P&ID to evaluate EHPWHs is shown in Figure 14. A detailed test plan for the evaluation of these systems can be found in Appendix D – EHPWH Evaluation Test Plan.

Due to limited access to the laboratory during the beginning of the COVID-19 pandemic, an alternative approach was used by GTI to achieve the goals associated with this project. Third-party published data from controlled environment evaluation procedures were used to develop performance mapping equations for these two EHPWHs. In the NREL’s [Laboratory Performance Evaluation of Residential Integrated Heat Pump Water Heaters](#) report, similar EHPWHs scoped by GTI were evaluated. In this report, detailed data and operating strategies of these systems were described. This allowed GTI to build the performance curves required for VTH evaluation.

Table 2 – EHPWH Evaluation: Devices Under Test

	Brand	AO Smith	Rheem
Model Number	Indoor Unit	PROPH50 T2 RH350 DCB	FPTU-80-130
Compressor Capacity, MBH		4.2	Not Listed
Upper Heating Element Capacity, kW		2	4.5
Lower Heating Element Capacity, kW		2	4.5

Tank Size, Gal	45	82
UEF	3.55	3.45

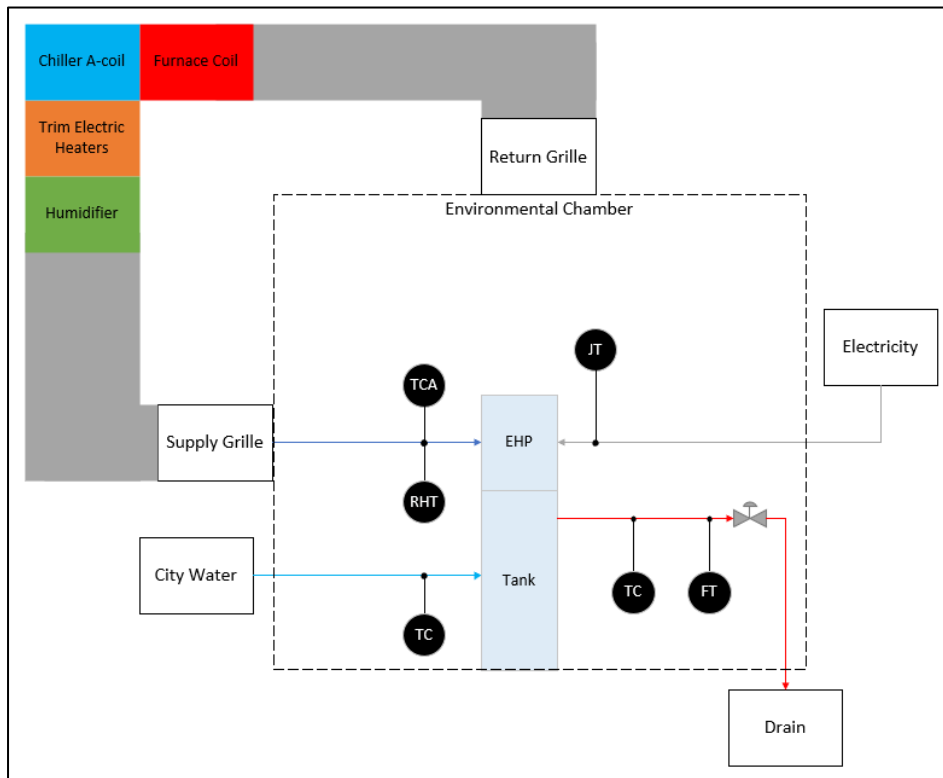


Figure 14 – EHPWH Simplified P&ID

Building Energy Modeling

EnergyPlus™ is the DOE’s flagship whole building energy simulation engine that permits the simultaneous simulation of a whole building’s energy consumption and its interaction with the surrounding environment. It is used by itself or on the back-end of other building energy modeling software such as BEopt. Its popularity has grown within the energy efficiency community and is commonly used by decision makers considering the best HVAC options for buildings, and in policy development.

Prior to GTI’s work in the VTH research sponsored by UTD (projects 1.16.H and 1.16.E), NEEA and CEC, developing advanced functions in EnergyPlus for furnaces, combi systems and electric heat pumps, were limited in the ability to compare state of the art gas and electric appliances. The software inputs were conducive to single-rating point entries for appliances and could not accurately capture part-load performance and the effects of improper equipment sizing.

Using data sets collected from the VTH evaluation of the baseline ASHP, ccASHPs and EHPWHs, space and water heating part-load performance characterizations were developed and implemented in EnergyPlus to estimate annual efficiencies and quantify annual metrics in various climate zones. Previous UTD projects developed performance characterizations and EnergyPlus modeling tools for

comparative fuel-fired equipment including furnaces and water heaters. For this project, building energy modeling was based on a 1,600 sq-ft residential model assuming 3 bedrooms, 2.5 bathrooms, 3 occupants, and 70°F winter and 75°F summer thermostat settings. The model was built to 2010 Building America Reference Home standards, which incorporated 2009 IECC building code measures. Performance characterizations for the 36 MBH ASHP was scaled proportionally to meet the loads for the 1,600 sq-ft model in the various climates.

Field Validation

GTI’s VTH methods were developed as an alternative to lengthy and costly field tests. Field demonstrations are sometimes plagued by data inconsistencies across long periods due to measurement difficulties, weather anomalies, and occupancy behaviors among other variables. Moreover, without a second lengthy and costly baseline field test, comparisons between baseline and new equipment performance must be done through utility billing analyses. Utility billing analyses have separate but significant data assessment challenges including those related to gas usage and weather correlation and gas usage disaggregation. However, field tests have provided valuable data for short-term performance of equipment. Data from various field tests conducted by GTI and other research organizations were used to validate the equipment performance characterizations GTI developed in the VTH.

ccASHP Space Heating Performance Characterizations

Background

Before assessing space heating performance of the three electric-driven air-source heat pumps evaluated in this project, it is important to understand the differences between ASHP and ccASHP systems. Table 3 summarizes the comparison between the two with respect to heating operation, defrost cycles, sizing and manufacturer rating.

Table 3 – ASHP and ccASHP Basic Principles

Parameter	ASHP	ccASHP
Heating Operation	With a single-speed compressor, the ASHP cycles based on heating calls.	Compressors modulate speed based on heating loads
Defrost Cycles	Time-accumulated activation defrost strategy is implemented for OATdb less than 40°F. During a defrost cycle, cold air is delivered to the space.	Defrost cycles are activated based on frost accumulation in the outdoor coil sensed by an instrument. Its duration depends on the ambient conditions. During the defrost cycles, no cold air is delivered to the space.
Heating Sizing	Heating capacity is selected based on ACCA Manual S	Heating capacity is selected to meet a balance point between

	summarized in Strategy Guideline: HVAC Equipment Sizing . Outdoor air temperature heating capacity curves are used for determining balance points and auxiliary heating equipment	5°F and 20°F OATdb. Auxiliary heating is sized for the supplemental heating required. Such practices follow Guide to Sizing and Selecting Air-Source Heat Pumps in Cold Climates developed by the Northeast Energy Efficiency Partnerships (NEEP).
Manufacturer Heating Capacity Rating	Heating capacity is specified by the manufacturer at 47°F OATdb	Heating capacity is specified by the manufacturer at a wide range (-5°F to 47°F OATdb)

Space Heating Capacity Characterization

The heating capacity of a system is determined by the compressor speed, return air temperature (RATdb) and wet-bulb outdoor air temperature (OATwb). The difference between RATdb and OATwb dictates the ability for an ASHP system to transfer heat indoors from outside humid air. Similar to air conditioning systems, ASHP system capacities increase with high moisture content in the air at the evaporator coil. Likewise, heat pump and air conditioner system capacities are limited by higher temperatures at the condenser coil. Figure 15 shows the heating capacity of the Goodman single-stage ASHP evaluated under this project. Despite being a single-stage compressor, small adjustments in compressor speed were observed due to changes in the RATdb at the AHU system.

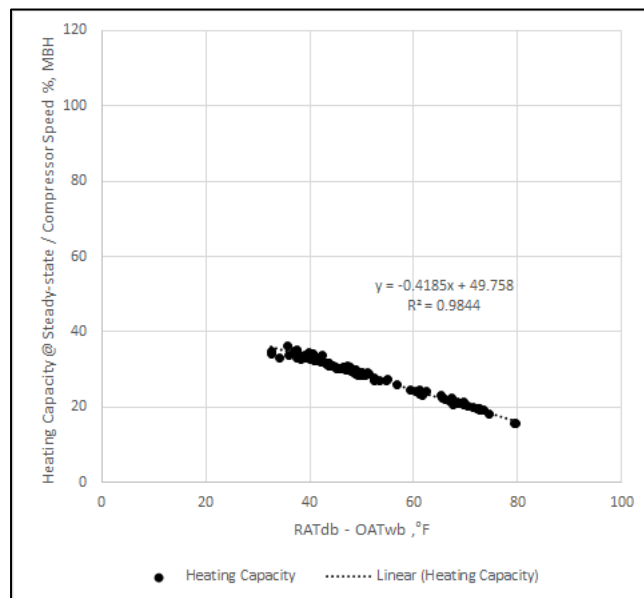


Figure 15 – Goodman ASHP Steady-state Heating Capacity Characterization

Figure 16 shows the heating capacity characterizations for the Mitsubishi (left) and Fujitsu (right) ccASHPS. Despite the large compressor speed range, ccASHP steady-state heating capacity can be characterized in a linear fashion at multiple compressor speed ranges.

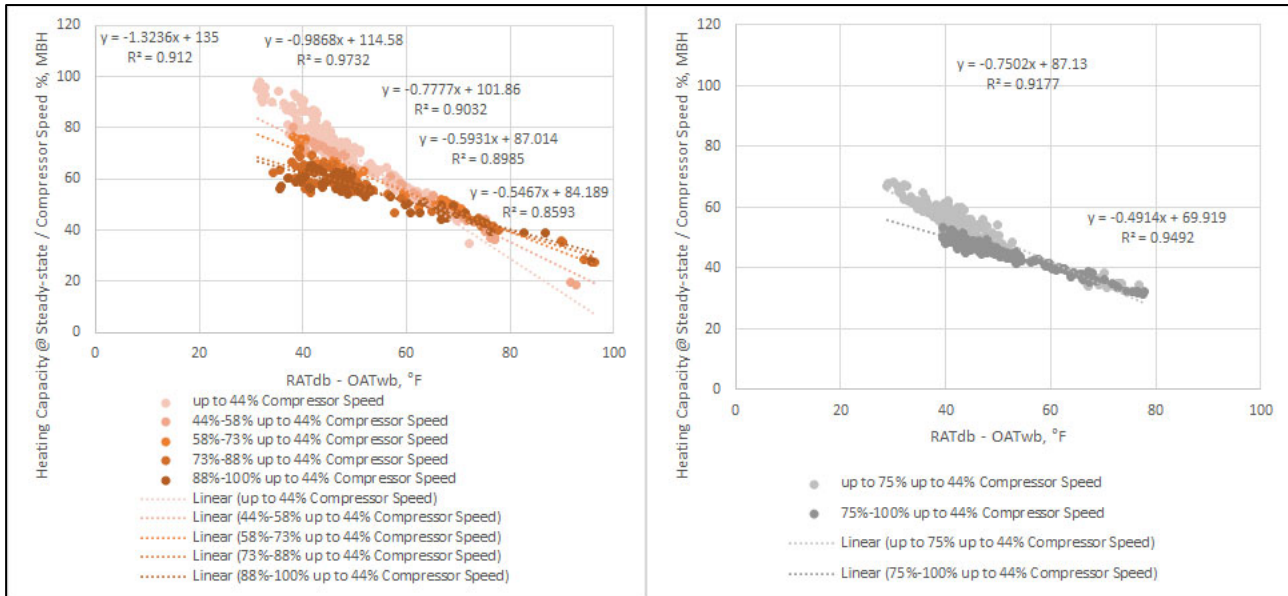


Figure 16 – Mitsubishi (left) and Fujitsu (right) ccASHP Steady-state Heating Capacity Characterizations

Coefficient of Performance Characterization

Similar to ASHPs and ccASHP heating capacities, the COP of these systems are affected by the difference between RATdb and OATwb. Figure 17 shows the Goodman ASHP steady-state COP characterization. The Mitsubishi and Fujitsu ccASHPs steady-state COP characterizations are shown in Figure 18. Similar characterization strategies implemented for heating capacity performance curves were used for ASHP and ccASHPs COP performance curves.

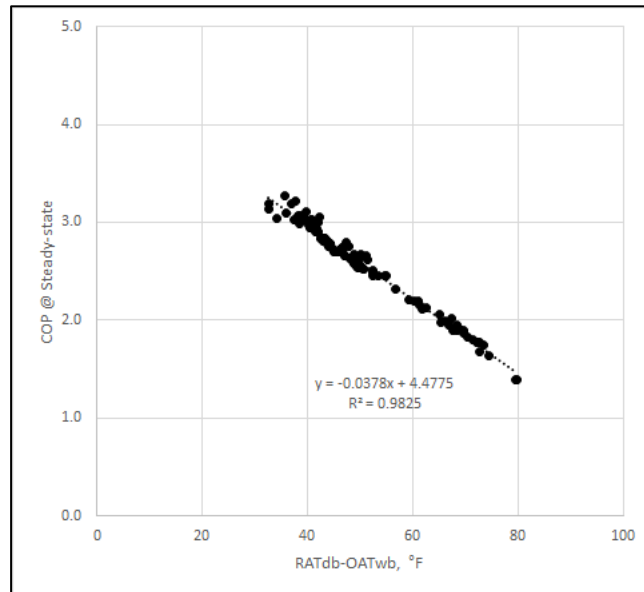


Figure 17 – Goodman ASHP Steady-state COP Characterization

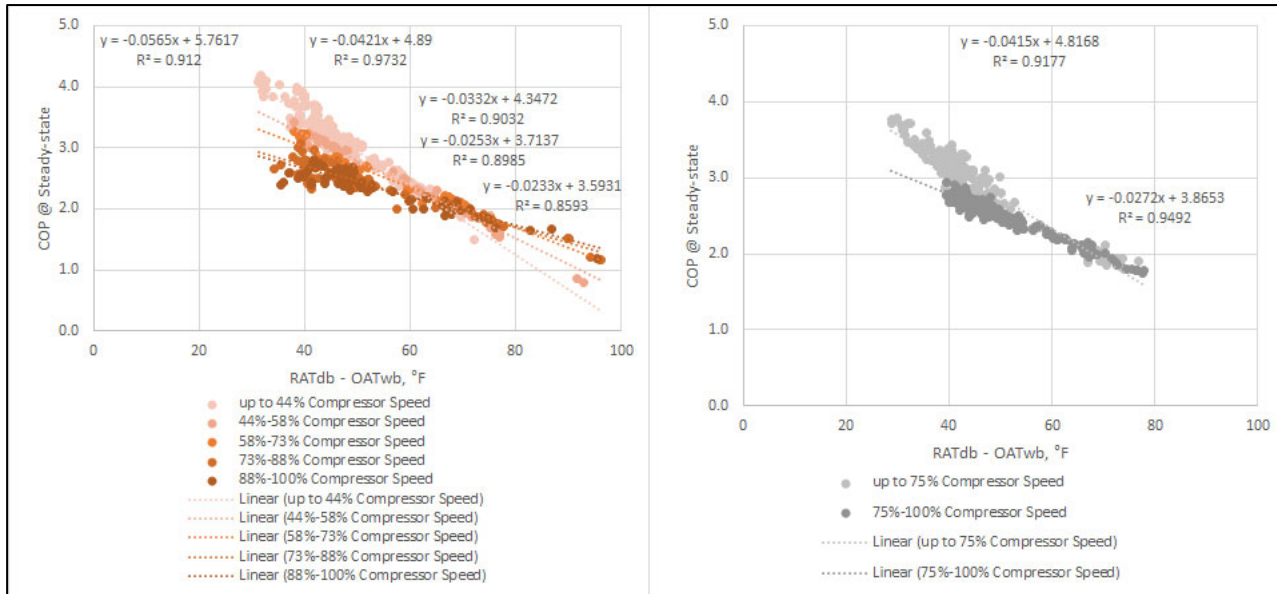


Figure 18 – Mitsubishi (left) and Fujitsu (right) ccASHP Steady-state COP Characterizations

Additional Operation Characterizations

Defrost, part-load degradation and standby power consumption were characterized for these systems. The most influential of these operating characteristics was the standby power consumption that affects system performance when cycling. Defrost operation and part-load degradation characterizations can be found in Appendix E – ASHP and ccASHP Additional Characterizations. The standby power consumption of the systems is shown in Figure 19. These standby power draws were observed to be constant across the monitoring period. All ASHP systems have a low-wattage crankcase heater, which is utilized to ensure adequate mixing of the refrigerant and compressor oil prior to circulation. This operation is required to prevent compressor damage. ccASHPs have additional mechanical and electrical components, such as pan heaters and DC inverter cards. Pan heaters are used for preventing ice formation below the outdoor units and operate most of the time at OATdb less than 32°F. DC inverter cards are implemented to modulate compressor speeds. Table 4 shows the main differences between electrical and mechanical components of these three systems. Similar components for the two ccAHPs might be responsible for the significant power consumption during standby periods. These power consumption rates were observed during OATdb between 5°F and 90°F.

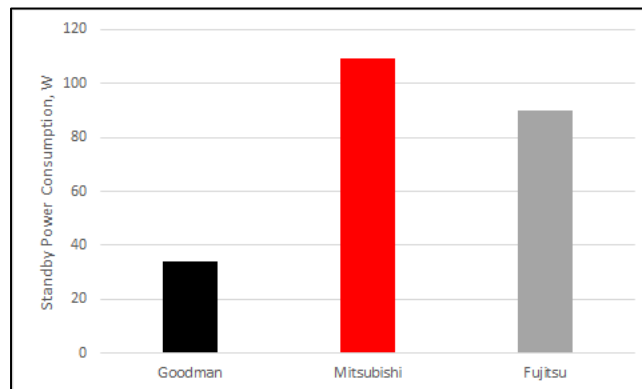


Figure 19 – Standby Power Consumption of the Electric Heat Pump Systems

Table 4 – Electric and Mechanical Component Matrix of Electric Heat Pumps

Outdoor Unit Component	Type	Goodman ASHP	Mitsubishi ccASHP	Fujitsu ccASHP
Crankcase Heater	Electrical	•	?	•
Pan Heater	Electrical		?	•
Reactor Coil	Electrical		•	•
DC Inverter Card	Electrical		•	•
Accumulator	Mechanical		•	•
Heat Inter-change Circuit	Mechanical		•	

ASHP and ccASHP Performance Comparison

Before evaluating and characterizing the performance of the baseline ASHP and two ccASHPs, it is important to establish reference outdoor operating conditions and the expected sizing strategy. HSPF ratings established by the ANSI/AHRI 210/240 Standard: *Performance Rating of Unitary Air-Conditioning and Air-Source Heat Pump Equipment* are used to differentiate ASHP systems. These HSPF ratings are based on the heating operation associated with Region IV defined by ANSI/AHI 210/240, shown in Figure 20. The outdoor conditions of Region IV were used in this section to evaluate the performance of the baseline ASHP relative to the two ccASHPs.

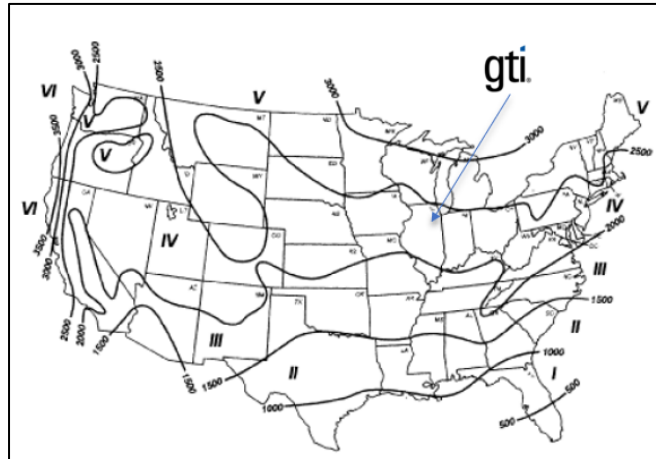


Figure 20 – ANSI/AHRI 210/240 Heating Regions

ASHPs and ccASHPs are sized differently as previously presented in Table 3. Figure 21 shows the expected heating output of the baseline ASHP and the two ccASHPs evaluated in the VTH reference model home (presented in the Building Energy Modeling section) located in Region IV with humid air conditions. The primary observations were:

- With a peak heating capacity of 27 MBH, the baseline ASHP was sized for 36 MBH while the two ccASHPs were sized for 24 MBH. Therefore, the ASHP balance point is at 15°F OATdb requiring significant auxiliary heating down to -5°F OATdb. On the other hand, the ccASHPs balance point is at 5°F OATdb requiring less than half of the auxiliary heating needed for the baseline ASHP scenario.
- The two ccASHPs modulation range starts at 40°F OATdb eliminating cycling penalties associated with part-load degradation while the ASHP cycles most of the heating season.

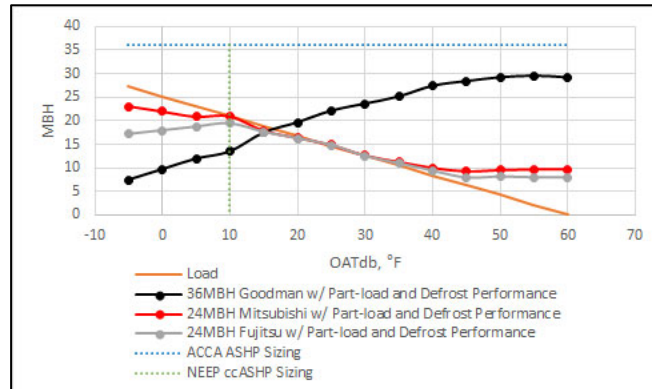


Figure 21 – ASHP and ccASHP Sizing in Modeling Home Located in Region IV with Humid Air Conditions

Figure 22 shows the daily COP for these three systems as implemented in the model home and located in the ASHRAE Region IV with humid air conditions. These daily COP model calculations account for part-load degradation, standby power consumption and defrost cycles. The primary observations were:

- As can be seen in Figure 21, the ccASHPs start modulating at 40°F OATdb. As can be seen in Figure 22 at temperatures above 40°F OATdb, the ccASHPs reached their maximum steady-state COP at 45°F to 50°F OATdb, but were significantly impacted by part-load degradation and standby power consumption as temperatures rose above about 50°F OATdb.
- As can be seen in Figure 22, the traditional ASHP had significantly lower COPs than for the ccASHPs as cycling occurred during most of the heating season OATdb range. The traditional ASHP reached maximum COPs of 2.0 to 2.5 between 30°F to 50°F.
- At OATdb's lower than 20°F, the ASHP and ccASHPs daily COPs dropped consistently to about 1.0 to 1.5. The gap in daily COP between the ASHP and the two ccASHPs is associated with less efficient defrost operation implemented in the conventional ASHPs as previously described in Table 3.
- Figure 22 also shows the daily modeled heating distribution for the model home heating season in the humid Region IV. This heating distribution curve shows that these systems would operate most of time from 25°F to 40°F OATdb during the heating season.

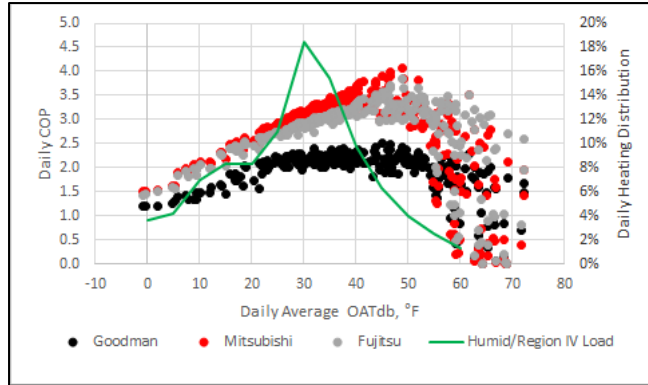


Figure 22 – ASHP and ccASHPs Daily COP in the Humid/Region IV

Figure 23 and Figure 24 show COP waterfall charts for the Goodman baseline ASHP and Mitsubishi ccASHP at three different OATdbs. These COP waterfall charts show how steady state COP is reduced due to part-load degradation (PLD), standby power consumption, defrost operation and auxiliary heating. The primary observations were:

- At 0°F OATdb, the Goodman and Mitsubishi ASHPs have the same steady-state COP. However, due to inefficient defrost operation and lower heating capacity output, the Goodman ASHP system COP is greatly reduced from about 1.8 to 1.2. On the other hand, the Mitsubishi system COP was only slightly impacted and reduced to just 1.6 due to smart defrost operation and lower auxiliary heating operation.
- At 20°F OATdb, the Mitsubishi ccASHP steady state COP was slightly greater than the Goodman baseline ASHP COP. The Mitsubishi ccASHP COP was only affected slightly by defrost operation at this OATdb. On the other hand, the Goodman ASHP COP was significantly affected by part-load degradation, defrost and auxiliary heating.
- At 50°F OATdb, the Mitsubishi ccASHP steady state COP was greater than the Goodman baseline ASHP COP. Both systems at this temperature were affected by part-load degradation and standby power consumption.

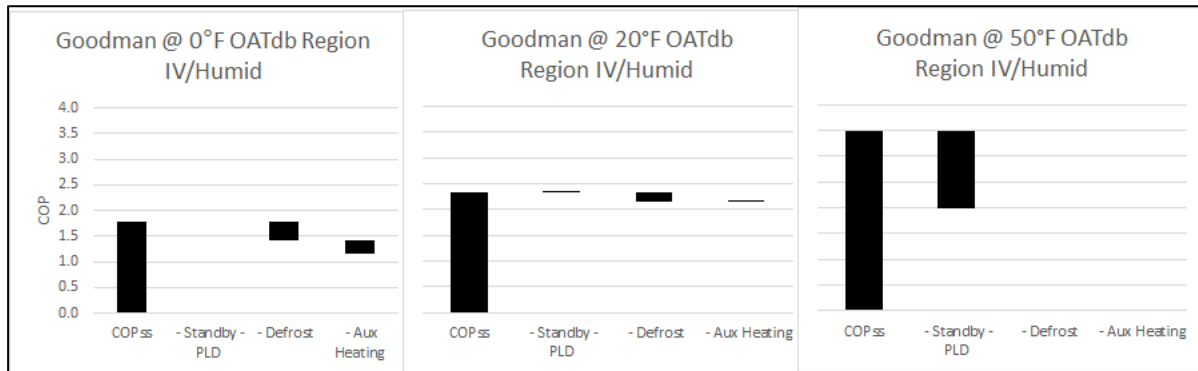


Figure 23 – Goodman Baseline ASHP COP Waterfall Chart at 0°F (left), 20°F (center), and 50°F (right)

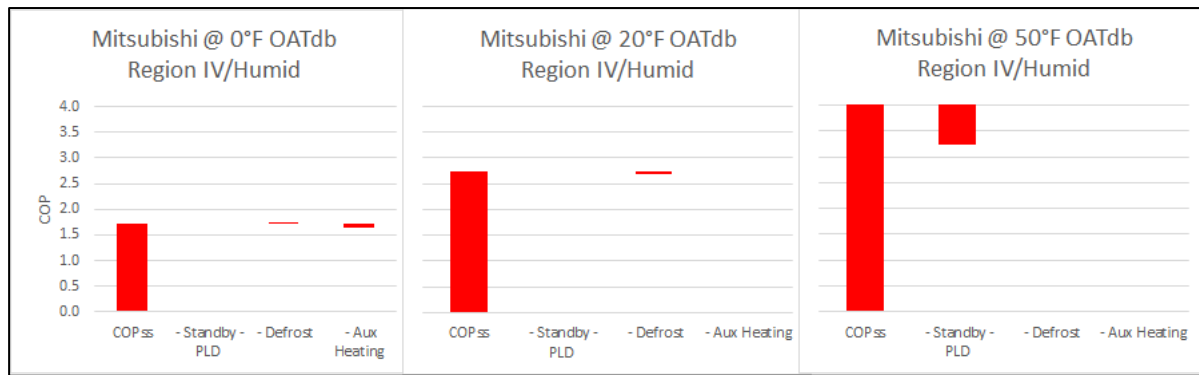


Figure 24 – Mitsubishi ccASHP COP Waterfall Chart at 0°F (left), 20°F (center), and 50°F (right)

Figure 25 shows the annual heating performance of the baseline ASHP and ccASHPs in all CSA EXP 07 – *Dynamic ASHP Test Procedure* climate zones with the corresponding heat load distribution per zone as a function of OATdb. The following observations were made:

- Both ccASHP systems are predicted to have significantly better annual COPs than the traditional ASHP.
- Both ccASHP systems are predicted to perform similarly in all climate zones with research data indicating a COP difference of about ± 0.25
- Modeling results suggested the Mitsubishi central ccASHP can perform at higher COPs in most of the CSA EXP 07 climates zones in comparison to the Fujitsu mini-split system.
- These systems would likely perform better in humid regions in comparison to dry regions due to the heating capacity boost associated with humidity in the heat transfer process.
- These systems would likely perform best in Marine climates due to the following:
 - high moisture content in the air
 - heating operation is often within 20°F to 60°F OATdbs
 - heat pump sizing is based on heating loads as opposed to cooling loads.
 - Despite having a similar heat load distribution range to the Marine region, the ASHP systems operates at lower COP in both hot-dry and -humid regions. The ASHP sizing in these hot regions are based on cooling loads. Therefore, the system is over-sized for heating and short cycles more frequently, creating greater standby losses.

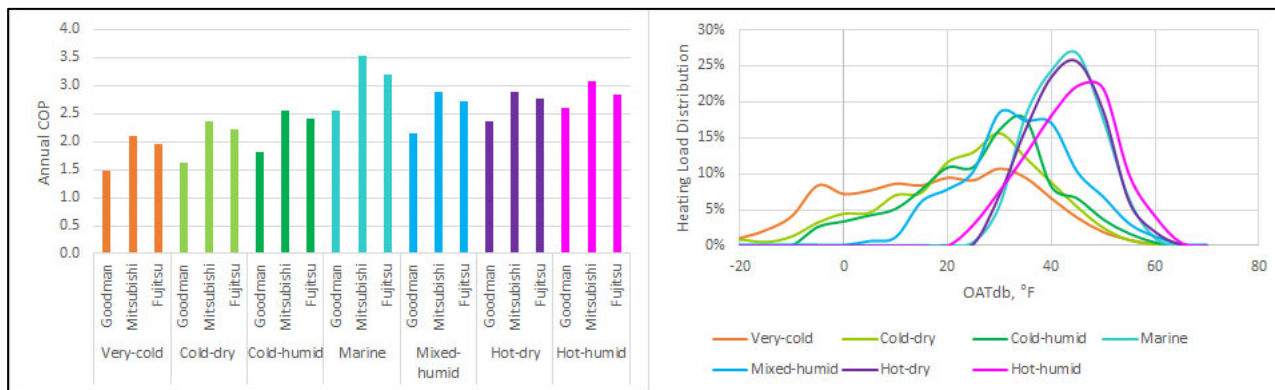


Figure 25 – ASHP and ccASHPs Annual Heating COPs in all CSA EXP 07 Climate Zones (left) and Heating Load Distribution as a Function of OATdb (right)

Validation

The performance characterization of the baseline ASHP and two ccASHPs were validated with manufacturer specifications and field demonstration data.

Manufacturer Specifications

The steady state heating capacities and COP at multiple OATdb were validated with manufacturer specifications. Figure 26 shows the comparison between manufacturers and VTH data for the steady-state heating capacity and COP as a function of OATdb. This plot demonstrates a strong correlation with expected performance of this equipment.

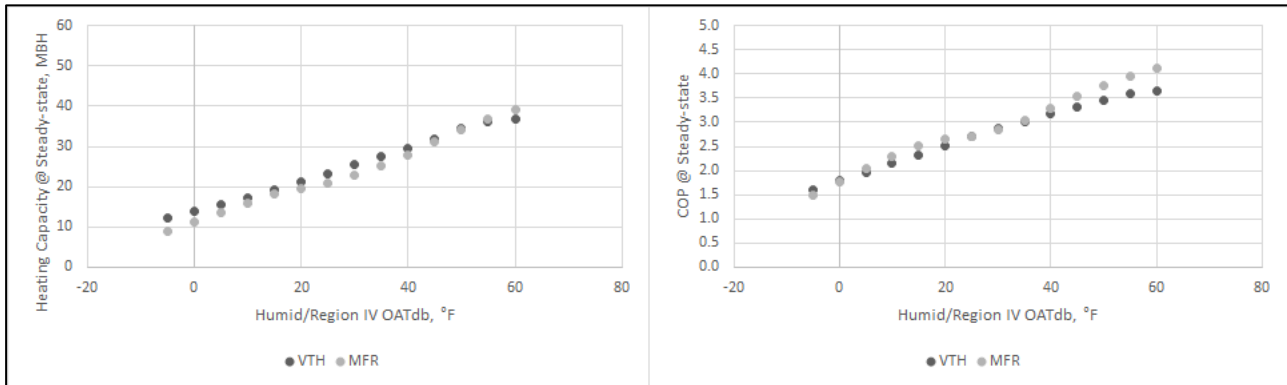


Figure 26 – Goodman ASHP Steady-state Heating Capacity (left) and COP (right) As a Function of OAT: VTH and MFR Comparison

Figure 27 and Figure 28 show the comparison between manufacturers and VTH data for the steady-state heating capacity and COP as a function of OATdb at the same compressor speed for the two ccAHPs. Similar to the Goodman ASHP analysis, manufacturer and VTH data correspond well for these two ccASHPs.

With validated heating capacities and COPs, the HSPFs were calculated for these three systems. Figure 29 shows the HSPF calculation based on the ANSI/AHRI 210/240 for Region IV. The results achieved with the VTH evaluation were similar to the rating published by the manufacturers.

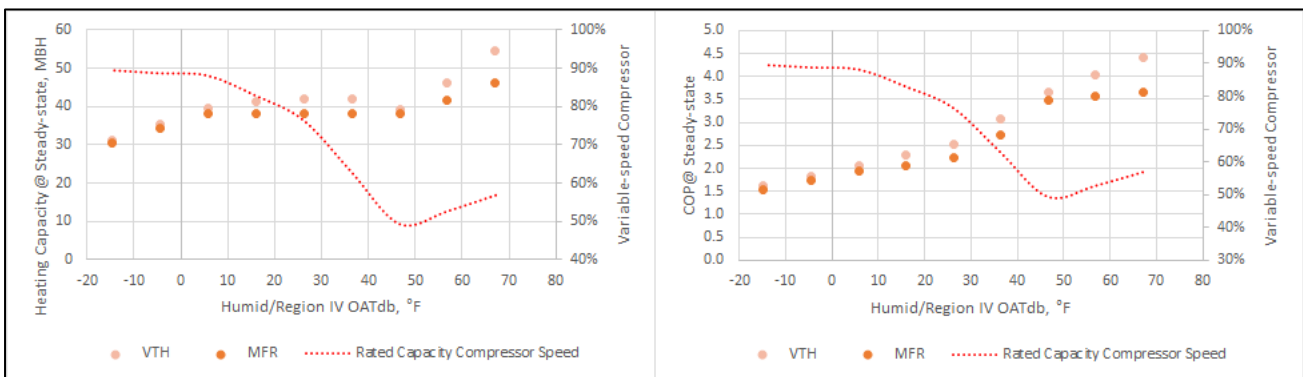


Figure 27 – Mitsubishi ccASHP Steady-State Heating Capacity (left) and COP (right) As a Function of OAT: VTH and MFR Comparison

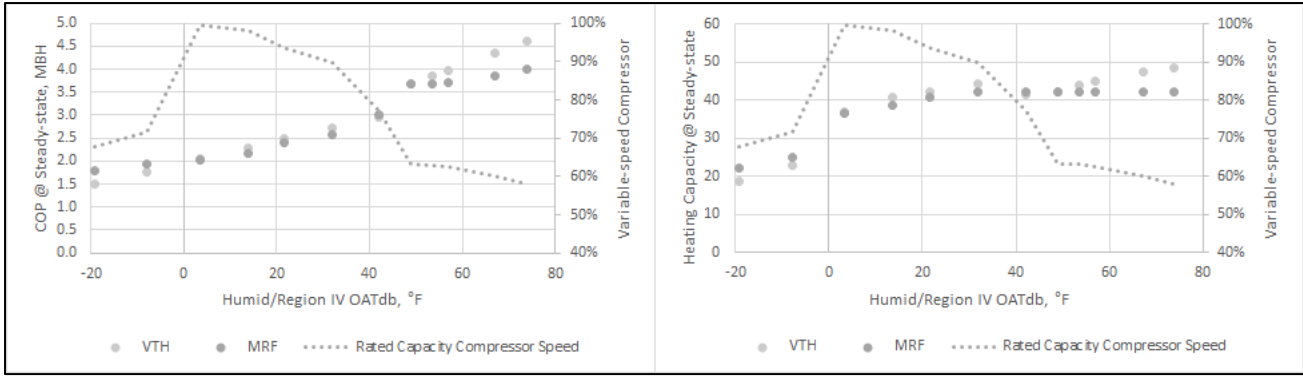


Figure 28 – Fujitsu ccASHP Steady-State Heating Capacity (left) and COP (right) As a Function of OAT: VTH and MFR Comparison

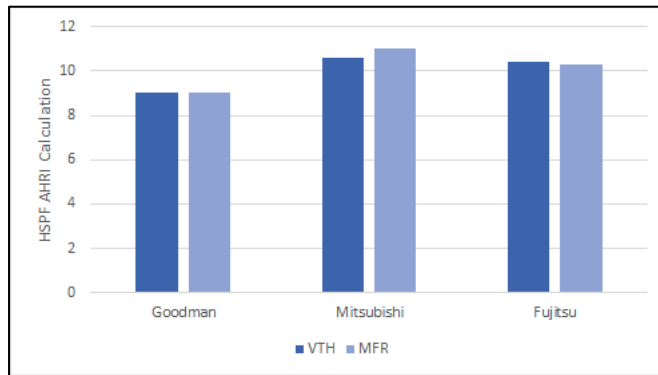


Figure 29 – ASHP and ccASHPs HSPF Calculation VTH and MFR Comparison

The left of Figure 30 shows the comparison between HSPF rating with VTH annual COP estimates and HSPF2 calculations. HSPF2 is an alternative HSPF rating derived by the DOE and addresses standby power amongst other operating characterizations for ASHP testing. The biggest difference between HSPF and HSPF2 is the heating distribution as a function of OATdb shown on the right side of Figure 30. The HSPF2 heating distribution is more closely aligned than HSPF in as-installed heating operation determined through VTH laboratory research and modeling.

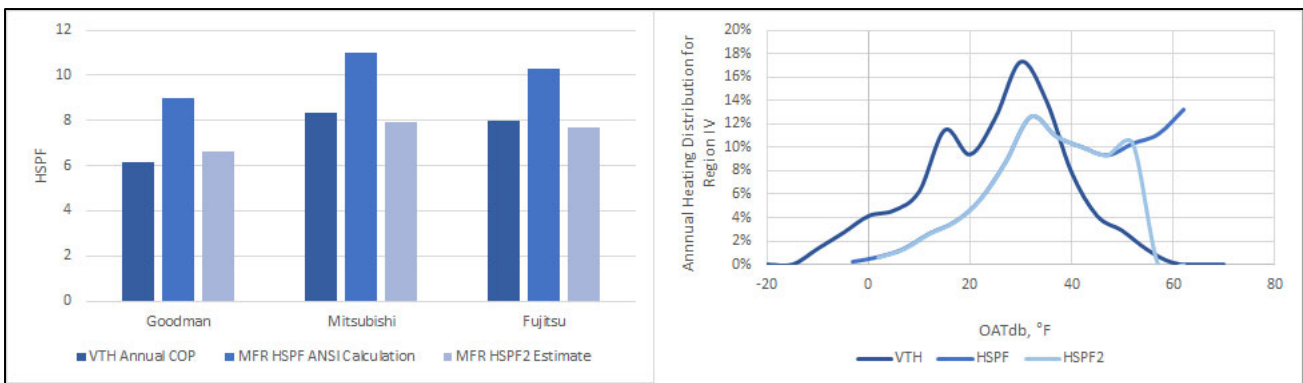


Figure 30 – HSPF, HSPF2 and VTH Calculation (left) and Heating Distribution as a Function of OATdb (right)

Field Demonstration

The Mitsubishi ccASHP system performance characterization was also validated with third-party field data presented in [Field Assessment of Ducted and Ductless Cold Climate Air Source Heat Pumps](#). With the heating load and balance point presented in [Field Test of Cold Climate Air Source Heat](#)

Pumps, the Mitsubishi ccASHP system was modeled and compared to the field data. Figure 31 shows modeled Mitsubishi ccASHP COPs with the third-party field collected COP data. Similar COP degradation as a function OATdb was observed. A magnitude of ± 0.25 COP was observed between the two data sets that can be attributed to measurement uncertainty and variation in return air and outdoor air conditions. Note, GTI’s performance models predicted the ccASHPs to be on the high side of the actual field data.

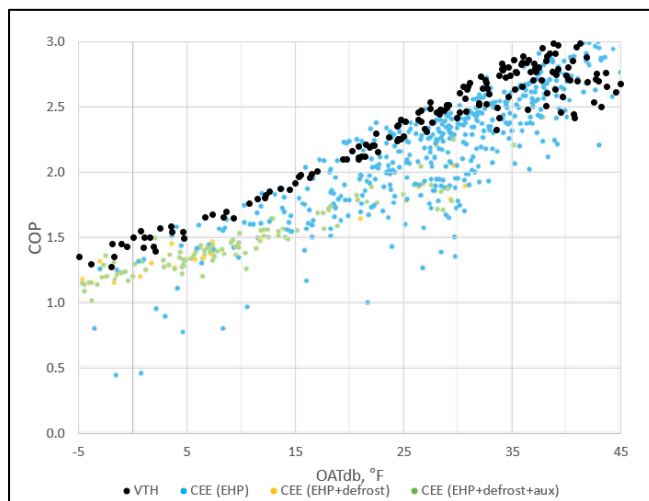


Figure 31 – Third-party Field Demonstration and VTH Comparison (Source: CEE)

EHPWH Water Heating Performance Characterizations

Background

Before assessing water heating performance of the two EHPWHs evaluated for this project, it is important to understand EHPWH operation and features. Table 5 shows the EHPWH operation and installation features that could be used in these systems.

Table 5 – EHPWH Basic Principles

Components

EHPWHs have two heating components: the heat pump and backup electric heating elements. This arrangement is commonly referred as hybrid heat pump water heater.

Heat Pump Size	Typically, heat pumps in EHPWHs are sized for 10 MBH of heating capacity to maintain hot water temperature at 125°F using room air dry-bulb temperature at 70°F
Heat Pump Heating Performance	Like ASHPs in cooling mode, the heat pump in the EHPWHs have a higher heating capacity and COP with warmer and humid indoor air conditions at the evaporator and lower water tank temperature set point. The heat pump has a small thermostat dead band in comparison to the backup heating element. This allows reduction of backup heating element operation.

<p>Backup Heating Elements</p>	<p>The EHPWHs commonly have two backup heating elements. Each element could have different thermostat dead bands. The upper heating element could be triggered first to maintain delivered hot water temperature. The lower heating element is trigger as a last resort to maintain delivered hot water temperature.</p>
<p>Installation Types</p>	<p>EHPWHs can use indoor air as well as outdoor air. EHPWHs are installed in warmer climates to take advantage of the cooling provided by the heat pump. The heat pump return and supply grilles can be ducted to outdoor air. The heat pump operates down to 40°F OATdb entering air temperatures. Below this threshold, the EHPWH only uses the backup heating elements and operates just like an electric water heater.</p>

EHPWH Heat Pump Capacity and COP Characterization

The heating capacity of the heat pump component in the EHPWH is determined by the wet bulb entering air (EATwb) and water tank temperature (WTdb). The difference between WTdb and EATwb dictates the ability for the heat pump component in the EHPWH to transfer heat to the water from indoor or outdoor humid air. Similar to air conditioning systems, the capacity and COP of the heat pump component in the EHPWH increase with high moisture content in the air at the evaporator coil. Likewise, the capacities and COPs of the heat pump in the EHPWHs are reduced due to higher temperatures at the condenser coil. Figure 32 and Figure 33 show heating capacity and COP characterizations of the heat pump component in the EHPWH for both systems. Similar heating capacities and COPs were observed in these systems. The EHPWH heating capacity breakdown based on EATwbs is associated with the power requirements of the compressor at the given WTdb. As the WTdb increases, the power consumption of the EHPWH increases to maximize heating capacity. The EHPWH COP in this section is defined as hot water production divided by power consumption.

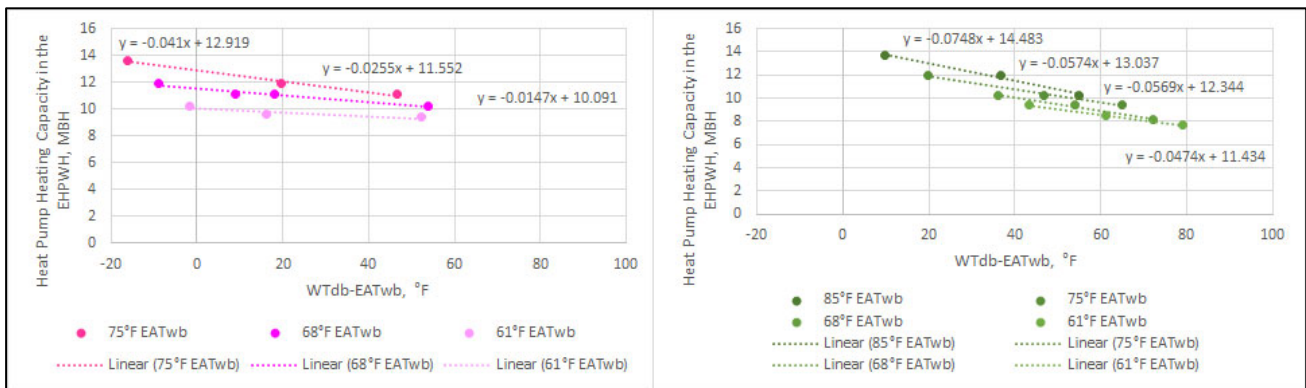


Figure 32 – Rheem (left) and AO Smith (right) EHPWH Heat Pump Component Heating Capacity Characterizations

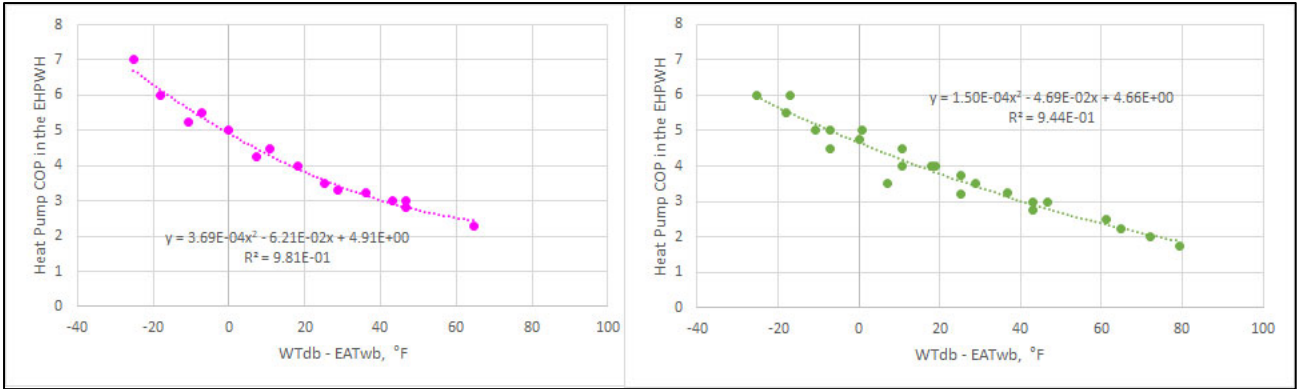


Figure 33 – Rheem (left) and AO Smith (right) EHPWH Heat Pump Component COP Characterizations

EHPWH Operation Characterization

Table 6 shows the tank heat loss factors and thermostat settings for the two heating elements for each EHPWH system used in this research.

Table 6 – EHPWH Tank Heat Loss Factor and Heating Elements Lower Thermostat Limit

Unit Brand	AO Smith	Rheem
Heat Loss, Btu/h-°F	3.7	3.9
Heat Pump Activation Temperature, °F	104	96
Backup Heating Element Activation Temperature, °F	95	80

EHPWH Performance Comparison

Figure 34 shows the daily COPs for these two systems and a baseline 50-gallon electric water heater in the model home located in the humid Region IV for a hot water set point of 120°F. These daily COPs account for tank heat losses for all systems. The primary observations were:

- Unlike traditional gas-fired water heaters, daily hot water consumption does not define daily COPs for EHPWHs as well as the combination of hot water draw heating capacity, EATwb, tank heat loss and daily hot water consumption.
- The highest daily COP in EHPWHs is accomplished by long hot water draws without using backup heating elements and daily hot water consumption greater than 50 gallons. This condition will maintain a lower average water tank temperature thereby reducing heat losses and maximizing EHPWH heating capacity and efficiency.

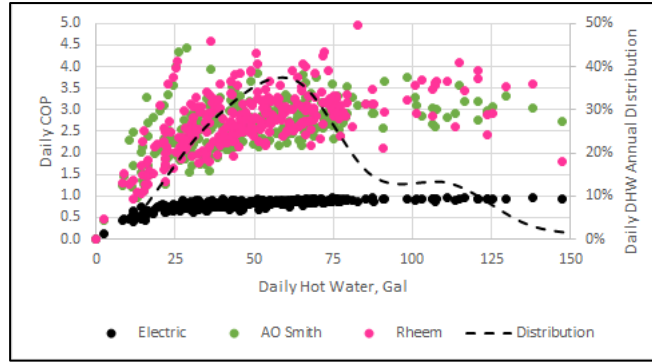


Figure 34 – EHPWH Daily COP for Indoor Installation in the Humid/Region IV

Figure 35 and Figure 36 show the COP waterfall charts for the baseline electric water heater and the Rheem EHPWH for three daily hot water usage patterns. These three daily hot water usage patterns are representative of the low-, medium- and high-usage pattern daily gallons from the [Appendix E to Subpart B of Part 43, Title 10, CFR - Uniform Test Method for Measuring the Energy Consumption of Water Heaters](#) developed by the DOE. These COP waterfall charts are based on average performance of these two systems in the water heating days that represented these three hot water consumptions from the hot water patterns developed by the NREL [Domestic Hot Water Event Schedule Generator](#). These COP waterfall charts show how EHPWH performance is reduced by auxiliary heating and standby losses. The following observations were made:

- The baseline electric water heater daily COP is greater for higher hot water usage where the standby losses become relatively small to the operating performance of electric elements.
- Similar to electric water heaters, the EHPWHs perform their best at higher hot water usage.
- For 32-gallon days, the daily COP of EHPWH is penalized by the standby losses.
- For 58-gallon days, the standby losses are relatively small to the hot water usage and very little auxiliary heating is implemented to maintain temperature in the tank.
- For 84-gallon days, the standby losses are neglectable and some auxiliary heating is used to maintain temperature in the tank.

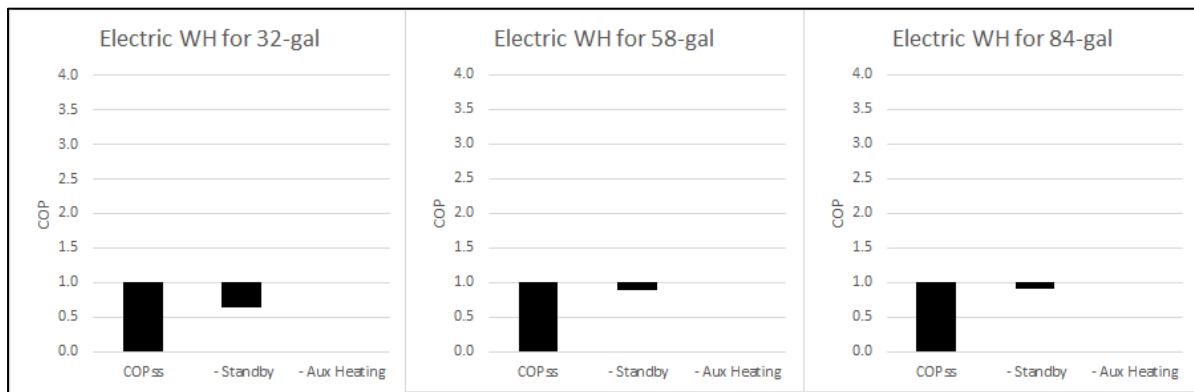


Figure 35 – Baseline Electric Water Heater Waterfall Charts for 32-gallon (left), 58-gallon (center), and 84-gallon (right) days

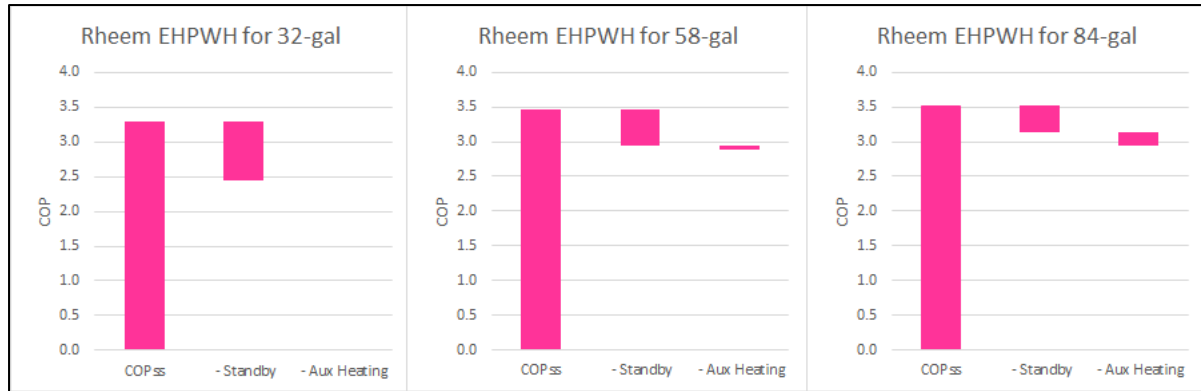


Figure 36 – Rheem EHPWH Water Heater Waterfall Charts for 32-gallon (left), 58-gallon (center), and 84-gallon (right) days

Figure 37 shows the water heating performance of the EHPWHs in all CSA EXP 07 climate zones with corresponding annual water heating load per zone in the model home. The primary observations were:

- The annual COP shown in Figure 37 does not account for the cooling benefits for the cooling season in all climates.
- The Rheem EHPWH performs slightly higher than the AO Smith EHPWH in all zones due to its smaller tank size.
- The lower the annual hot water consumption is, the lower the annual COP is for both EHPWHs.
- The lower annual COPs for both EHPWHs are found in hot regions where the city water is not as cold as the cold regions.

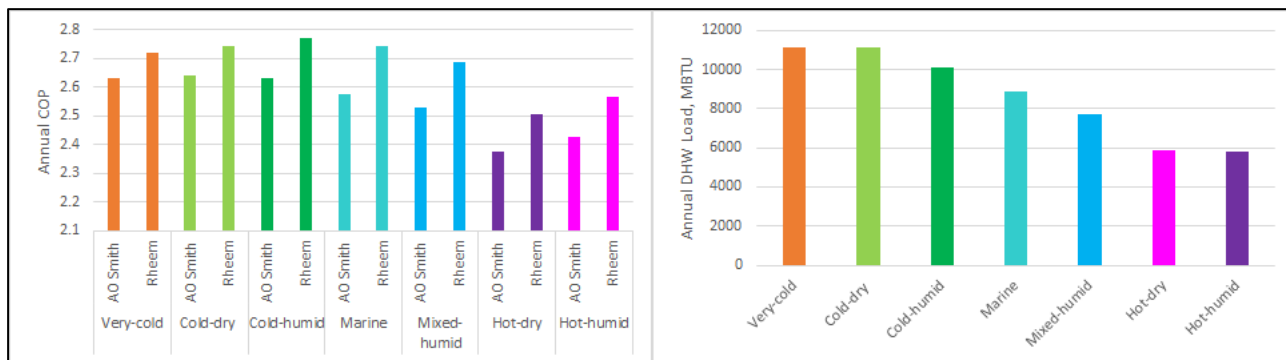


Figure 37 – EHPWHs Annual COPs in all CSA EXP 07 Climate Zones (left) and Water Heating Load Distributions as a Function of OATdb (right)

Figure 38 shows the difference between conventional and ducted installations for the Rheem EHPWH. In the conventional installation, the EHPWH borrows heat from the conditioned space. For the ducted installation, ductwork is used to draw air from the outside into the EHPWH HP. Ductwork is also connected to exhaust cold air used by the EHPWH back outside. The following observations were made:

- The ducted installation performs poorly compared to the conventional installation in most of the climate zones because the heat pump component does not operate under freezing temperatures during the heating season.

- In cold climates, the ducted installation performs only slightly better than a typical electric resistance water heater.
- The ducted installations are unlikely to perform better than the conventional installation.
- In hot climates zones, both installation performances are comparable. However, the cooling benefit from the EHPWH is lost from the ducted installation, making the conventional installation beneficial to reducing cooling loads during the cooling season.

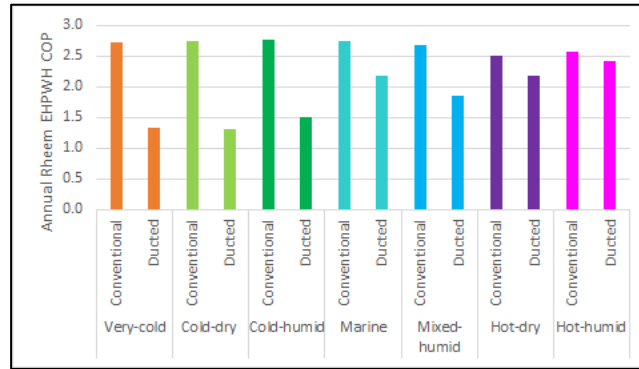


Figure 38 – Rheem EHPWH Annual COP for Conventional and Ducted Installations

Validation

The performance characterization of these EHPWHs were validated with manufacturer specification and field demonstration data.

Manufacturer Specifications

The manufacturer published UEFs were compared to the VTH modeling using their corresponding UEF profile tests from [Appendix E to Subpart B of Part 43, Title 10, CFR - Uniform Test Method for Measuring the Energy Consumption of Water Heaters](#) for validation purposes. Figure 39 shows a small difference in UEF calculation reported by manufacturer and VTH modeling for these two EHPWHs and a baseline 50-gallon electric water heater.

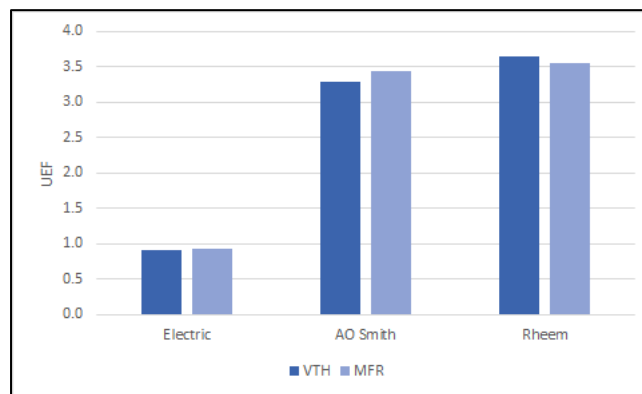


Figure 39 – EHPWH UEF Calculation Comparison

Figure 40 shows the difference between the UEF ratings and VTH evaluations for humid/Region IV. This comparison highlights the difference between test profiles and dynamic annual performance in EHPWHs. Figure 40 also shows the entering air temperature difference between the UEF and

EHPWHs installed in the model home in multiple climate zones. The UEF EATwb is generally only representative of hot-dry and -humid climates.

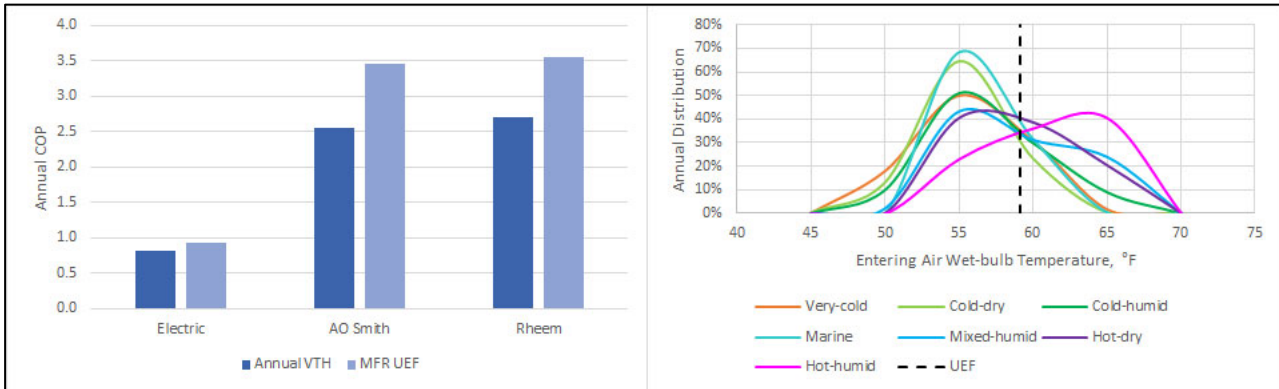


Figure 40 – UEF and VTH Calculation (left) and Entering Air Temperature (right) Comparison

Field Demonstration

Two field demonstrations were modeled with data from the VTH for validation purposes. These models used the daily water heating load ranges, EATwb, and water heating set point while using the daily patterns associated with location in the NREL [Domestic Hot Water Event Schedule Generator](#). The AO Smith EHPWH for indoor installation was modeled based on the [Field Performance of Heat Pump Water Heaters in the Northeast](#) published by the DOE. The AO Smith EHPWH was modeled using the reported average EATwb 49°F and 0 to 150-daily hot water gallons. Figure 41 shows the comparison between DOE field demonstration data and the VTH analysis. Similar daily COP ramp-ups were observed within 0- to 100-daily hot water gallons. Likewise, both field demonstration data and VTH demonstrated a daily COP band between 2 and 3 for hot-water gallons greater than 50. Here again, the VTH assessment tends to predict slightly better performance than what is seen in the field.

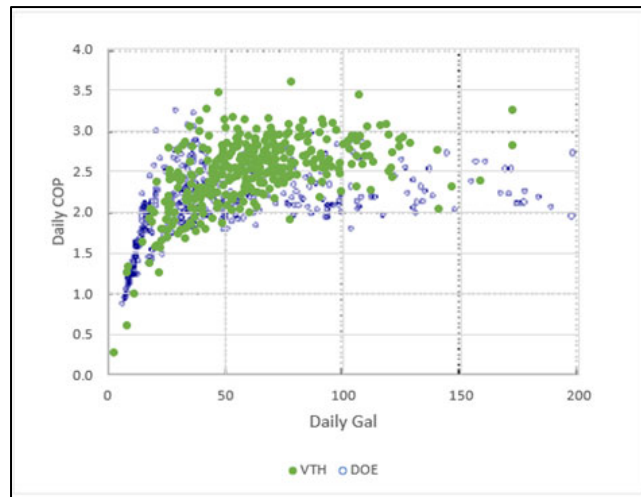


Figure 41 – Third-party Field Demonstration and VTH Comparison for the AO Smith EHPWHH with Conventional Installation (Source: DOE)

The Rheem EHPWH was simulated for ducted installation and compared to the operating conditions published by Energy 350 in the [CO₂ & Integrated Heat Pump Water Heater Performance Report](#). Figure 42 shows the weekly COP for the Rheem EHPWH operating with outdoor air conditions from

the cold-dry region and 0 to 150 gallons of hot water. Similar weekly COP degradation was observed between the third-party field demonstration and VTH modeling.

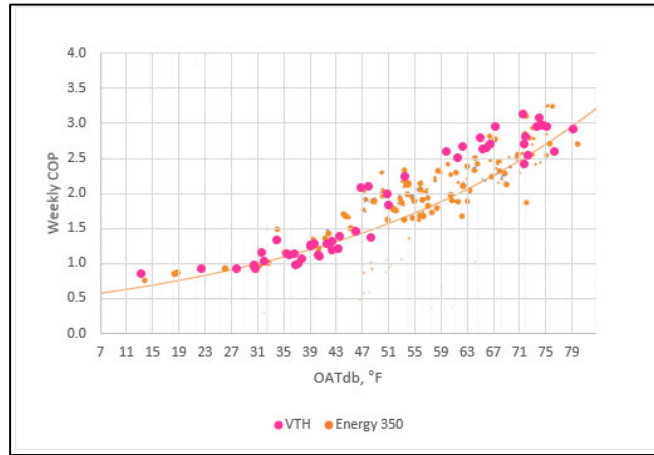


Figure 42 – Third-party Field Demonstration and VTH Comparison for the Rheem EHPWH with Ducted Installation (Source: Energy 350)

Performance Perspective

Conventional installation of EHPWHs provides for better performance compared to ducted installation. However, the increase in EHPWH performance negatively impacts the space heating and positively impacts cooling loads. During the cooling season, the EHPWH removes cooling load to heat water while decreasing the outdoor unit runtime as shown in Figure 43. However, in the heating season, the EHPWH adds heating load to the system as the EHPWH borrows energy to heat water in the tank.

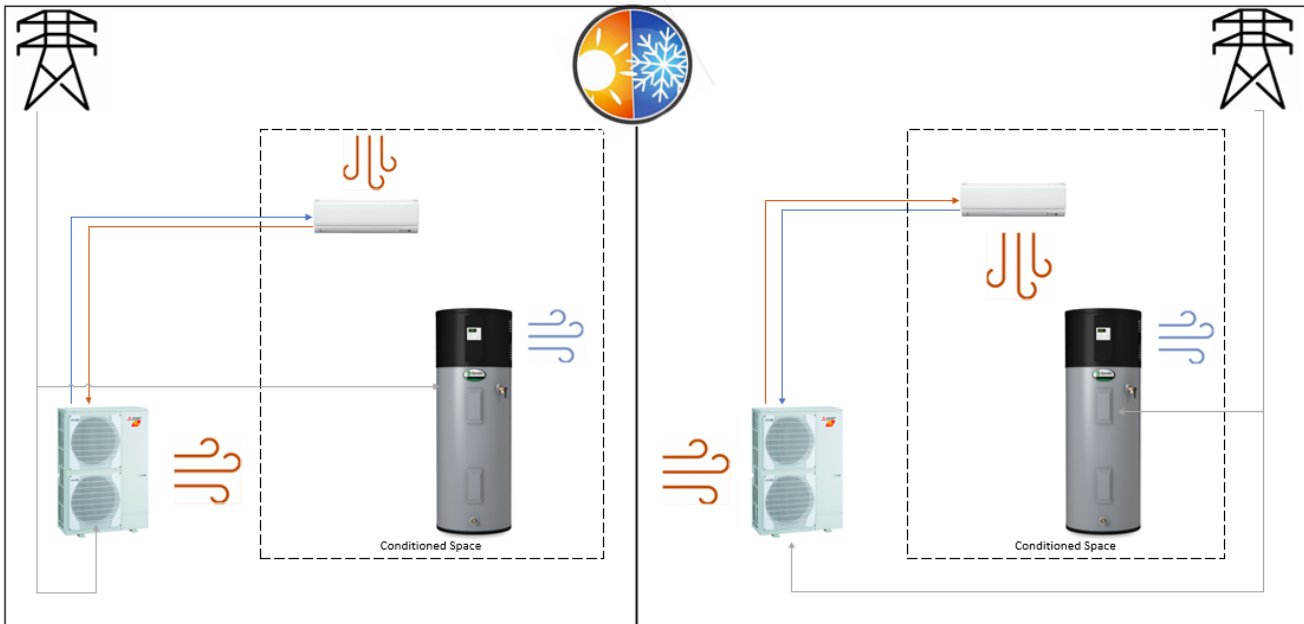


Figure 43 – EHPWH and ccASHP Energy Streams in the Cooling and Heating Seasons

The addition and removal of energy in the HVAC (cooling and heating) system is not considered in UEF ratings nor is it addressed in Figure 34 though Figure 42. In order to compare EHPWHs with other water heating systems that do not add/remove energy, a separate analysis must be done. Therefore, in the following analysis, the Mitsubishi ccASHP is applied to space heating and cooling in the model home where the EHPWH is installed without ducting. The electric power required or eliminated for the Mitsubishi ccASHP for additional heating or reduced cooling is integrated in the EHPWH COP equation as:

$$COP_{EHPWH} = \left(\frac{Q_{HW}}{E_{EHPWH} + E_{aSH} - E_{rSC}} \right)$$

where:

COP_{EHPWH} = annual EHPWH coefficient of performance

Q_{HW} = annual hot water load, MWh

E_{EHPWH} = annual EHPWH power consumption, MWh

E_{aSH} = annual additional ccASHP power consumption due to induced EHPWH space heating load, MWh

E_{rSC} = annual ccASHP power consumption reduction due to EHPWH operation during the cooling season, MWh

Figure 44 compares the conventional installation with and without the HVAC impact for the EHPWH performance in all CSA EXP 07 climate zones for the ducted installation. In all of these climate zones, the conventional installation provides better benefits for the EHPWH. However, the consideration of HVAC impact significantly changes the performance rating. For mild and cold climates, the EHPWH performs below the expected EHPWH COP due to the additional energy required to meet the space heating load induced by the EHPWH. Conversely, the EHPWH performs above expectations in warm climates because it produces hot water and reduces cooling load in the home.

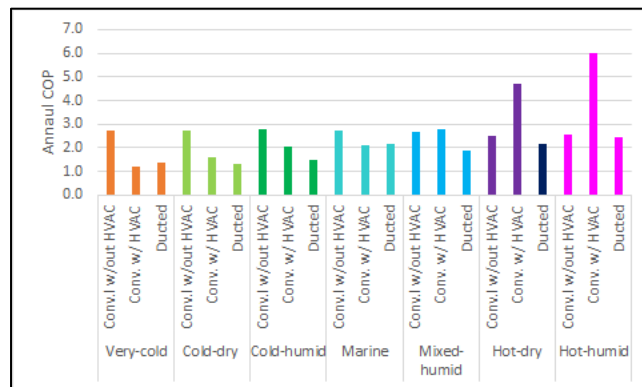


Figure 44 – Rheem EHPWH Annual COPs for Conventional with- and without HVAC Impact and Ducted Installations

Individual Space and Water Heating Performance Comparison

Modeling analyses were conducted to assess predicted performance attributes of ASHP, ccASHPs, EHPWHs and select gas appliances, as summarized in Table 7, in residential applications across

multiple climates. Analyses in this section present modeled predictions for energy, GHG, and cost metrics based on equipment performances determined in GTI’s VTH and validated with manufacturer’s data and in-field performance. Analyses were done for 14 cities across the nation that represent all the IECC and CSA EXP 07 climate zones shown by cyan and black dots in Figure 45. The model home referenced in the Building Energy Modeling section of this report was used to make assessments for equipment annual operating cost, site- and source-energy efficiency, and GHG emissions. The EHPWH performance in the analyses included the impacts on space heating and cooling loads associated with non-ducted EHPWH installed in the building envelope as presented in the Performance Perspective section of this report. Performance characterizations for the gas-fired system were developed in previous UTD research and can be found in Appendix B – iFLOW + Navien Combi Space and Water Heating Performance Curves.

Table 7 – Space and Water Heating Equipment System Performance Comparison

Space Heating	11 HSPF Mitsubishi Central ccASHP
	10 HSPF Fujitsu Mini-split ccASHP
	iFLOW + Navien Combi
Water Heating	Baseline 50-gal Electric Water Heater
	3.45 UEF AO Smith EHPWH
	3.55 UEF Rheem EHPWH
	0.97 UEF Navien Tankless

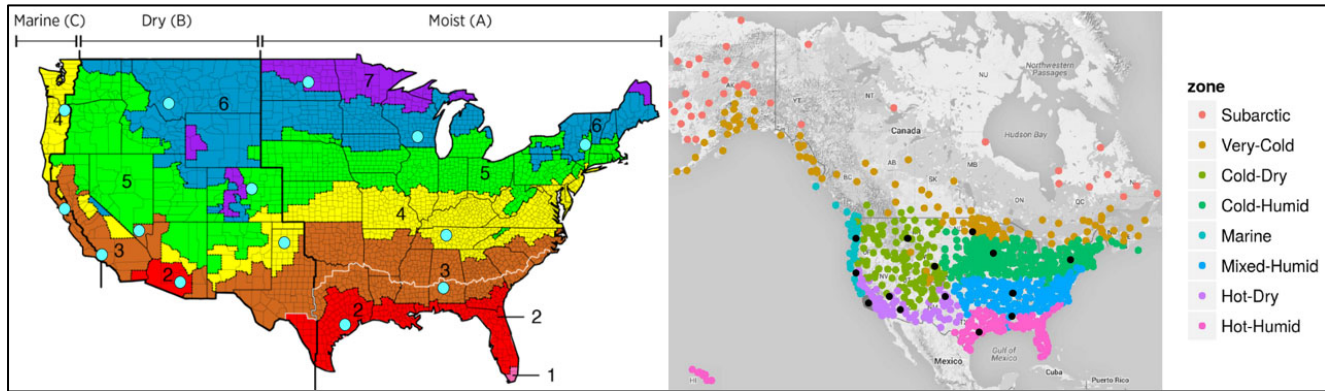


Figure 45 – Market Impact Considerations Cities in the IECC (left) and CSA EXP 07(right) Maps

Annual COP and Energy Consumption

Predicted annual COPs for the electric and gas space heating equipment are shown on the left side of Figure 46. Similar to the CSA EXP 07 climate zone analysis shown in Figure 25, the two ccASHPs outperformed the baseline ASHP for heating dominant climates. The predicted annual EHPWH performances shown on the right side of Figure 46 demonstrate similar patterns observed in the CSA EXP 07 climate zone analysis shown in Figure 37. The two EHPWHs were predicted to perform

similarly across all 14 cities. Both iFLOW + Navien advanced combi demonstrated similar space and water heating COP across the 14 cities.

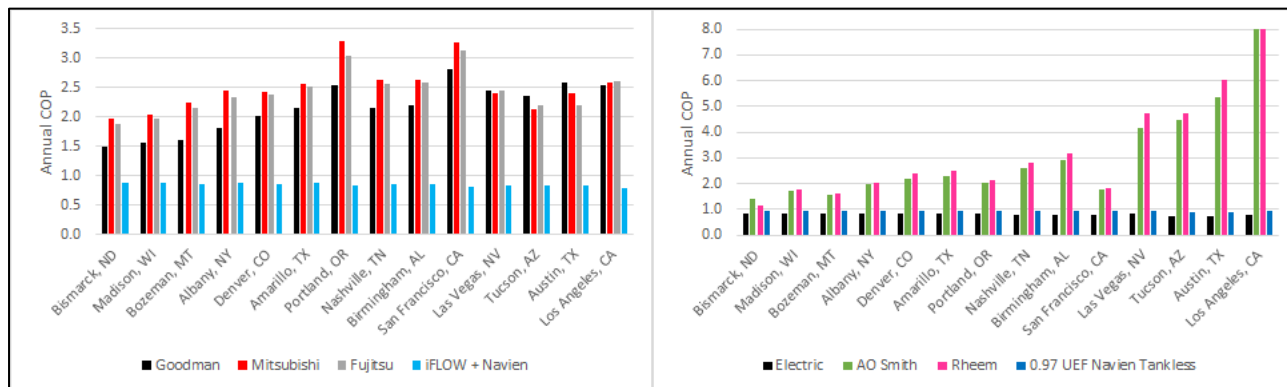


Figure 46 – Space (left) and Water (right) Heating Equipment Annual COPs

The total annual energy consumptions for the electric and gas space and water heating equipment are shown in Figure 47. Significantly less site-energy consumption is observed for all electric-driven heat pump technology than for the gas-fired technology, which was to be expected. However, Figure 48 and Figure 49 show energy consumptions in terms of source-energy as represented by source-energy factors for non-baseload and total perspectives. The source-energy factors are based on the latest (2018) data from the [Emissions & Generation Resource Integrated Database \(eGRID\)](#) developed by the U.S. Environmental Protection Agency (EPA). This data can be found in Appendix F – Modeling. Non-baseload is also referred to as the marginal power mix and total considers all sources of power generation. Which perspective used to calculate emissions from consumed grid electricity can be a source of contention because each option nets quite different results. It may seem logical to use all sources of power (total or baseload perspective) for the emissions calculation, especially since clean nuclear and renewable power will have a positive impact on the calculations. However, as the term baseload implies, those sources of power will always stay on. It is the non-baseload, or marginal power that will be displaced by energy efficiency measures. Results and observations for the source-energy analyses for non-baseload and total are provided below:

- Non-baseload Perspective
 - The gas-fired iFLOW + Navien advanced combi is similar to ccASHPs and EHPWHs in most of the 14 cities analyzed.
 - The iFLOW + Navien advanced combi consumes less source-energy for space heating in cold climates than the ccASHPs.
- Total Perspective
 - The ccASHPs are similar in cold climates to the iFLOW + Navien advanced combi, and consumes less source-energy than the iFLOW + Navien advanced combi in moderate and mild climates.
 - EHPWH consumes similar source-energy as the Navien tankless in mild climates, and outperforms the tankless in terms of source-energy consumption in hot climates.

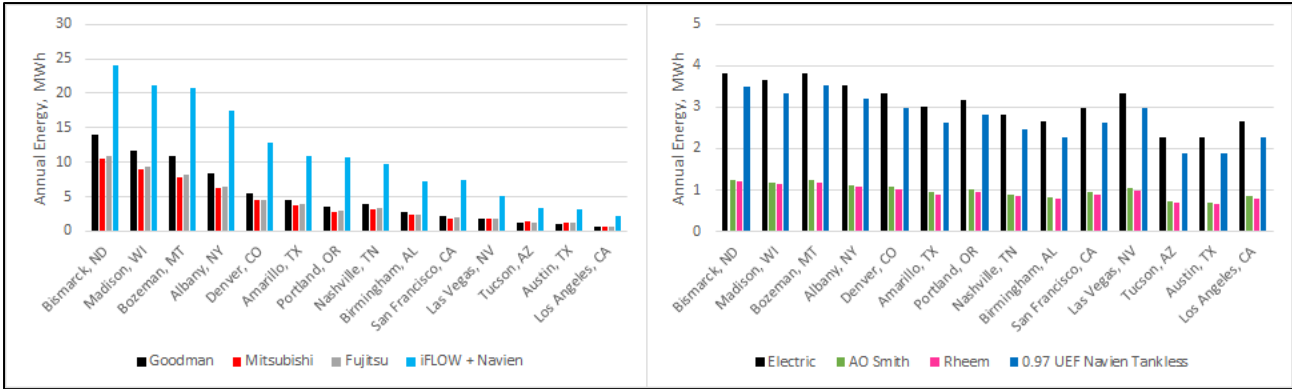


Figure 47 – Space (left) and Water (right) Heating Equipment Annual Energy (Gas + Electricity) Consumption

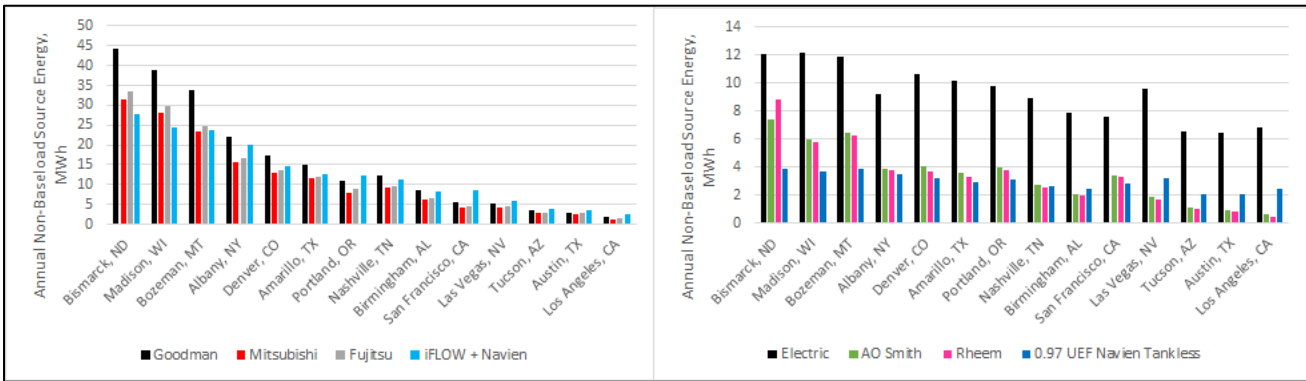


Figure 48 – Space (left) and Water (right) Heating Equipment Annual Non-baseload Source-energy (Gas + Electricity) Consumptions

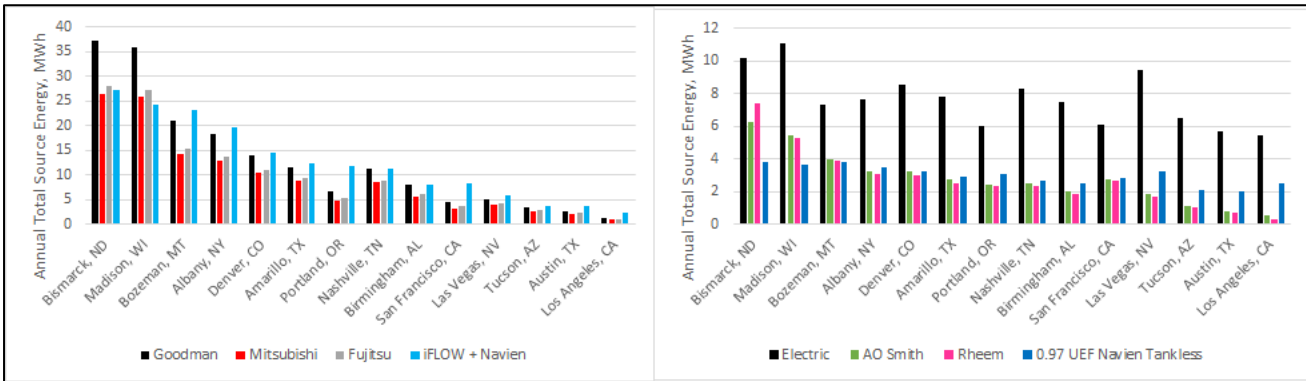


Figure 49 – Space (left) and Water (right) Heating Equipment Annual Total Source-energy (Gas + Electricity) Consumptions

Annual Operating Cost

Maximizing efficiency and GHG savings and minimizing operating cost can sometimes be conflicting goals. For example, heat pump operations may be very efficient at times, but very costly to operate depending on electric utility tariffs.

Predicted annual operating costs for the electric and gas space and water heating equipment are shown in Figure 50. The 2019 electric and natural gas monthly rates from [U.S. Energy Information Administration](#) (EIA) were used in these analyses and can be found in Appendix F – Modeling . The iFLOW + Navien advanced combi space heating annual operating cost was predicted to be

significantly lower in cold climate zones than with the ASHP and ccASHP technologies. For the rest of the climate zones, operating costs for electric and gas space heating technologies were similar on an annual basis. EHPWH operating costs are generally the lowest and highest in the hot and cold climates, respectively.

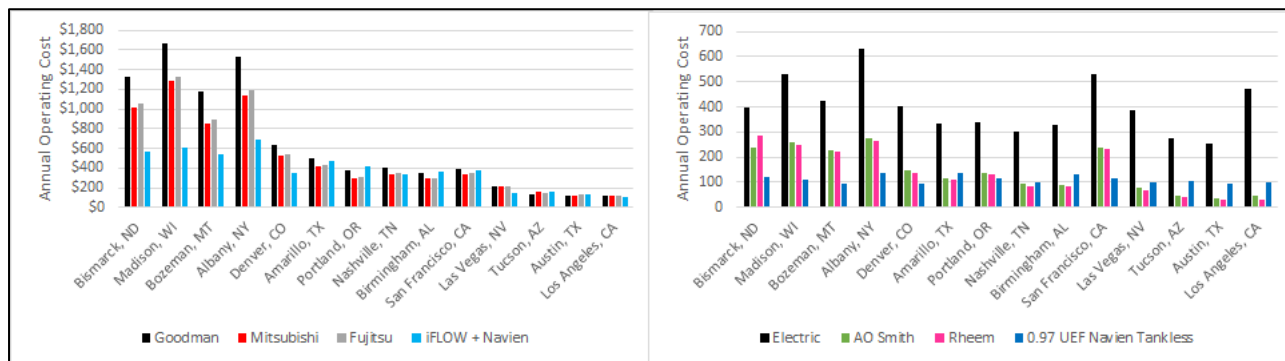


Figure 50 – Space (left) and Water (right) Heating Equipment Annual Operating Costs

Annual GHG Emissions

The predicted annual non-baseload and total GHG emissions for the electric and gas space and water heating equipment are shown in Figure 51 and Figure 52, respectively. The latest (2018) GHG emission factors from eGRID used in these analyses and are provided in Appendix F – Modeling . The following observations were made:

- Non-baseload Perspective
 - GHG emission for the iFLOW + Navien advanced combi are similar to ccASHPs in moderate, mild, and hot climates.
 - The iFLOW + Navien advanced combi operation would likely be cleaner than the ccASHPs in cold climates.
 - The 0.97 UEF Navien tankless operation is significantly cleaner than EHPWHs in cold and mild climate cities.
- Total Perspective
 - In many cases, ccASHP and EHPWH technology could be cleaner than the advanced gas-fired combi system, particularly in warm climates. However, all-plant grid emission intensities are key factors. For example, the iFLOW + Navien advanced combi system is cleaner than the ccASHP and EHPWH technology in Madison, WI, but not in Albany, NY as can be seen in Figure 52.
 - EHPWH technology provides the lowest GHG emissions in hot climates as it also reduces space cooling loads.

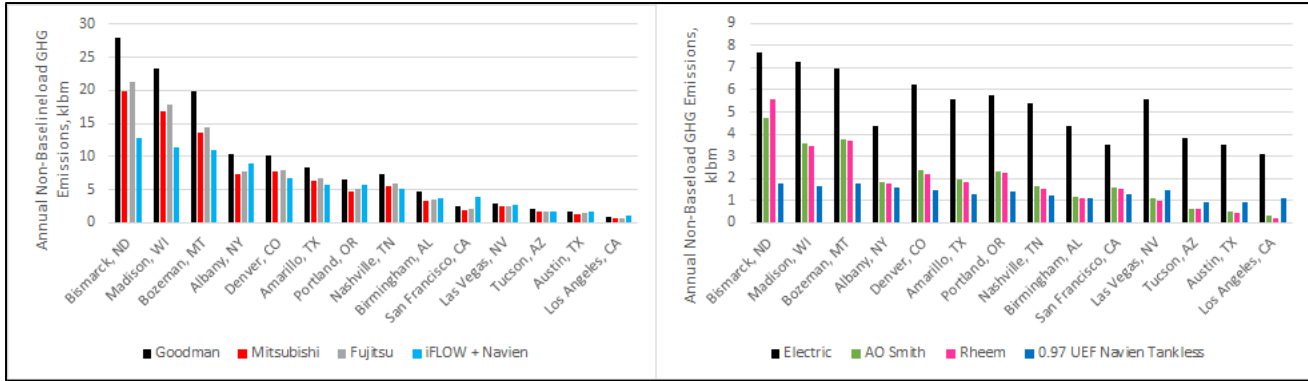


Figure 51 – Space (left) and Water (right) Heating Equipment Annual Non-baseload GHG Emissions

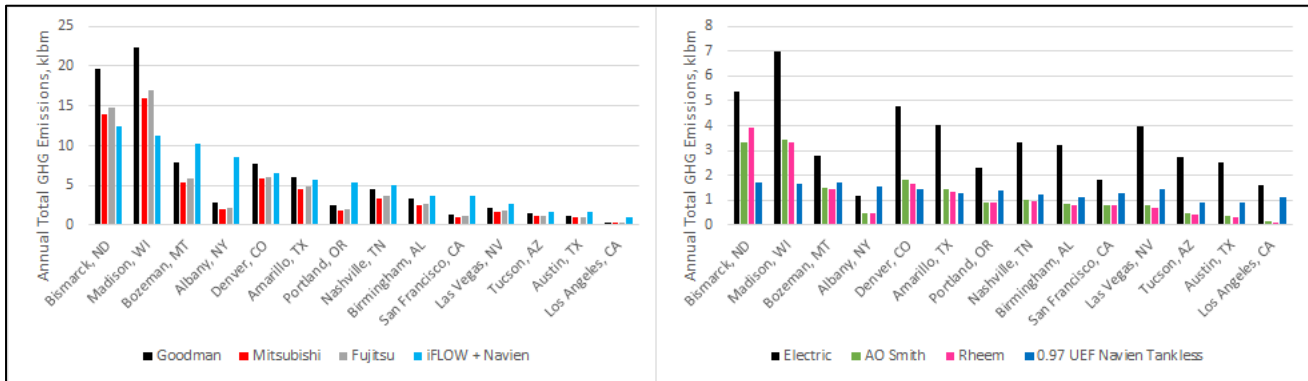


Figure 52 – Space (left) and Water (right) Heating Equipment Annual Total GHG Emissions

Discussion

The analyses presented in this section are useful for assessing the attributes of individual space and water heating technologies. However, the interaction of these systems is very important to understand. For example, it is clear from the analyses that EHPWHs impact the HVAC loads. A coupled space heating/cooling and water heating system analysis is needed to better understand how advanced electric and gas-fired systems perform relative to one another and as hybrid solutions.

System Market Impact Considerations

The following section presents coupled system modeling analyses for five systems across 14 cities, representing most of the IECC and CSA EXP 07 climate zones (as shown by cyan and black dots in Figure 45). The five coupled systems that were analyzed for this research are shown in Figure 53 and Table 8. These five systems are:

- Baseline Electric
- Advanced Electric
- iFLOW + Navien advanced combi with an air conditioner (AC)
- Two gas-fired systems that GTI has developed with goals for achieving efficiencies greater than 1.0
 - Gas-driven thermal heat pump (THP) and AC

- Integrated energy system with micro-combined heat and power (IES-mCHP)

All these systems were characterized in the VTH to fully understand their performance across a very wide range of conditions and to provide accurate modeling to determine potential energy, cost and GHG savings potential. The modeling approach implemented for this section is detailed in Appendix G – Modeling System Market Impact Considerations.

Table 8 – Market Impact Consideration Equipment

System Name	Baseline Electric	Advanced Electric	Advanced Gas + AC	THP + AC	IES-mCHP
Space Heating	15SEER / 9HSPF Goodman ASHP	Mitsubishi ccASHP	iFLOW + Navien	SMTI THP connected to a storage tank for space and water heating loads	18SEER / 10HSPF Goodman ASHP driven by mCHP with thermal storage and tankless
Water Heating	Electric Water Heater	Rheem EHPWH			
Space Cooling	15SEER / 9HSPF Goodman ASHP	Mitsubishi ccASHP	18SEER Goodman AC	18SEER Goodman AC	18SEER / 10HSPF Goodman ASHP
Grid Resiliency	No	No	No	No	Yes

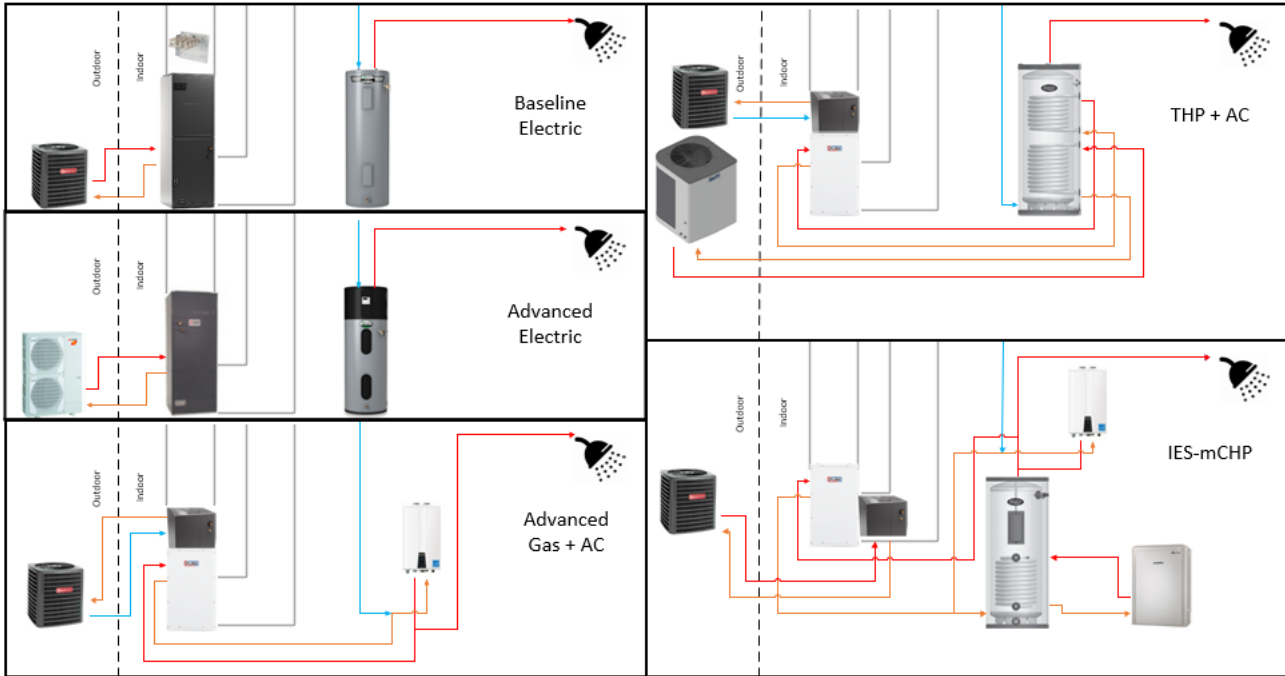


Figure 53 – Market Impact Consideration System Configurations. Baseline Electric (upper left), Advanced Electric (middle left), Advanced Gas (lower left), THP + AC (upper right) and IES-mCHP (lower right)

Annual COP

The predicted annual COPs for the five systems are shown in Figure 54. As expected, the advanced electric system shows the highest COP in all 14 cities due to its electrically driven heat pump technology.

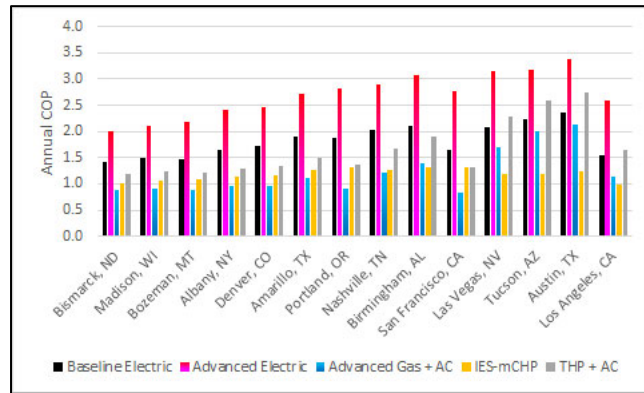


Figure 54 – Annual COPs for the Five HVAC & DHW Systems

Annual Source-Energy COP

The annual source-energy COPs (SCOPs) for total and non-baseload perspectives are shown in Figure 55. The source-energy factors are based on the latest (2018) information from eGRID can be found in Appendix F – Modeling . The SCOP analysis suggests:

- Total Perspective

- In cold climates, the IES-mCHP and THP + AC systems were predicted to provide the highest SCOP due to their advanced gas-fired heating technologies and integration with electric-based technology.
- The models indicated the advanced electric system in mild climates and in regions with clean electricity from the grid provide for very clean operation.
- In warm climates, the advanced gas + AC system would likely be as effective as the advanced electric system in reducing GHG emissions.
- Gas-fired cooling, albeit very resilient in warm climates, would likely be less efficient than electrically driven cooling given the current state of technologies.
- Non-baseload Perspective
 - The models indicated the advanced electric system provides clean operation, but not as clean as the other hybrid solutions.
 - Models indicated the IES-mCHP and THP + AC solutions would likely provide the cleanest operations in all the regions.

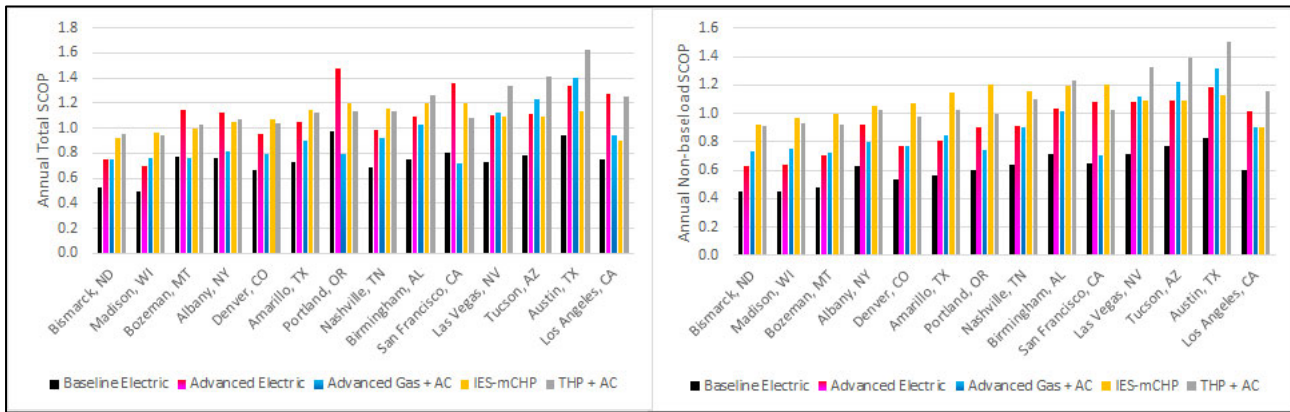


Figure 55 – Annual Total (left) and Non-baseload (right) SCOPs for the Five HVAC & DHW Systems

Annual Source-Energy

The annual total and non-baseload source-energy consumptions for these five systems are shown in Figure 56. The source-energy factors are based on the latest (2018) source-energy factors eGRID can be found in Appendix F – Modeling . The source-energy analysis suggests:

- Total Perspective
 - In very-cold climates, the IES-mCHP and THP + AC systems would likely provide the lowest source-energy consumption of the five systems.
 - The advanced electric system would likely consume less source-energy in comparison to the advanced gas + AC system in many cold cities.
 - In warm climates, gas-fired space and water heating would likely be more effective at reducing source-energy than all-electric alternatives.
- Non-baseload Perspective
 - Modeling indicates IES-mCHP and THP + AC would be more effective at reducing source-energy than the advanced electric system in all the cities analyzed in this report.

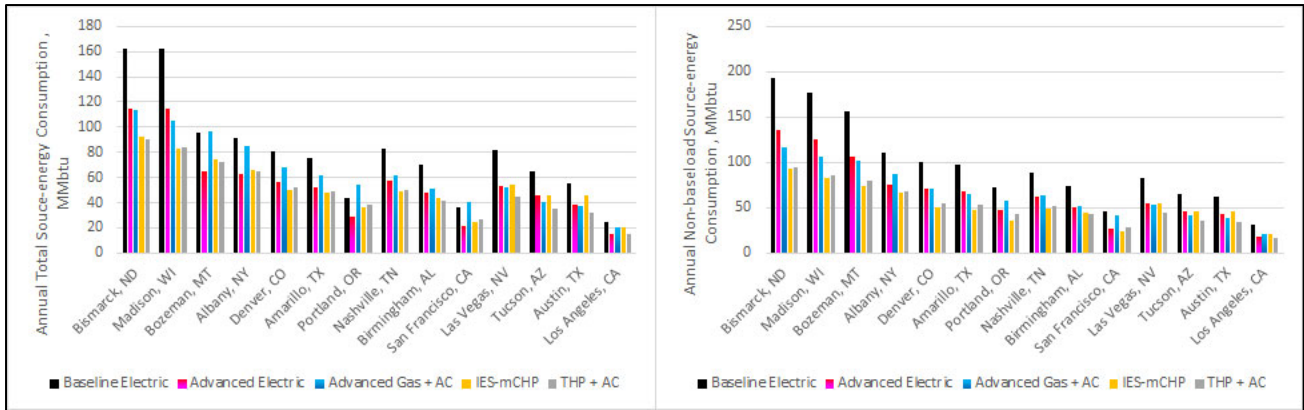


Figure 56 – Annual Total (left) and Non-baseload (right) Source-energy Consumptions for the Five HVAC & DHW Systems

Annual GHG Emissions

The predicted annual non-baseload and total GHG emissions for the electric and gas space and water heating technology are shown in Figure 57. The GHG analyses for these five systems have similar trends observed in the previous Annual Source-Energy section.

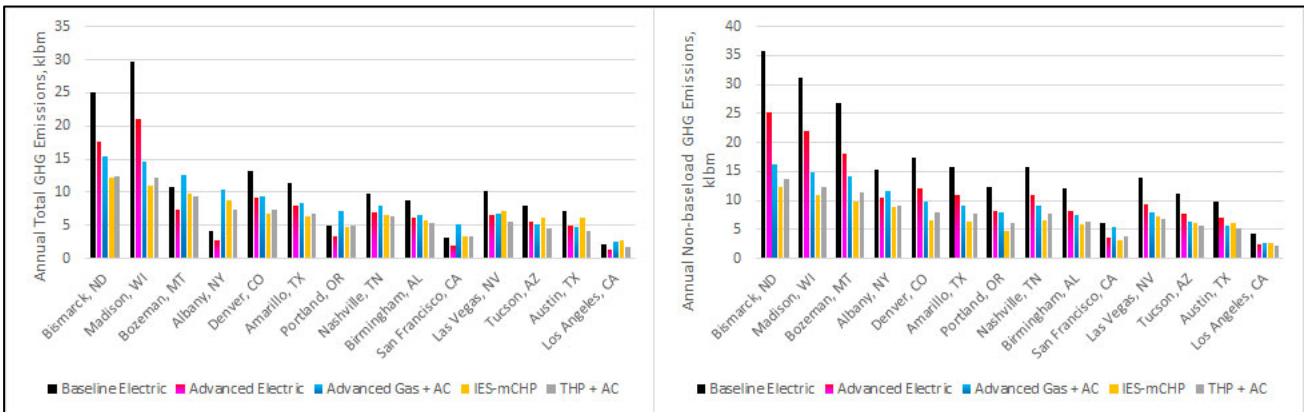


Figure 57 – Annual Total (left) and Non-baseload (right) GHG Emissions for the Five HVAC & DHW Systems

Annual Operating Cost

The predicted annual electric and gas HVAC and water heating operating costs for the five systems are shown in Figure 58. This analysis suggests:

- Modeling indicated the advanced electric system is a more costly alternative than the advanced gas + AC system in non-cold climate cities.
- THP + AC and IES-mCHP systems would likely provide the lowest operating cost in all cities. Moreover, each provides certain resilience attributes that an all-electric option cannot provide.
- Grid-resilient gas-cooling was more expensive than electric cooling.

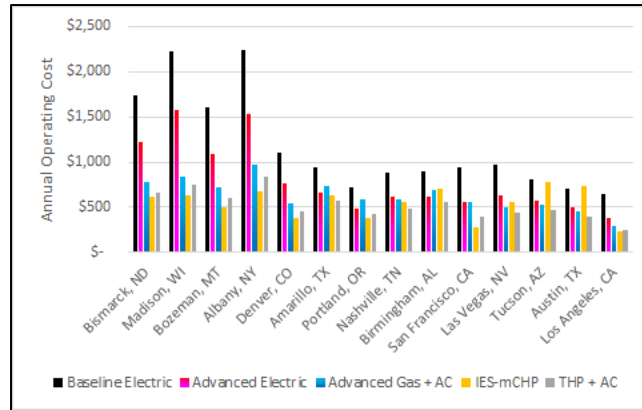


Figure 58 – Annual Operating Costs for the Five HVAC & DHW Systems

Conclusion & Next Steps

GTI evaluated the best-in-class electrically driven heat pump technology for space and water heating in the VTH in order to determine the detailed performance of the technology and to better understand how hybrid gas-electric systems can be implemented to achieve the most efficient, cost-effective and comfortable space heating. Extensive evaluations were performed to identify variables that affect operating mode, heating output and detailed electrical power requirements of these two systems. ccASHP and EHPWH performance characterizations were developed from VTH evaluations. Additionally, advanced building energy modeling was performed to formulate conclusions based on extensive laboratory, in-field and modeling research using these performance characterizations and previous VTH best-in-class gas-fired system performance curves. Results of this holistic research across 14 cities representing most of the IECC climate zones suggest:

- Annual non-baseload source-energy consumption and GHG emissions for the all-electric alternative the advanced electric system would likely be higher than the advanced gas + AC system in most of the cities.
- Annual operating cost of an advanced electric system would likely be higher than the advanced combi alternative the advanced gas + AC system in all of the cities researched in this study except the cities in IECC climate zones 4
- Advanced gas-fired systems such as the THP + AC and IES-mCHP could offer the lowest source-energy consumption, GHG emissions and operating cost in all 14 cities of the five systems evaluated in this research project.

Next Steps

GTI recognizes the advantages of hybrid systems to reduce operating costs and GHG emissions. GTI recommends integrating ccASHP and EHPWH in the IES-mCHP configuration to optimize system controls for various climates to further increase the potential for annual energy, GHG emissions and operating cost reductions. This research is already underway as part of UTD projects 1.20.G and 1.20.J.

Appendix A – VTH Evaluation Methods

Space Heating

The laboratory test setup was designed such that energy in warm air delivered by the furnaces could be determined using accurate airflow measurements along with supply- and return-air temperature measurements. However, that energy was not delivered to a conditioned space, like it would be in a home. Rather, the test setup was designed to expel the warm air from the lab space. As such, the furnaces did not operate on actual calls from their thermostats. Instead, for each incremental part-load test, algorithms in a computer-generated, or virtual home were used to calculate room air temperatures and simulate thermostat cycle times (on/off or modulation calls). During the on cycles, the amount of energy delivered in warm air by the furnace was calculated every five seconds using measurements from the test setup. Knowing the energy delivered at 5-second intervals, and the required heating demand for the particular part-load test, room air temperatures in the virtual home were calculated every five seconds as well. It is important to note, conditioned space volume is also needed to determine how the room air temperatures change. Since part-loads were based on the Building America B10 Benchmark reference house, building volume and construction were arbitrarily defined by that reference model. The model used to define the volume can be arbitrary as only the resulting cycle times are important in order to map the part-load force-air system performance with single-stage or modulation operation.

Thermostats operate based on room air temperature set points and deadbands, which are adjustable. The thermostat deadband is important because it could negatively affect efficiency as a result of short cycling. For instance, the smaller the deadband, the shorter the furnace cycle time, and the lower the efficiency. The deadband allows a force-air system to cycle on or modulate between allowable minimum and maximum room air temperatures. The force-air cycling algorithms developed for this project used a 2°F deadband, allowing the room air temperature in the virtual home to be between 69°F and 71°F. Therefore, the force air system came on at 69°F and shut off at 71°F. Examples of force-air system operation with single- and modulating capacity is shown on the left and right of Figure 59, respectively.

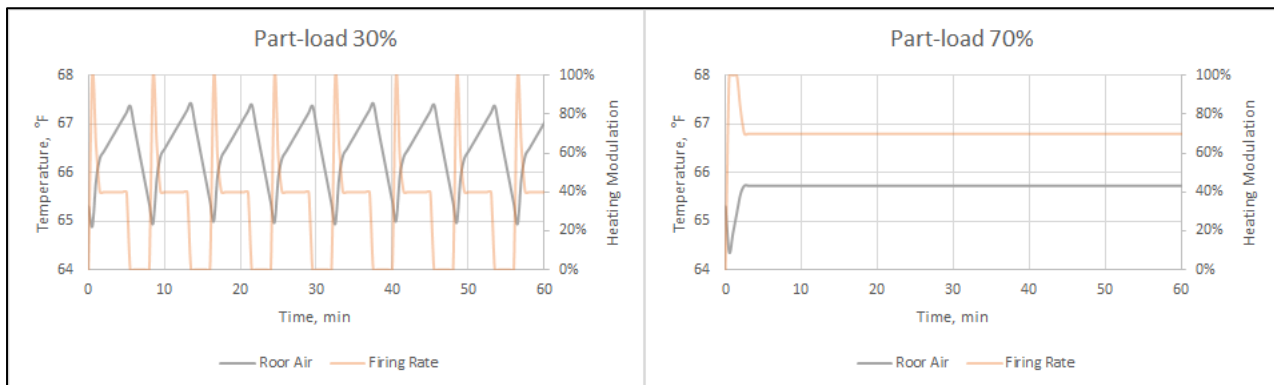


Figure 59 – Thermostat Simulation Strategies

Tankless Water Heating

As with space heating, the experimental methods employed for evaluating combi water heating capabilities also used the VTH. Here again, the methods are collectively an alternative to standardized test methods such as ASHRAE 118.2 for rating water heaters. The VTH was used to conduct

simulated-use tests under controlled conditions with water draw events at various conditions. Efficiencies were calculated using an input-output method rather than a UEF as applied in ASHRAE 118.2.

A 6-hour water heating evaluation was conducted for each of the combis in order to develop efficiency profiles for various DHW draws. Similar DHW draws were used for coincidental space heating and water heating experiments described in the next section. The data set of direct energy input and output measurements were collected for each of the combis operating at 1, 2, 3, and 4 gallons-per-minute (gpm) draws each for 1, 3, 5, 7 and 10 minutes. Between each scenario, the water heater was cooled down to about 65°F.

Appendix B – iFLOW + Navien Combi Space and Water Heating Performance Curves

iFLOW + Navien

Figure 60 shows the performance characterization for the iFLOW + Navien combi used in the Individual Space and Water Heating Performance Comparison and System Market Impact Considerations sections. Left of Figure 60 shows the steady-state gas efficiency and electric rate (as a function of gas consumption) of the iFLOW + Navien system in the space heating output range of 15 MBH to 100 MBH. Right of Figure 60 shows degradation factor as a function of hourly part-load for both gas efficiency and electric rate to correct for deficiencies associated to cycling.

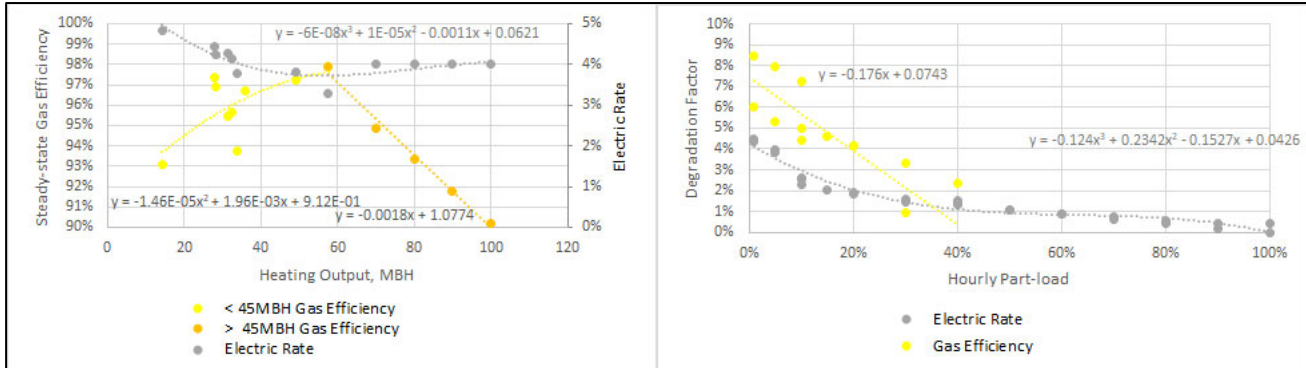


Figure 60 – iFLOW + Navien Performance Characterization

Navien Tankless

Figure 61 shows the performance characterization curves for the 0.97 Navien tankless. Unlike space heating modeling, the tankless modeling is performed in the daily DHW demand. Both daily gas and electricity consumption can be modeled using the daily DHW load.

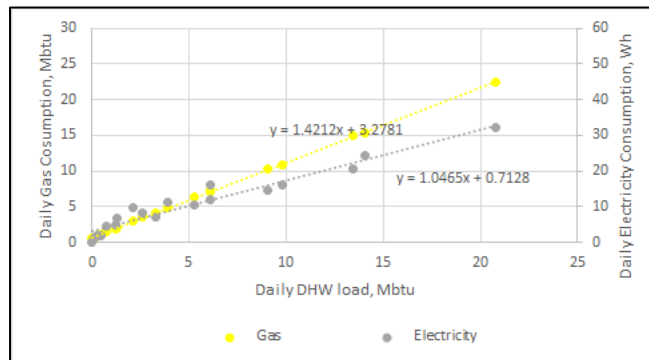


Figure 61 – Navien Tankless Performance Characterization

Appendix C – ASHP and ccASHP Evaluation Test Plan

The objective of this test plan is to compare the performance of two ccASHPs against a baseline ASHP with a hybrid lab/field demonstration approach. The outdoor units will be installed outside of GTI laboratories with the goal of exposing the condensers to a diverse climate conditions in Des Plaines, IL starting on December 2019 and ending on June 2020. The indoor units will be installed in a controlled environment inside of GTI laboratories with their corresponding thermostats. The heat calls will be determined by the heating load applied to GTI laboratories during the testing period. For GTI laboratories backup heating, an RTU will be used and operated with a lower thermostat set point. The installation of the ccASHP and baseline ASHP thermostats will be at the same location of the GTI laboratories RTU thermostat.

Evaluation Matrix

The baseline ASHP and ccASHP will be running to maintain their corresponding thermostat temperature set points. The temperature set point in the thermostats will be changed to obtain different compressor responses in the ccASHPs. Data sets with a diverse of operating conditions will be carefully reviewed to characterize the following variables:

- Steady state heating capacity
- Compressor power consumption and range
- Part-load degradation
- Steady state COP
- Defrost power consumption, cooling delivered and duration
- Standby power consumption

Instrument Plan

Table 9 through Table 11 list the instruments that will be used in the this performance evaluation illustrated in Figure 62 through Figure 64 respectively, including the parameter to be measured, the instrument make and model, and the instrument’s accuracy.

Table 9 – ASHP and ccASHP Evaluation Mechanical Room Instrumentation

Parameter	I.D.	Make / Part #	Range	Accuracy
ASHP 01 + AHU 01 Power Consumption	JT01	CCS / WNB-3D-240-P	0 – 50amps/leg	±0.5% nominal
ccASHP 01 + AHU 02 Power Consumption	JT02	CCS / WNB-3D-240-P	0 – 50amps/leg	±0.5% nominal
ccASHP 02 + AHU 03 and 04 Power Consumption	JT03	CCS / WNB-3D-240-P	0 – 50amps/leg	±0.5% nominal
ASHP 01 + AHU 01 L1 Current	CT01	AcuAMP / ACTR050-42L-S	0 – 50amps/leg	±1% full-scale
ccASHP 01 + AHU 02 L1 Current	CT02	AcuAMP / ACTR050-42L-S	0 – 50amps/leg	±1% full-scale
ccASHP 02 + AHU 03 and 04 L1 Current	CT03	AcuAMP / ACTR050-42L-S	0 – 50amps/leg	±1% full-scale

Table 10 – ASHP and ccASHP Evaluation Outdoor Testing Bay Instrumentation

Parameter	I.D.	Make / Part #	Range	Accuracy
-----------	------	---------------	-------	----------

ASHP 01 Entering Outdoor Air Temperature	TCA 43-46	Omega / 5TC-TT-T-24-72	-454 to 700°F	± 1.8F (±1C) or 0.75%
ccASHP 01 Entering Outdoor Air Temperature	TCA 47-50	Omega / 5TC-TT-T-24-72	-454 to 700°F	± 1.8F (±1C) or 0.75%
ccASHP 02 Entering Outdoor Air Temperature	TCA 51-54	Omega / 5TC-TT-T-24-72	-454 to 700°F	± 1.8F (±1C) or 0.75%
ASHP 01 Entering Outdoor Air Relative Humidity	RHT 01	Dwyer Instruments / RHP-2010	0 to 100% @ -40 to 140°F	± 2.0% of reading
ccASHP 01 Entering Outdoor Air Relative Humidity	RHT 02	Dwyer Instruments / RHP-2010	0 to 100% @ -40 to 140°F	± 2.0% of reading
ccASHP 02 Entering Outdoor Air Relative Humidity	RHT 03	Dwyer Instruments / RHP-2010	0 to 100% @ -40 to 140°F	±2.0% of reading

Table 11 – ASHP and ccASHP Evaluation Indoor Instrumentation

Parameter	I.D.	Make / Part #	Range	Accuracy
AHU 01 Return Air Relative Humidity	RHT 04	Dwyer Instruments / RHP-2D10	0 to 100% @ -40 to 140°F	± 2.0% of reading
AHU 02 Return Air Relative Humidity	RHT 05	Dwyer Instruments / RHP-2D10	0 to 100% @ -40 to 140°F	± 2.0% of reading
AHU 03 and 04 Return Air Relative Humidity	RHT 06	Dwyer Instruments / RHP-2D10	0 to 100% @ -40 to 140°F	± 2.0% of reading
AHU 01 Supply Air Relative Humidity	RHT 07	Dwyer Instruments / RHP-2D10	0 to 100% @ -40 to 140°F	± 2.0% of reading
AHU 02 Supply Air Relative Humidity	RHT 08	Dwyer Instruments / RHP-2D10	0 to 100% @ -40 to 140°F	± 2.0% of reading
AHU 03 and 04 Supply Air Relative Humidity	RHT 09	Dwyer Instruments / RHP-2D10	0 to 100% @ -40 to 140°F	± 2.0% of reading
AHU 01 Return Air Temperature	TCA 04-07	Omega / 5TC-TT-T-24-72	-454 to 700°F	± 1.8F (±1C) or 0.75%
AHU 02 Return Air Temperature	TCA 08-11	Omega / 5TC-TT-T-24-72	-454 to 700°F	± 1.8F (±1C) or 0.75%
AHU 03 Return Air Temperature	TCA 12-15	Omega / 5TC-TT-T-24-72	-454 to 700°F	± 1.8F (±1C) or 0.75%
AHU 01 Supply Air Temperature	TCA 16-24	Omega / 5TC-TT-T-24-72	-454 to 700°F	± 1.8F (±1C) or 0.75%
AHU 02 Supply Air Temperature	TCA 25-33	Omega / 5TC-TT-T-24-72	-454 to 700°F	± 1.8F (±1C) or 0.75%
AHU 03 and 04 Supply Air Temperature	TCA 34-42	Omega / 5TC-TT-T-24-72	-454 to 700°F	± 1.8F (±1C) or 0.75%
AHU 01 Airflow Temperature	TC 01	Omega / TMQSS-125G-6	-454 to 700°F	± 1.8F (±1C) or 0.75%
AHU 02 Airflow Temperature	TC 02	Omega / TMQSS-125G-6	-454 to 700°F	± 1.8F (±1C) or 0.75%
AHU 03 and 04 Airflow Temperature	TC 03	Omega / TMQSS-125G-6	-454 to 700°F	± 1.8F (±1C) or 0.75%
AHU 01 Airflow Pressure	PT 01	Setra / 2641-R25WD-11-T1-F	0 to 0.25inWC	± 0.25% full-scale

AHU 02 Airflow Pressure	PT 02	Setra / 2641-R25WD-11-T1-F	0 to 0.25inWC	± 0.25% full-scale
AHU 03 and 04 Airflow Pressure	PT 03	Setra / 2641-R25WD-11-T1-F	0 to 0.25inWC	± 0.25% full-scale
AHU 01 Pressure Rise	PT 04	Setra / 2641-2R5WD-11-T1-F	0 to 2.5inWC	±0.25% full-scale
AHU 02 Pressure Rise	PT 05	Setra / 2641-2R5WD-11-T1-F	0 to 2.5inWC	± 0.25% full-scale
AHU 03 and 04 Pressure Rise	PT 06	Setra / 2641-2R5WD-11-T1-F	0 to 2.5inWC	± 0.25% full-scale
AHU 01 L1 Current	CT04	AcuAMP / ACTR005-42L-S	0 – 2amps/leg	±1% full-scale
AHU 02 L1 Current	CT05	AcuAMP / ACTR005-42L-S	0 – 2amps/leg	±1% full-scale
AHU 03 L1 Current	CT06	AcuAMP / ACTR005-42L-S	0 – 2amps/leg	±1% full-scale
AHU 04 L1 Current	CT07	AcuAMP / ACTR005-42L-S	0 – 2amps/leg	±1% full-scale
AHU 01 Power Consumption	JT04	CCS / WNB-3D-240-P	0 – 20amps/leg	±0.5% nominal
AHU 02 Power Consumption	JT05	CCS / WNB-3D-240-P	0 – 20amps/leg	±0.5% nominal
AHU 03 Power Consumption	JT06	CCS / WNB-3D-240-P	0 – 20amps/leg	±0.5% nominal
AHU 04 Power Consumption	JT07	CCS / WNB-3D-240-P	0 – 20amps/leg	±0.5% nominal
AHU 01- 03 Airflow	AFS01-03	FE-1500-1-A-0-16x08-R-0-FX-1	300 – 1800 cfm	± 2% of reading ±0.12% full-scale

Figure 62 shows the instrumentation location of the Power Panel 1 at the Mechanical Room of GTI laboratories that will contain the instrumentation associated to total power and current measurement of every ASHP system. An electrical-power transmitter JT and current transducer (CT) will be used to measure power consumption and current draw. Figure 63 shows the Outdoor Testing Bay where the ASHPs will be installed. A 4-thermocouple array TCA and a relative humidity transmitter RHT will be installed in every outdoor unit intake grill to measure the entering outdoor air temperature and relative humidity.

Figure 64 shows the instrumentation required to measure energy delivered to the air and the indoor unit power consumption and current draw. Room air will be conditioned using either hot or cold water through the hot-water coil (ESV Coil) shown in Figure 64, to accomplish return air temperatures between 65°F and 70°F. The indoor unit or AHU airflow will be measured independently with a low-pressure pitot-tube array (AFS) attached to a low-differential pressure transmitter (PT) in combination with a thermocouple (TC) for density corrections. A 4-thermocouple array and an RTH will be used to measure the return air temperature and relative humidity entering the AHU. The AHU supply air temperature and relative humidity will be measured with a 9-thermocouple array and 2 RHTs in order to capture the temperature and relative humidity profiles across the supply ductwork. The AHU pressure-rise associated with the operating stage will be monitored with a higher range PT.

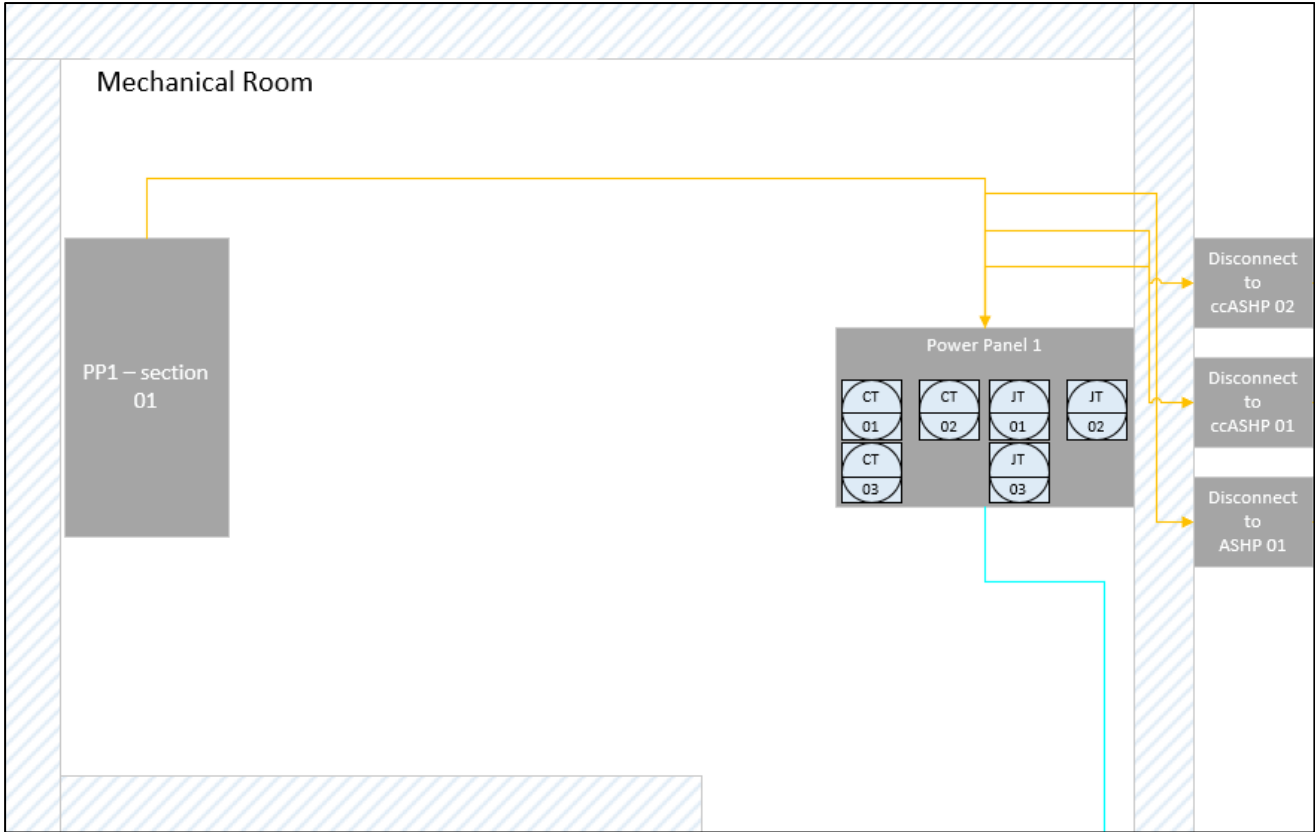


Figure 62 – Mechanical Room P&ID

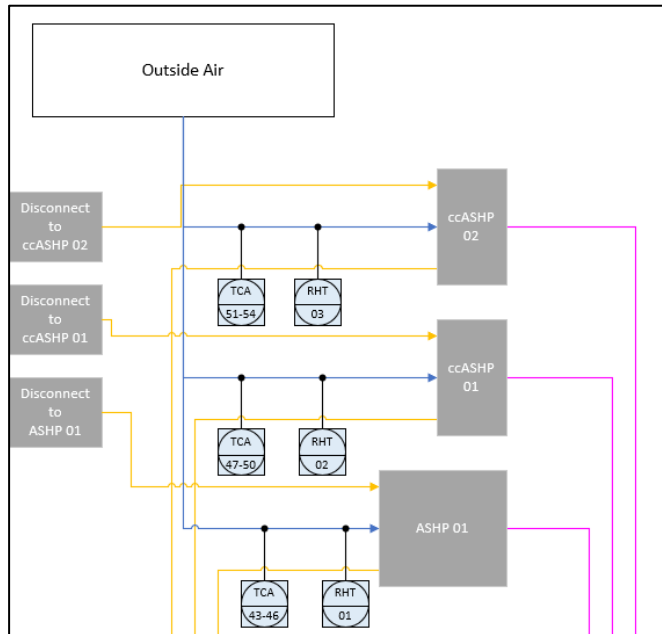


Figure 63 – Outdoor Testing Bay P&ID

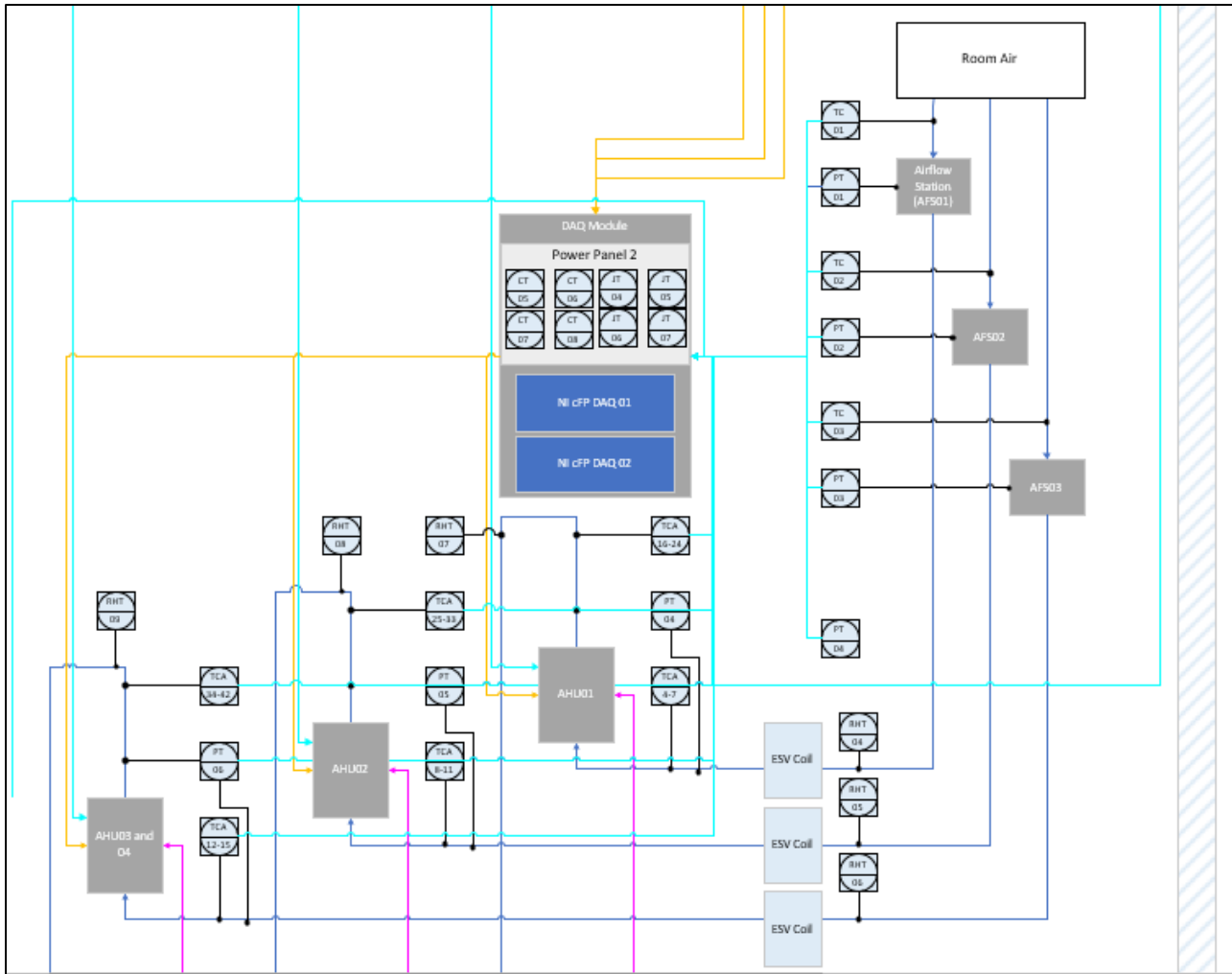


Figure 64 – AHU Test Rig P&ID

Data Sampling

A data acquisition system shall be used to record all data continuously throughout the data collection period. A maximum data sample interval of 5 seconds and minimum data collection period of at least 4 months shall be used for each ASHP's system. Barometric pressure measurements shall be made daily using a local weather station.

Air Source Electric Heat Pump and System Boundary conditions

The ASHP and System boundaries are shown in Figure 65. These boundaries define the energy stream associated with the energy delivered to the AHU and air stream and power consumption by the indoor and outdoor units independently.

ASHP Boundary

The ASHP boundary is defined by the amount of energy delivered to the AHU and power consumed by the outdoor unit. This boundary is defined by the pink dash rectangle in Figure 65. The energy delivered to the AHU will be determined by the energy delivered to the air.

System Boundary

The System boundary is defined by the amount of energy delivered to the air by the AHU and power consumed by the indoor and outdoor units. This boundary is defined by the purple dash rectangle in Figure 65.

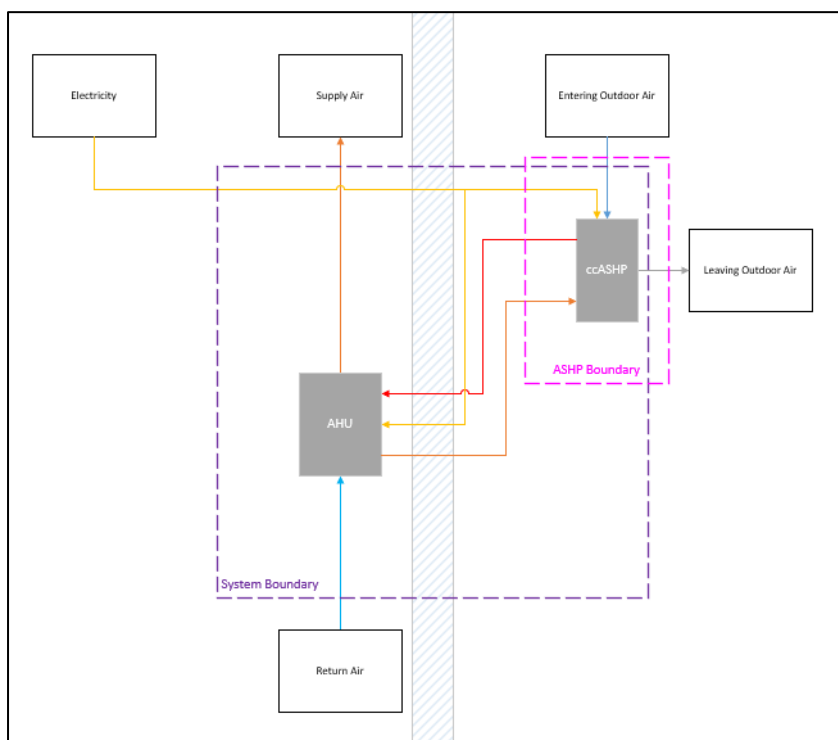


Figure 65 – ASHP and System Boundary

Calculation of Performance Parameters

Electrical Input

Electrical input shall be calculated and reported based on the real power indication (electrical output) as measured at the customer interconnection location and shall include parasitic losses, as appropriate.

ASHP Electrical Input

The ASHP electrical input is based on the difference between the direct measurement taken during testing at the Power Panel 1 and Power Panel 2 using an electrical power transmitter.

System Electrical Input

The System electrical input is based on direct measurement taken during testing at the Power Panel 1 and Power Panel 2 using an electrical power transmitter.

$$E_{ASHP} = E_{sys} - E_{AHU}$$

where:

E_{sys} = accumulated electrical power at the ASHP system, (kWh)

E_{AHU} = accumulated electrical power at the AHU, (kWh)

E_{ASHP} = accumulated electrical power at the ASHP, (kWh)

Thermal Output

Thermal output of ASHP and System boundaries is determined by measuring airflow rate and the leaving and entering enthalpies measured at the customer interconnection locations and applying appropriate specific heat values and densities to the following the basic heat transfer equation during the testing period.

ASHP Heating Output

ASHP heating output is based on calculated heat delivered to the air shown in the section below.

AHU Heating Output

AHU heating output is based on the direct measurement taken during testing at heat transferred at the ASHP System boundary calculated with the following equation for heating:

$$Q_{heat} = \dot{V} \cdot \rho \cdot c_p \cdot \Delta T \cdot t$$

where:

Q_{heat} = accumulated total thermal output at the AHU, (Btu)

\dot{V} = AHU airflow, (cfm)

ΔT = positive temperature difference between leaving and entering air temperatures at the AHU, (°F)

c_p = air specific heat at the average operating temperature, (Btu/lbm-°F)

ρ = air density based on fluid temperature at the flow meter, (lbm/cF)

t = data collection time step, (min)

Cooling Output Associated to Defrost Events

The defrost events associated to ASHP operations under freezing temperatures is based on the direct measurement taken during testing at cooling energy delivered to the air calculated with the following equation for heating:

$$Q_{cool} = \dot{V} \cdot \rho \cdot -\Delta h \cdot t$$

where:

Q_{cool} = accumulated total cooling output at the AHU, (Btu)

\dot{V} = AHU airflow, (cfm)

Δh = negative enthalpy difference between leaving and entering air temperatures at the AHU, (°F)

ρ = air density based on fluid temperature at the flow meter, (lbm/cF)

t = data collection time step, (min)

Enthalpy Calculation

The air enthalpy is calculated with following series of equations:

$$h = 0.24 \cdot T + x \cdot (0.444 \cdot T + h_{we})$$

where:

h = air enthalpy, (Btu/lbm)

T = air temperature, (btu)

h_{we} = evaporation heat of water, (1061 Btu/lbm)

x = mass of water vapor

$$x = 0.62198 \cdot \frac{p_v}{p - p_v}$$

where:

p = humid air density, (Pa)

p_v = dry air density, (Pa)

$$p_v = (RH/100) \cdot 6.1078 \times 10^{\frac{[7.5 \cdot (T-32)]}{(T-32)+237.3 \cdot 1.8}}$$

where:

RH = air relative humidity, (%)

Net Thermal Output

The net thermal output accounts for the amount of heat delivered by the ASHP system minus the cooling load during a defrost cycle in a heat call.

$$Q_{out} = Q_{heat} - Q_{cool}$$

where:

Q_{out} = accumulated total thermal output at the AHU, (Btu)

ASHP Efficiency

The ASHP efficiency shall be calculated using thermal output over the electrical input with the following equation:

$$\eta_{ASHP} = \left(\frac{Q_{out}}{E_{ASHP}} \right)$$

where:

η_{ASHP} = ASHP efficiency

System Efficiency

The ASHP system efficiency shall be calculated using thermal output over the electrical input with the following equation:

$$\eta_{sys} = \left(\frac{Q_{out}}{E_{sys}} \right)$$

where:

η_{ASHP} = ASHP efficiency

Appendix D – EHPWH Evaluation Test Plan

The objective of this test plan is to characterize two EHPWHs in the VTH. The EHPWHs will be installed in an environmental chamber to provide a variety of wet-bulb air temperatures to characterize EHPWHs for conventional and ducted installations. Mains water will be used for DHW simulations.

Evaluation Matrix

The two EHPWHs will be evaluated with the following tests:

- Heat pump heating only at constant entering air temperature and relative humidity with changing water average tank temperature
- Heat recovery at multiple hot water set points
- Two 24-hr profiles

This evaluation will identify:

- EHPWH heat pump component heating capacity as a function of ETAWb and tank average WTdb
- EHPWH COP as a function of ETAWb and tank average WTdb
- EHPWH heat pump component and backup heating element triggering by tank average WTdb
- EHPWH heat loss coefficient

Instrument Plan

Table 12 lists the instruments that will be used in the EHPWH performance evaluation illustrated in Figure 66, including the parameter to be measured, the instrument brand and model, and the instrument’s accuracy.

Table 12 – EHPWH Evaluation Instrumentation List

Parameter	I.D.	Make / Part #	Range	Accuracy
EHPWH 1 Power Consumption	JT01	CCS / WNB-3D-240-P	0 – 30amps/leg	±0.5% nominal
EHPWH 2 Power Consumption	JT02	CCS / WNB-3D-240-P	0 – 30amps/leg	±0.5% nominal
EHPWH 1 Com+Fan Current	CT01	AcuAMP / ACTR050-42L-S	0 – 20amps/leg	±1% full-scale
EHPWH 1 R1 Current	CT02	AcuAMP / ACTR050-42L-S	0 – 20amps/leg	±1% full-scale
EHPWH 1 R2 Current	CT03	AcuAMP / ACTR050-42L-S	0 – 20amps/leg	±1% full-scale
EHPWH 2 Com+Fan Current	CT04	AcuAMP / ACTR050-42L-S	0 – 20amps/leg	±1% full-scale
EHPWH 2 R1 Current	CT05	AcuAMP / ACTR050-42L-S	0 – 20amps/leg	±1% full-scale
EHPWH 2 R2 Current	CT06	AcuAMP / ACTR050-42L-S	0 – 20amps/leg	±1% full-scale
EHPWH 1 Water Flow	FT01	Dwyer Instruments / MFS2-3	0.6 to 13 GPM	±1% of reading
EHPWH 2 Water Flow	FT02	Dwyer Instruments / MFS2-3	0.6 to 13 GPM	±1% of reading
EHPWH 1 Entering Air Temperature	TC01	Omega / 5TC-TT-T-24-72	-454 to 700°F	± 1.8F (±1C) or 0.75%
EHPWH 1 Entering Air Relative Humidity	RHT01	Dwyer Instruments / RHP-2D10	0 to 100% @ -40 to 140°F	± 2.0% of reading
EHPWH 1 Water Inlet Temperature	TC02	Omega / 5TC-TT-T-24-72	-454 to 700°F	± 1.8F (±1C) or 0.75%

EHPWH 1 Water Outlet Temperature	TC03	Omega / 5TC-TT-T-24-72	-454 to 700°F	± 1.8F (±1C) or 0.75%
EHPWH 2 Entering Air Temperature	TC04	Omega / 5TC-TT-T-24-72	-454 to 700°F	± 1.8F (±1C) or 0.75%
EHPWH 2 Entering Air Relative Humidity	RHT 02	Dwyer Instruments / RHP-2D10	0 to 100% @ -40 to 140°F	± 2.0% of reading
EHPWH 2 Water Inlet Temperature	TC05	Omega / TMQSS-125G-6	-454 to 700°F	± 1.8F (±1C) or 0.75%
EHPWH 2 Water Outlet Temperature	TC06	Omega / TMQSS-125G-6	-454 to 700°F	±1.8F (±1C) or 0.75%
EHPWH 1 Thermocouple Tree	TC07-09	Omega / 5TC-TT-T-24-72	-454 to 700°F	± 1.8F (±1C) or 0.75%
EHPWH 2 Thermocouple Tree	TC 10-12	Omega / 5TC-TT-T-24-72	-454 to 700°F	± 1.8F (±1C) or 0.75%

Figure 66 shows the instrumentation location for the EHPWH evaluation. City water and domestic hot water streams will be measured using TC probes. A inline FT will be installed in the city water line to measure water flow rates. These instruments will measure the energy delivered to the water from the EHPWH. A TC tree will be installed inside the tank to measure the average water temperature of the tank all times. A TC and RHT will be installed at the EHPWH inlet grille to measure the entering wet-bulb air temperature. To vary DHW draws, a control valve will be used controlled by a data acquisition system (DAQ) input signal. A JT will be used to measure the total power consumption of the EHPWH. Three CTs will be use to map power consumption from each heating element, the EHPWH heat pump component and the two backup heating elements.

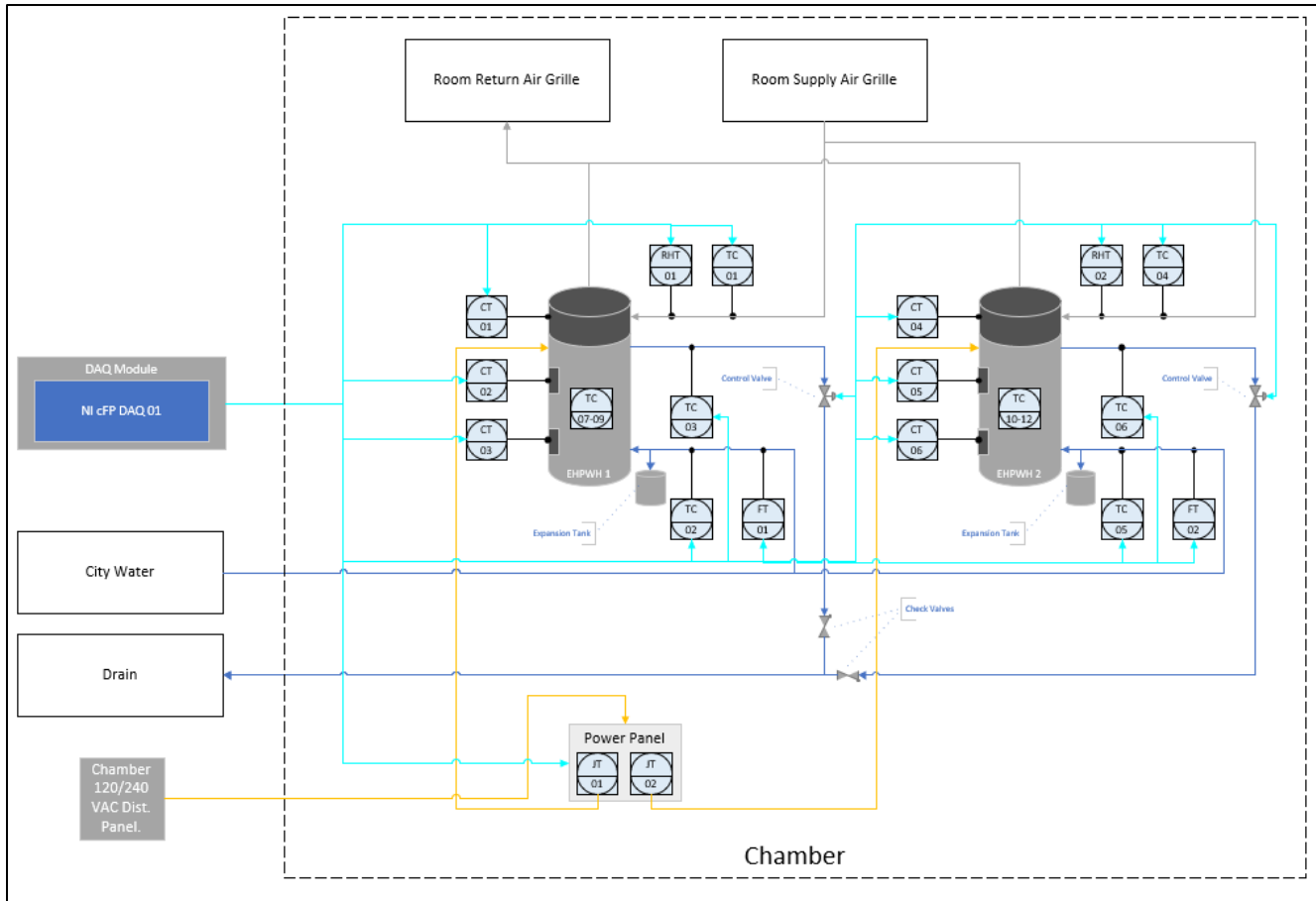


Figure 66 – EHPWH Evaluation P&ID

Data Sampling

A data acquisition system shall be used to record all data continuously throughout the data collection period with a maximum data sample interval of 5 seconds.

Calculation of Performance Parameters

Electrical Input

Electrical input shall be calculated and reported based on the real power indication (electrical output) as measured at the customer interconnection location and shall include parasitic losses, as appropriate. The EHPWH electrical input is based on direct measurement taken during testing at the Power Panel using an electrical power transmitter.

Thermal Output

Thermal output of EHPWH is determined by measuring water flow rate and the leaving and entering water temperatures measured at the customer interconnection locations and applying appropriate specific heat values and densities to the following the basic heat transfer equation during the testing period. The heat transferred to the water stream is calculated with the following equation:

$$Q_{out} = \dot{V} \cdot \rho \cdot c_p \cdot \Delta T \cdot t$$

where:

Q_{out} = accumulated total thermal output at the AHU, (Btu)

\dot{V} = water flow entering the EHPWH, (gpm)

ΔT = positive temperature difference between leaving and entering water temperatures at the EHPWH, (°F)

c_p = water specific heat at the average operating temperature, (Btu/lbm-°F)

ρ = water density based on fluid temperature at the flow meter, (lbm/gal)

t = data collection time step, (min)

EHPWH COP

The EHPWH COP shall be calculated using thermal output over the electrical input with the following equation:

$$\eta_{EHPWH} = \left(\frac{Q_{out}}{E_{EHPWH}} \right)$$

where:

η_{EHPWH} = EHPWH efficiency

E_{EHPWH} = EHPWH power consumption, (Btu)

EHPWH Heat Recovery

The EHPWH heat recovery is calculated for UEF testing. This shall be calculated when the EHPWH continues to heat water without DHW draw while consuming power with the following equation:

$$Q_{HR} = V_{tank} \cdot \rho \cdot c_p \cdot (\Delta T_{tank})/t$$

where:

Q_{HR} = accumulated total thermal output at the AHU, (Btu)

V_{tank} = tank water volume, (gal)

ΔT_{tank} = temperature rise in the EHPWH TC tree while consuming power without DHW draw as a function of time, (°F)

c_p = water specific heat at the average operating temperature, (Btu/lbm-°F)

ρ = water density based on fluid temperature at the flow meter, (lbm/gal)

t = time for water tank temperature rise, (hr)

Appendix E – ASHP and ccASHP Additional Characterizations

Part-load Degradation

Figure 67 and Figure 68 show the part-load degradation characterization for the ASHP and ccASHP systems evaluated in the VTH. In the y-axis PRL Capacity is the percentage of steady-state heating capacity at a given compressor speed. The PRL Time in the x-axis is the percentage of running time of a heating call over hours. Figure 67 shows that the Goodman ASHP required at least 36 minutes (60% of an hour) to reach to steady-state heating capacity after receiving a heating call. Figure 68 shows that both ccASHPs required about 24 minutes (40% of an hour) to reach to the steady-state heating capacity while cycling and not modulating.

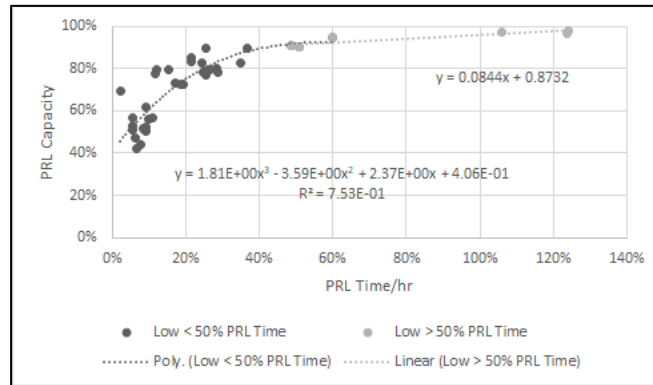


Figure 67 – Goodman ASHP Part-load Degradation Characterization

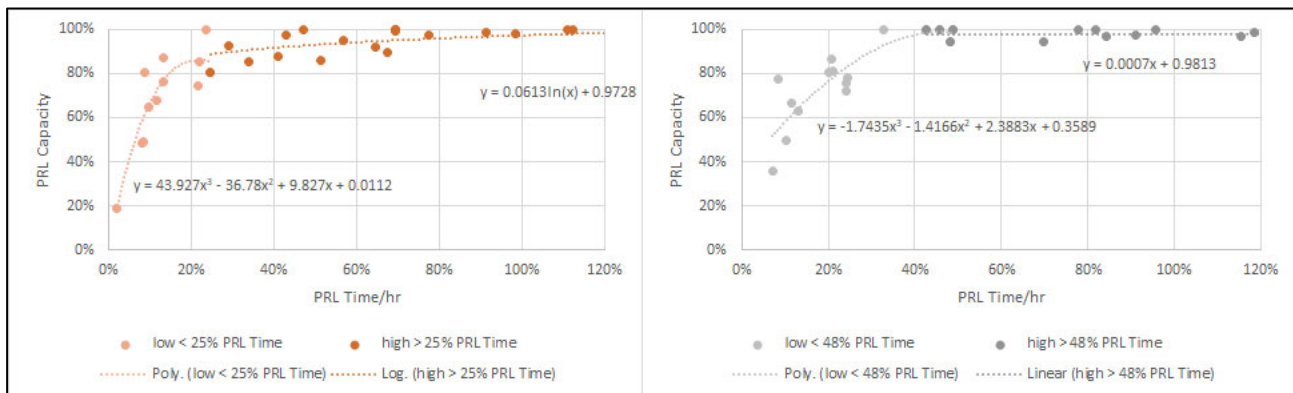


Figure 68 – Mitsubishi (left) and Fujitsu (right) ccASHP Part-load Degradation Characterizations

Compressor Speed

Figure 69 shows the compressor speed characterization in the baseline ASHP as a function of return air enthalpy (RAH). The compressor speed in the ASHP seemed to adjust based on the ability to reject heat in the indoor unit. As the return air temperature increases, it is more difficult to reject heat for an ASHP. Therefore, the compressor works harder requiring more power.

Figure 70 show the maximum compressor speed the Mitsubishi (left) and Fujitsu (right) ccASHPs. Both units had similar compressor speed limitations. For warmer OATdb's, the compressor speed was limited to low speeds. This control strategy is beneficial by avoiding short-cycling efficiency degradation when space heating loads are low. On the other hand, the compressor speed declined

below 0°F OATdb with lower maximum power consumption. Similar behavior in the power consumption in the ASHP was observed as the OATdb decreased.

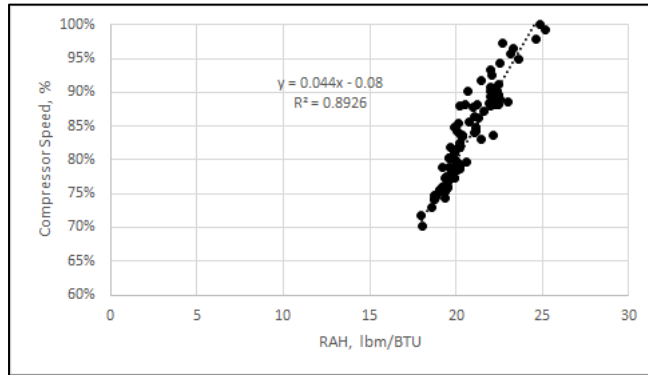


Figure 69 – Goodman ASHP Compressor Speed Characterization

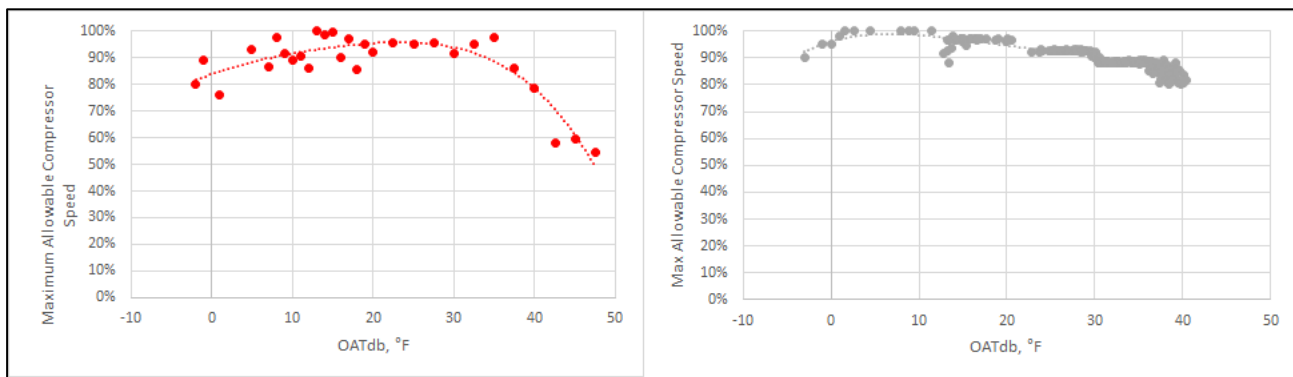


Figure 70 – Mitsubishi (left) and Fujitsu (right) ccASHP Maximum Compressor Speed Characterizations

Defrost Cycles

Power Consumption and Cooling Delivered

Figure 71 shows cooling delivered and power consumption of the ASHP during defrost cycles as a function of outdoor air relative humidity (OARH) for OATwb lower than 40°F. Figure 72 shows the power consumption during defrost cycles for both ccASHPs. Unlike the baseline ASHP, the two ccASHPs stopped the AHU fan to prevent cool air delivered to the space. In doing so, these two ccASHPs consumed at least two times the amount of power.

Defrost Duration

Figure 73 and Figure 74 shows the defrost duration as a function of power consumption for the baseline ASHP and ccASHPs, respectively. The Fujitsu mini-split ccASHP took longer to defrost for the same power consumption in comparison to the other two systems.

Defrost Activation Cycles

The ASHP defrost activation cycle shown to be based on 1-hour run time under OATdb less than 40°F. Unlike the baseline the ASHP, the two ccASHPs had similar activation strategies shown in Figure 75. As the OARH increased, the defrost cycles were more frequent. For OATwb less than 40°F and OARH less than 70%, the defrost cycles at least every two hours. These systems appeared to monitor the frost buildup in the outdoor refrigerant coil and activate the defrost cycle when needed.

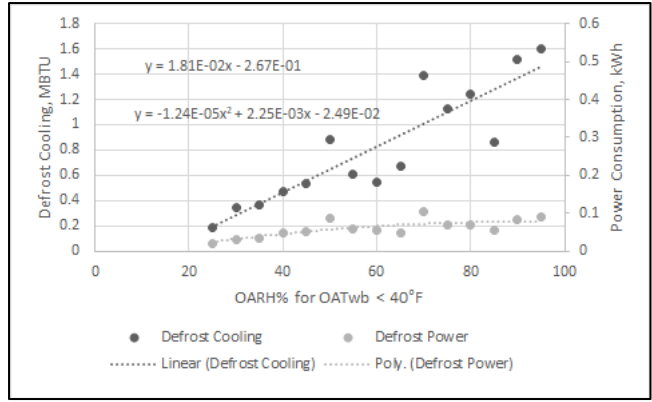


Figure 71 – Goodman ASHP Defrost Cooling (left Y-axis) and Power Consumption (right Y-axis) Characterizations

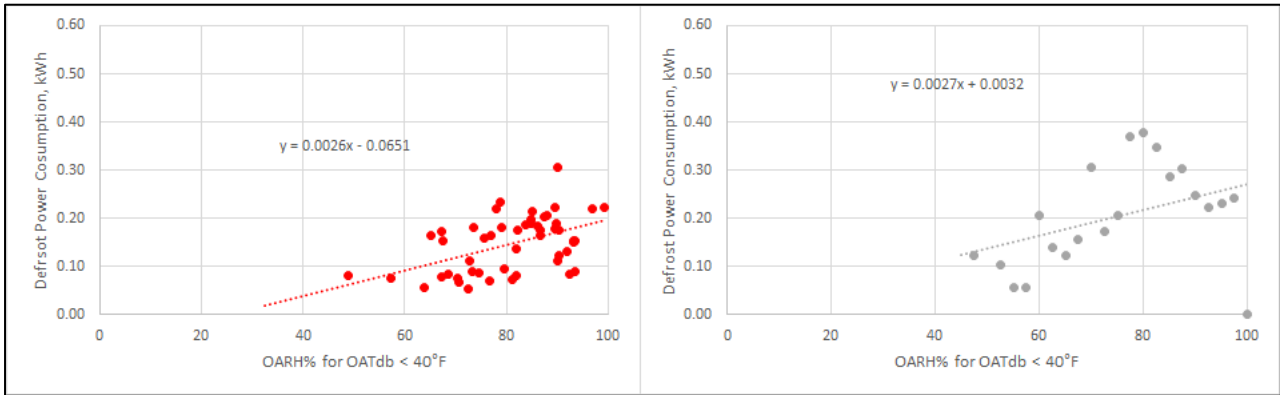


Figure 72 – Mitsubishi (left) and Fujitsu (right) ccASHP Defrost Power Consumption Characterizations

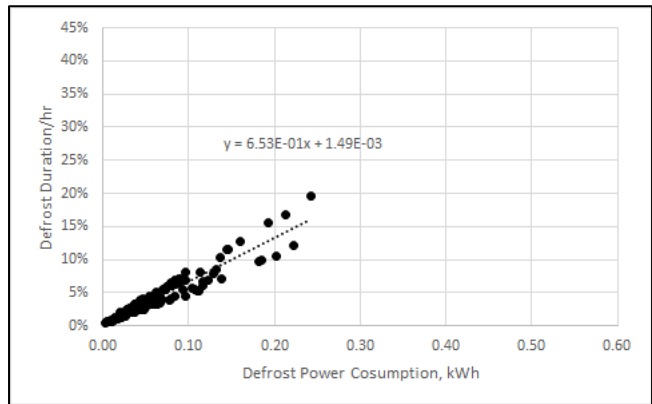


Figure 73 – Goodman ASHP Defrost Duration Characterization

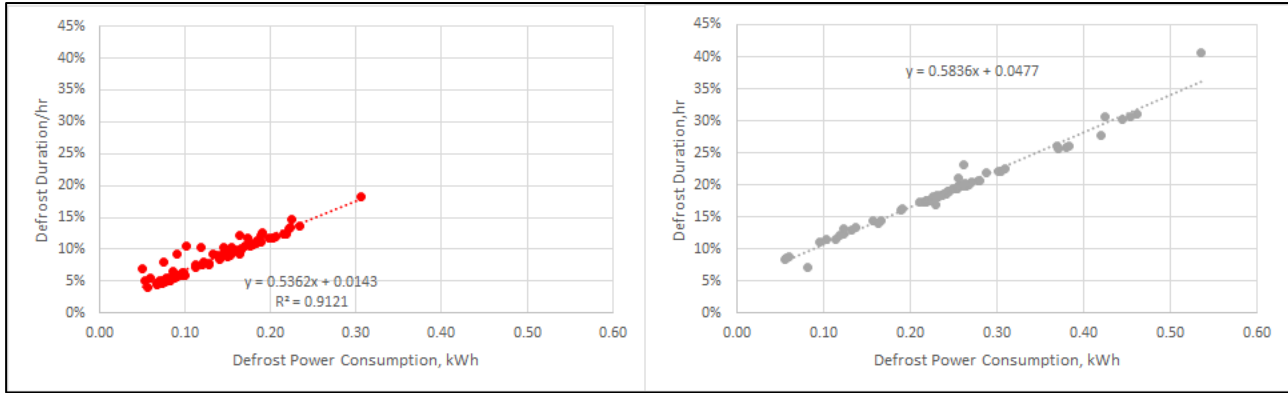


Figure 74 – Mitsubishi (left) and Fujitsu (right) ccASHP Defrost Duration Characterizations

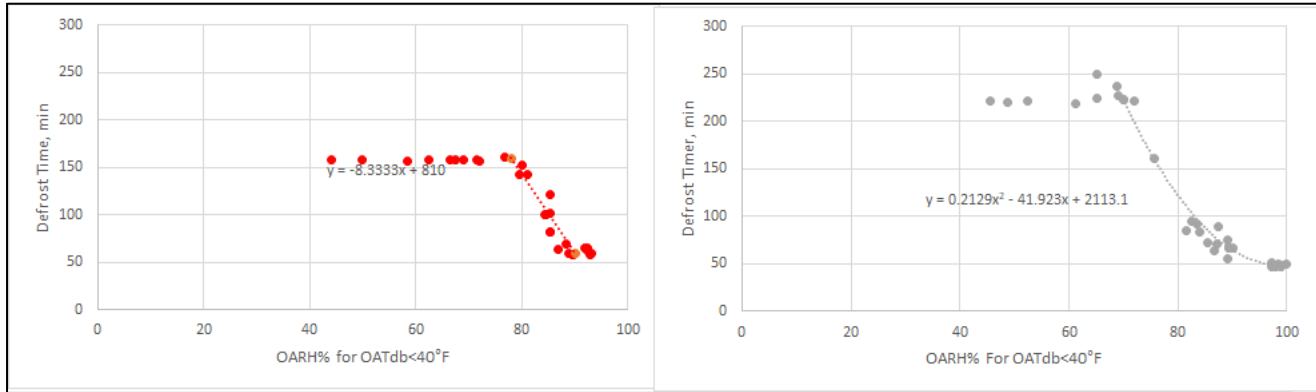


Figure 75 – Mitsubishi (left) and Fujitsu (right) ccASHP Defrost Duration Characterizations

Appendix F – Modeling Individual Space and Water Heating Performance Comparison

Table 13 and Table 14 show the electricity and natural gas rates implemented in the annual operating cost analysis in the Individual Space and Water Heating Performance Comparison and System Market Impact Considerations sections obtained from [U.S. Energy Information Administration](http://www.eia.doe.gov).

Table 13 – EIA State Electricity Monthly Rates

States	\$ / 100kWh											
	Jan	Feb	Mar	Apr	May	Jun	Jul	Aug	Sep	Oct	Nov	Dec
Alabama	12.11	12.97	12.82	12.71	12.73	12.79	12.08	12.22	12.27	12.56	12.29	12
Arizona	11.31	11.66	11.73	12.49	13.04	12.94	12.71	12.78	12.77	12.69	12.16	11.3
California	18.44	18.68	18.87	17.66	18.29	19.39	18.49	18.88	18.23	18.35	17.93	18.15
Colorado	11.6	11.89	11.93	12.14	12.1	12.75	13.14	12.89	12.78	12.57	12.16	11.78
Michigan	15.23	15.41	15.38	15.4	15.85	15.86	15.37	15.87	15.77	15.77	15.46	15.28
Montana	10.67	10.61	10.74	10.93	11.29	11.73	11.6	11.5	11.62	11.35	11.19	10.79
Nevada	12.69	13.46	13.6	13.48	13.52	13.12	13.12	12.63	12.87	13.21	13.61	12.95
New York	19.28	19.75	18.92	17.72	18.5	18.77	20.48	19.51	19.41	19.43	19.45	19.26
Oregon	10.4	10.53	10.56	10.69	10.86	10.97	10.95	11.06	10.91	10.98	10.93	10.68
Tennessee	10.45	10.52	10.63	10.68	10.74	10.93	10.76	10.54	10.56	10.63	10.95	10.81
Texas	11.49	11.62	11.56	12.1	12.04	11.78	12.05	12.05	12.03	12.07	11.98	11.81
Wisconsin	14	14.34	14.51	14.75	15.35	15.05	14.94	14.37	14.77	14.76	14.58	13.93

Table 14 – EIA State Natural Gas Monthly Rates

States	\$ / 1000 CF											
	Jan	Feb	Mar	Apr	May	Jun	Jul	Aug	Sep	Oct	Nov	Dec
Alabama	13.43	14.63	14.71	16.46	20.85	21.42	21.81	21.85	21.87	21.22	19.09	14.48
Arizona	14.36	18.88	18.94	18.94	19.21	21.54	23.6	24.03	23.7	21.92	17.48	16.55
California	13.17	12.73	12.48	12.58	13.04	13.21	12.5	12.9	13.34	13.39	12.4	13.16
Colorado	8.05	7.97	8.5	9.3	10.23	12.81	15.45	15.47	13.58	10.06	8.08	8.15
Michigan	8.61	8.64	9.15	9.9	11.14	13.15	14.08	14.65	13.26	10.09	8.89	9.03
Montana	8.39	8.29	8.8	9.79	10.92	12.45	13.39	13.58	11.18	10.08	8.52	8.26
Nevada	10.42	11.4	11.84	13.3	14.34	15.51	16.72	16.75	16.14	15.5	12.44	10.61
New York	11.18	11.32	11.78	12.49	14.55	17.99	19.25	18.99	18.42	16.12	12.27	11.43
Oregon	11.18	12.37	13.23	14.17	15.69	16.31	16.2	17.09	15.53	13.54	12.69	11.94
Tennessee	8.72	9.1	9.65	11.57	14.18	17.54	18.86	19.64	18.54	16.12	11.74	9.22
Texas	8.63	8.56	10.08	12.53	16.33	18.67	20.22	21.08	20.9	19.55	15.49	10.06
Wisconsin	8.83	9.62	13.82	11.56	14.55	13.6	14.35	15.05	14.3	9.2	8.99	9.46

Table 15 shows the source-energy factors and GHG rates implemented in the annual operating cost analysis in the Individual Space and Water Heating Performance Comparison and System Market Impact Considerations sections obtained from eGRID.

Table 15 – eGRID Source-energy Factor and GHG Emissions for Natural Gas and Electricity Per City

City	Source-energy Factor		GHG, lbm/MMBtu	
	Natural Gas	Electricity	Natural Gas	Electricity
Bismarck, ND	1.09	2.66	145	414
Madison, WI	1.09	3.02	145	565
Bozeman, MT	1.09	1.91	145	221
Albany, NY	1.09	2.16	145	116
Denver, CO	1.09	2.58	145	436
Amarillo, TX	1.09	2.60	145	355
Portland, OR	1.09	1.91	145	221
Nashville, TN	1.09	2.90	145	393
Birmingham, AL	1.09	2.76	145	393
San Francisco, CA	1.09	2.02	145	198
Las Vegas, NV	1.09	2.58	145	221
Tucson, AZ	1.09	2.84	145	358
Austin, TX	1.09	2.53	145	355
Los Angeles, CA	1.09	2.02	145	198

Appendix G – Modeling System Market Impact Considerations

This appendix presents the details associated with the modeling used for the System Market Impact Considerations section.

ccASHP + EHPWH Space Heating and Cooling Loads

The space heating and cooling loads for the ccASHP were modified based on the amount of heat transferred by the EHPWH from the conditioned air.

Air Conditioning Performance Characterization

The air conditioning performance curves implemented in this report were based on the manufacturer specifications for Mitsubishi ccASHP ([PUZ-HA36NHA5 Engineering Manual](#)) and both Goodman 15 SEER ([GSZ14 Manufacturer Specifications](#)) and 18 SEER ASHPs ([GSZC18 Manufacturer Specifications](#)).

Cooling Capacity

The steady-state cooling capacities for the Mitsubishi ccASHP and both ASHPs are shown in Figure 76. The derating associated with OATdb increase is shown in Figure 77. This derating factor represents the limitations for an air conditioner to reject heat outdoors as the OATdb increases.

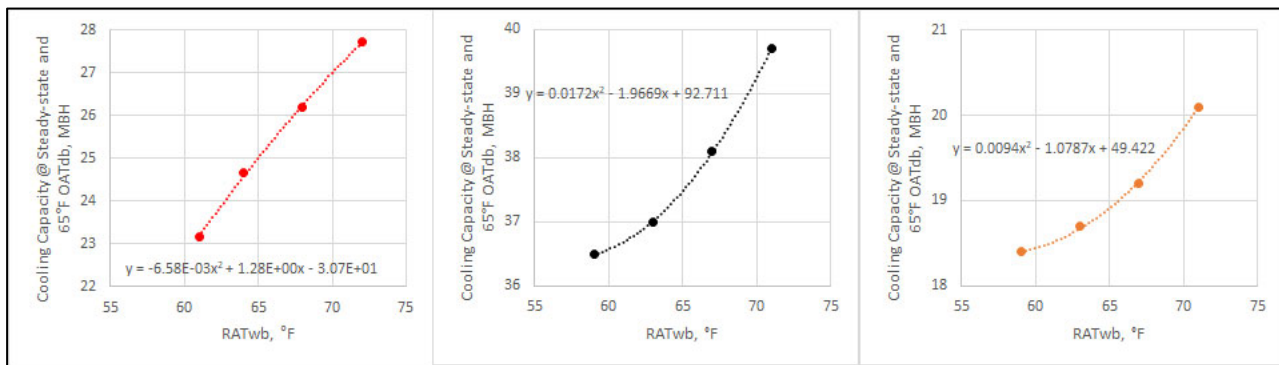


Figure 76 – Steady-state Cooling Capacity Curves for the Mitsubishi ccASHP (left) and Both Goodman 15SEER (center) and 18SEER (right) ASHPs

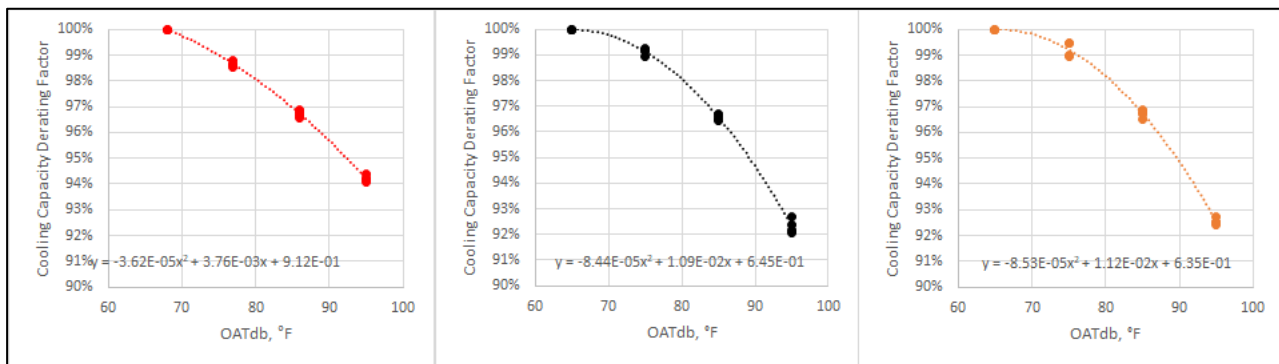


Figure 77 – Cooling Capacity OATdb Derating Factor for the Mitsubishi ccASHP (left) and Both Goodman 15SEER (center) and 18SEER (right) ASHPs

Coefficient of Performance

The steady-state COP for the Mitsubishi ccASHP and both ASHPs are shown in Figure 78. Similar heating characterization for electric-driven heat pumps/air conditioners COP is characterized based on

the difference between operating evaporator dry-bulb temperature and condenser wet-bulb temperatures. It is important to indicate that the COP curve for the 18 SEER Goodman ASHP is for the first stage of operation only.

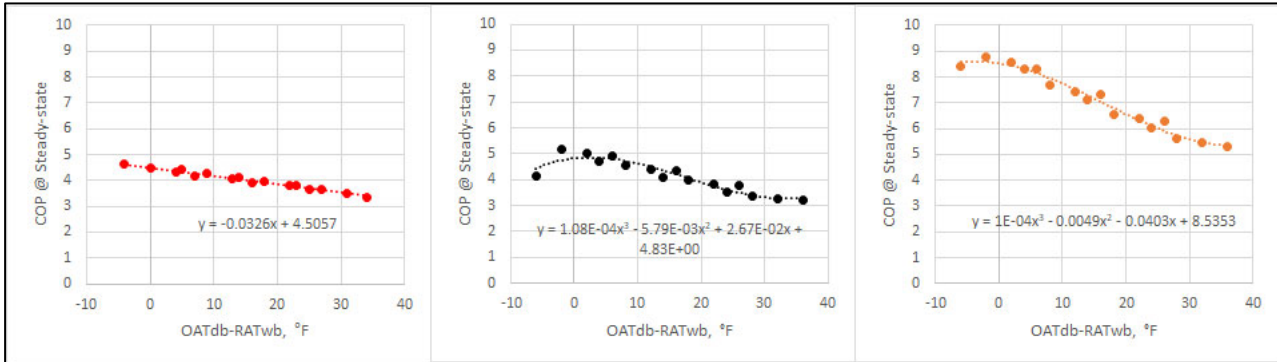


Figure 78 – Cooling COP Curves for the Mitsubishi ccASHP (left) and Both Goodman 15 SEER (center) and 18 SEER (right) ASHPs

Goodman Two-stage 10 HSPF ASHP Heating Performance Characterization

The Goodman two-stage 10 HSPF ASHP was analyzed in the UTD Report 1.16.E: *Low Capacity Heating Systems Portfolio – Phase 2*. The performance curves have been updated in this report with the same nomenclature for comparison purposes.

Heating Capacity

With dual-stage capability, the Goodman 10 HSPF ASHP heating capacity curves are shown in Figure 79.

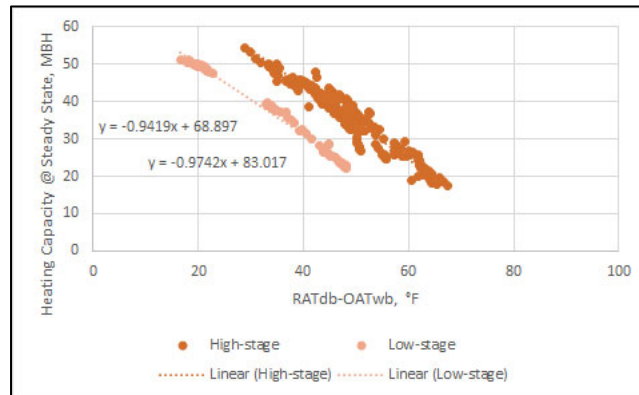


Figure 79 – Goodman 10HSPF ASHP Steady-state Heating Capacity

Coefficient of Performance

Similar to the other three ASHP systems analyzed in this report, the Goodman 10 HSPF ASHP COP was similar between stages as shown in Figure 80. Unlike the other three ASHP COP curves in this report, the power used during defrost operation is integrated.

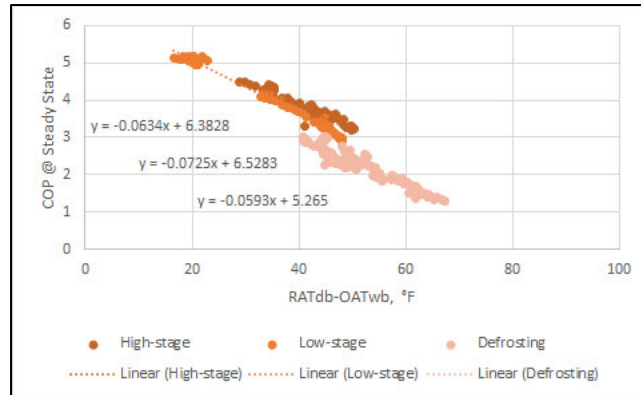


Figure 80 – Goodman 10 HSPF ASHP Steady-state COP

Defrost Operation

Similar to the Goodman 9 HSPF single-stage ASHP, this system operated with a defrost timer based on a selected time interval. The defrost operation time and cooling delivered to the air are shown in Figure 81.

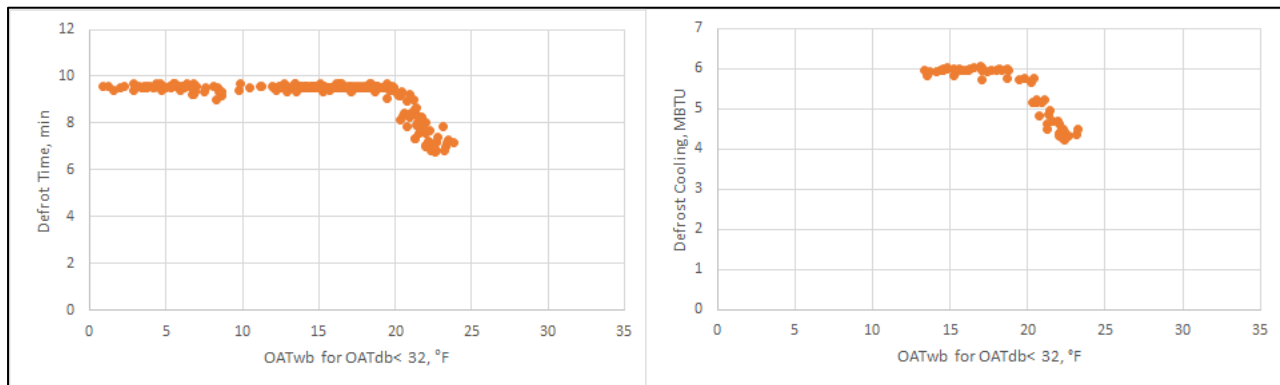


Figure 81 – Goodman 10 HSPF ASHP Defrost Operation Duration (left) and Cooling Delivered (right)

Additional Operating Features

- Similar to the Goodman 9 HSPF ASHP, this system had a 40W-crankcase heater attached to the accumulator.
- Part-load degradation curve was similar to the one observed in the Goodman 9 HSPF ASHP.

THP Performance Characterization

The performance curves for the THP is based on combined VTH testing and field demonstration results that are referenced in the UTD Report 1.18.D, 1.18.G, 2.18.G: *Integrating Micro-CHP & PV; Gas Heating & Cooling; Thermal Energy Storage; and in Advanced Gas/Renewable Homes*. The following equations were developed to determine the gas consumption of the THP considering:

- THP heating capacity
- Entering dry-bulb air temperature to the THP condenser
- Return glycol/water mixture to the THP from the process
- THP heating part-load
- THP cycling effect
- THP defrost cycling effect

- Electric consumption

The THP heating capacity as a function of entering air dry-bulb temperature and return glycol/water temperature to the THP is calculated with the following equation:

$$CAPFT = 3.413 \cdot (a_1 \cdot T_{EAT} + a_2 \cdot T_{EAT}^2 + b_1 \cdot T_{EWT} + b_2 \cdot T_{EWT}^2 + c_1 \cdot T_{EAT} \cdot T_{EWT} + c_0)$$

where:

$CAPFT$ = THP heating output as function of entering air dry-bulb temperature and return glycol/water temperature, (btu/h)

T_{EAT} = THP entering air dry-bulb temperature, ($^{\circ}C$)

T_{EWT} = THP return glycol/water temperature, ($^{\circ}C$)

a_1 = 4.28×10^{-3}

a_2 = -8.60×10^{-5}

b_1 = 4.09×10^{-3}

b_2 = 1.38×10^{-4}

c_1 = 2.26×10^{-6}

c_0 = 1.01×10^0

The THP heating capacity is calculated with the following equation:

$$Q_{out_{max}} = Q_{nom} \cdot CAPFT \cdot 3.413$$

where:

$Q_{out_{max}}$ = maximum THP heating output at current operating conditions, (btu/h)

Q_{nom} = THP nominal heating output, (W)

The THP heating part load is calculated with the following equation considering the firing rate modulation limits of the THP:

$$PRL = \frac{Q_{out_a}}{Q_{out_{max}}}$$

where:

PRL = THP heating part-load

Q_{out_a} = actual load, (btu/h)

$Q_{out_{max}}$ = maximum THP heating output, (btu/h)

The THP cycling effect is calculated with the following equation considering the firing rate modulation limits of the THP:

$$CRF = 0.4167 \cdot \frac{PRL}{0.25} + 0.5833$$

where:

CRF = THP cycling effect in gas efficiency

The THP heating capacity modulation efficiency derate as function of entering air dry-bulb temperature and return glycol/water temperature to the THP is calculated with the following equation:

$$EIRFT = 3.413 \cdot (a_1 \cdot T_{EAT} + a_2 \cdot T_{EAT}^2 + b_1 \cdot T_{EWT} + b_2 \cdot T_{EWT}^2 + c_1 \cdot T_{EAT} \cdot T_{EWT} + c_0)$$

where:

$EIRFT$ = THP heating output modulation efficiency derate as function of entering air dry-bulb temperature and return glycol/water temperature, (btu/h)

$$a_1 = -3.18 \times 10^{-3}$$

$$a_2 = 6.60 \times 10^{-5}$$

$$b_1 = 1.18 \times 10^{-2}$$

$$b_2 = -6.10 \times 10^{-5}$$

$$c_1 = -4.77 \times 10^{-5}$$

$$c_0 = 3.38 \times 10^{-1}$$

The THP defrost cycling effect as function of entering air dry-bulb temperature is calculated with the following equation:

$$EIRdef = 3.413 \cdot (-0.006 \cdot T_{EAT} - 0.0011 \cdot T_{EAT}^2 + 1.0317)$$

where:

$EIRdef$ = THP defrost cycling effect as function of entering air dry-bulb temperature within -8.88°C and 3.33°C EATs

The THP defrost cycling effect as function of entering air dry-bulb temperature is calculated with the following equation:

$$EIRdef = 3.413 \cdot (-0.006 \cdot T_{EAT} - 0.0011 \cdot T_{EAT}^2 + 1.0317)$$

where:

$EIRdef$ = THP defrost cycling effect as function of entering air dry-bulb temperature within -8.88°C and 3.33°C EATs

The THP heating performance derate as a function modulation is calculated with the following equation:

$$EIRFPRL = 0.0864 \cdot \max(PRL, 0.25)^2 - 0.0681 \cdot \max(PRL, 0.25) + 0.9814$$

where:

THP_E = THP power consumption, (btu/h)

The THP gas consumption is calculated with the following equation:

$$THP_G = Q_{out_a} \cdot EIRFT \cdot EIRdef \cdot EIRFPLR \cdot CRF^{-1}$$

where:

THP_G = THP gas consumption, (btu/h)

mCHP Performance Characterization

The performance mapping equations referenced in the UTD Report 1.18.D, 1.18.G, 2.18.G: *Integrating Micro-CHP & PV; Gas Heating & Cooling; Thermal Energy Storage; and in Advanced Gas/Renewable Homes* for the mCHP implemented in this report will not be presented due to the current NDA with the manufacturer.